

THE COMPLEXITY OF DIAGNOSING AND MONITORING GLAUCOMA



JOSINE VAN DER SCHOOT

The Complexity of Diagnosing and Monitoring Glaucoma

Josine van der Schoot

Proefschrift

The studies presented in this thesis were supported by Alcon Laboratories, Inc., Glaucoomfonds, Landelijke Stichting voor Blinden en Slechtzienden, Merck & Co. Inc., Pfizer Inc., the Rotterdam Eye Hospital Research Foundation (SWOO-Prof. Dr. H.J. Flieringa), Stichting Nederlands Oogheeskundig Onderzoek, Stichting Oogfonds Nederland, Stichting voor Ooglijders.

The publication of this thesis was financially supported by:
JoZien Oogheelkunde

ISBN: 978-94-92683-52-6

This thesis is also available online on <https://epubs.ogc.nl/?epub=j.vanderschoot>



Cover illustration: www.istockphoto.com

Layout and printing: Optima Grafische Communicatie, Rotterdam, the Netherlands

© Josine van der Schoot, 2017

All rights reserved. No part of this thesis may be reproduced, stored in a retrieval system of any nature, or transmitted in any form or by any means without permission of the author or, when appropriate, of the publishers of the publications

The Complexity of Diagnosing and Monitoring Glaucoma

*De complexiteit van het diagnosticeren
en monitoren van glaucoom*

Proefschrift

ter verkrijging van de graad van doctor aan de
Erasmus Universiteit Rotterdam
op gezag van de rector magnificus

Prof.dr. H.A.P. Pols

en volgens besluit van het College voor Promoties.

De openbare verdediging zal plaatsvinden op
woensdag 21 juni 2017 om 11.30 uur

door

Johanna Gesina van der Schoot
geboren te Groningen

Promotiecommissie:

Promotor: Prof. Dr. J.C. van Meurs

Overige leden: Prof. Dr. J.R. Vingerling
Prof. Dr. C.A.B. Webers
Prof. Dr. N.M. Jansonius

Copromotor: Dr. H.G. Lemij

TABLE OF CONTENTS

Chapter 1.	General Introduction & Outline of this thesis	7
Chapter 2.	Short wavelength automated perimetry is a poor predictor of conversion to glaucoma	27
Chapter 3.	Converting from ocular hypertension to glaucoma: Scanning laser polarimetry or standard automated perimetry?	41
Chapter 4.	Does topical Betaxolol or Timolol prevent ocular hypertension from converting to glaucoma? The Rotterdam Ocular Hypertension Trial	55
Chapter 5.	Accuracy of matching optic discs with visual fields: The European Structure And Function Assessment Trial (ESAFAT)	65
Chapter 6.	Detecting progression in glaucoma; a comparison between visual fields and stereoscopic photographs of the optic nerve head	79
Chapter 7.	Transient peripapillary retinoschisis in glaucomatous eyes	93
Chapter 8.	The effect of glaucoma on the optical attenuation coefficient of the retinal nerve fiber layer in spectral domain optical coherence tomography images	107
Chapter 9.	General Discussion	125
Chapter 10.	Summary & Samenvatting	139
	Dankwoord	151
	List of Publications	155
	Portfolio	157
	Curriculum Vitae	159

1

General Introduction &
Outline of this thesis

GENERAL INTRODUCTION

Glaucoma is a heterogeneous group of *progressive optic neuropathies* characterised by an *accelerated degeneration of retinal ganglion cells (RGCs)* and their axons, resulting in a *typical appearance of the optic nerve head* and a matching pattern of irreversible *visual field loss*.¹⁻³

Anatomy

The optic nerve connects the eye with the brain. The optic nerve leaves the eye at the optic nerve head (ONH), also referred to as optic disc because of its discoid shape when viewed from anteriorly. The optic nerve is formed by approximately one million nerve fibers. Before the axons converge in the ONH, they comprise the retinal nerve fiber layer (RNFL), which is the innermost layer of the retina. Like the retinal bloodvessels, the axons forming the RNFL follow an arcuate pattern towards the ONH. The ONH is about 1.5mm in diameter and vertically oval. The convergence of the axons, travelling from the RNFL to the optic nerve, forms a rim of neuroretinal tissue and a central depression, known as the cup.³ The neuroretinal rim is thickest in the inferior region, followed by the superior, nasal and temporal regions, following the ISNT-rule.⁴ In glaucoma, an increased loss of retinal ganglion cells and its axons occurs, leading to a typical excavation of the ONH and the subsequent loss and thinning of the retinal nerve fiber layer.

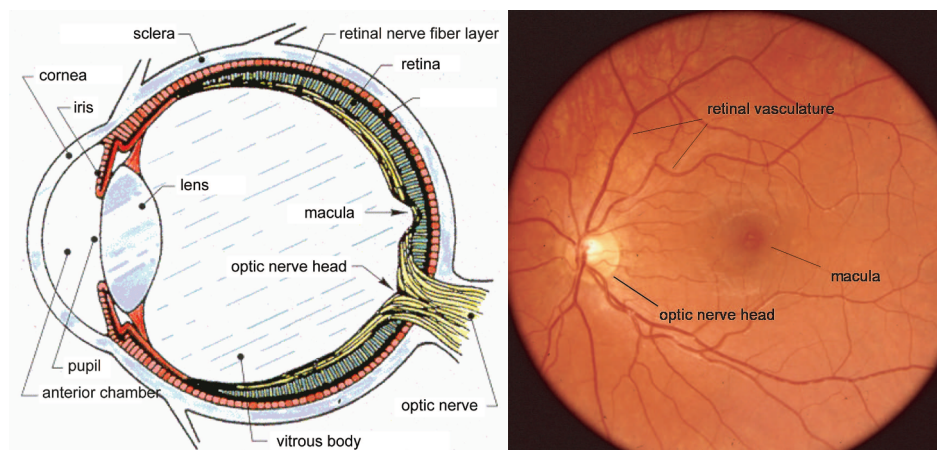


Figure 1 The schematic drawing on the left shows a cross-section of a human eye. The photograph on the right presents a anterior-to-posterior view on the retina, showing the macula, the retinal vasculature and the optic nerve head.

Epidemiology

When left untreated, glaucoma can lead to severe visual field loss and therefore progressive loss of visual function. Worldwide, glaucoma is the second leading cause of blindness, after cataract, whereas cataract is a potentially reversible disease and glaucoma leads to irreversible blindness.⁵ Approximately 12% of all blindness is due to glaucoma.⁵ As glaucoma is an age-related disease, the number of people affected by glaucoma will rise in the upcoming years, due to the increasing population aged 50 years and older. According to calculations by Quigley and Broman⁶, in 2020, 79.6 million people worldwide will have glaucoma. The prevalence among people of European descent aged 40 years and older varies between 1.1 and 2.1%, leading to an estimated prevalence of (open angle) glaucoma in the Netherlands somewhere between 180.000 and 360.000.⁷⁻¹⁰

Classification of Glaucoma

Traditionally, glaucoma has been classified as open angle or closed angle glaucoma and as primary or secondary glaucoma. The first classification is based on the anatomy of the anterior chamber angle and is mainly interesting from a treatment point of view. Primary glaucoma refers to glaucomatous damage when there is no identifiable underlying ocular or systemic disorder, whereas secondary glaucoma refers to those glaucomas caused by an ophthalmological or extraocular disease, drugs or treatment. Primary open angle glaucoma (POAG) is the most common form of glaucoma in Western countries.³

Risk factors

Glaucoma is a multifactorial disease with increased intraocular pressure (IOP) as the most important risk factor. An increased or highly fluctuating IOP is related to a higher prevalence, incidence and progression of POAG.¹¹ Historically, an elevated IOP was included in clinically defining glaucoma. However, approximately 20-75% of all patients with POAG have IOPs within the normal range, a condition referred to as 'normal tension glaucoma'.¹¹ However, an increased IOP does not necessarily lead to glaucomatous damage. Eyes with an increased IOP but without any signs of an optic neuropathy or any visual field loss are referred to as having ocular hypertension.¹ Other risk factors for POAG include increased age, African descent, a positive family history of glaucoma, myopia, a thinner cornea, and a reduced perfusion pressure.^{1;2;11} The role of various systemic factors, such as diabetes, systemic hypertension, migraine and ischemic vascular diseases, in the development of glaucoma has been widely debated, but the evidence is still inconclusive.¹¹

Pathophysiology

The exact pathophysiology of glaucoma is not fully understood, although the death of RGCs is related to the level of increased IOP³ and a reduced ocular blood supply.¹² Although no obstruction of the trabecular meshwork can be seen by gonioscopy in patients with POAG, the resistance to aqueous outflow is increased.³ When the level of IOP rises above physiological levels, the pressure gradient across the lamina cribrosa, an array of perforated connective tissue sheets through which the optic nerve fibers transverse to form the optic nerve, also increases. The increased IOP leads to *mechanical* stress of the lamina cribrosa and the retinal ganglion cell axons. The *vascular* factor causing glaucoma is a reduced retinal or ONH blood supply, leading to local ischemia and/or hypoxia and subsequent death of RGCs and optic nerve fibers. Various other contributing factors include a blockade of axonal protein transport by increased IOP, poorly functioning cellular pumps and glutamate transporters, inflammatory cytokines, aberrant immunity and apoptosis of RGCs secondary to initial optic nerve injury.^{3;12}

Treatment

Glaucoma care in Europe aims to enhance the patient's health and quality of life by preserving visual function without causing untoward effects from treatment.¹ Of all risk factors that play a role in glaucoma, the IOP is presently the only one that can be altered therapeutically. Lowering IOP has been shown to slow down the progression of glaucoma.^{13;14} Treatment options are either pharmaceutically (eyedrops or oral medication) or surgically (laser surgery, filtering surgery or implant surgery). Topical treatment decreases the IOP by reducing the aqueous production and/or increasing the trabecular or uveoscleral outflow. Surgical treatment aims for a permanent IOP reduction by increasing the aqueous outflow.

Ocular Hypertension

Ocular hypertension (OH) refers to those eyes with an elevated IOP without an optic neuropathy or visual field loss.¹ The prevalence of OH is 4.5% in whites aged 40 years and older.¹⁵ The higher the IOP, the higher the risk of developing glaucoma.¹⁶ Several large studies have presented conflicting results whether or not to treat ocular hypertension. The Ocular Hypertension Treatment Study (OHTS) found a 50% reduction of the risk to develop glaucoma by topical medication.¹⁷ The European Glaucoma Prevention Study (EGPS) shows no advantage of dorzolamide against placebo in preventing or delaying the onset of glaucoma.¹⁸ The European Glaucoma Society therefore advises to assess each patient individually when deciding whether or not to treat.¹

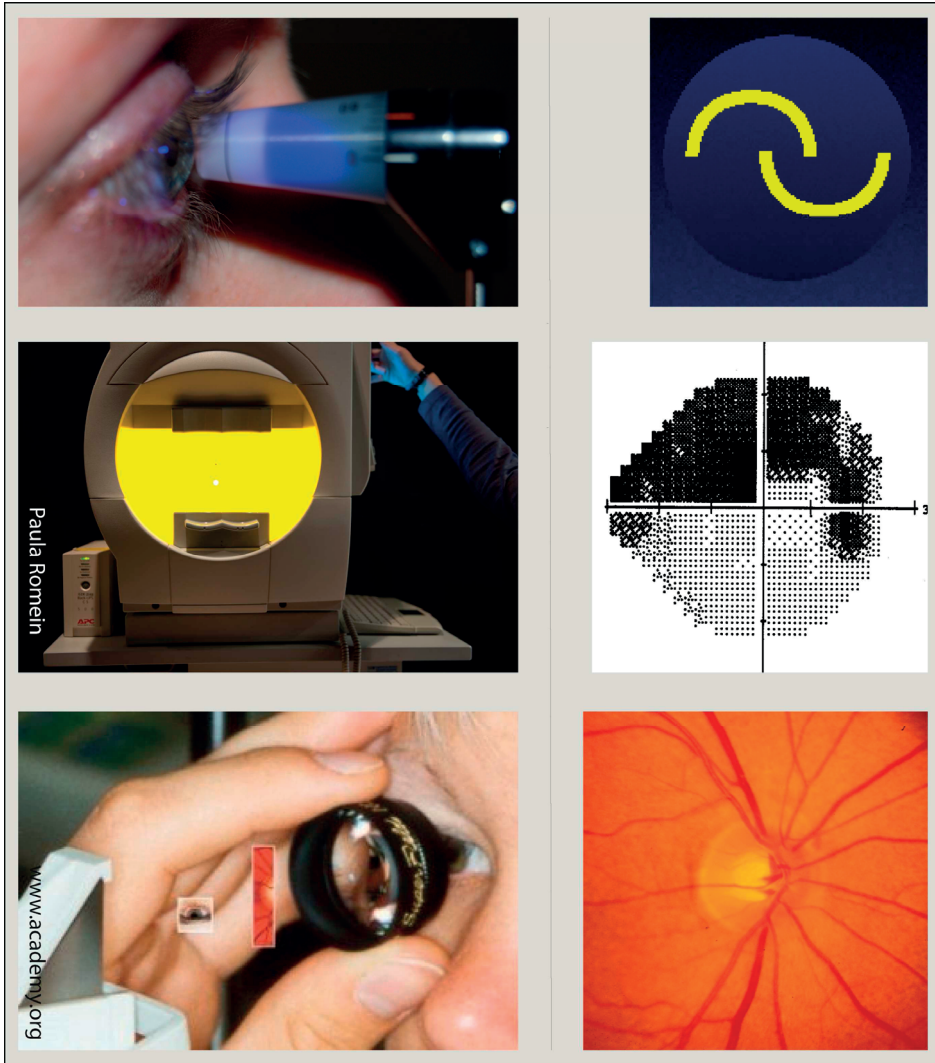


Figure 2 Illustration of the 3 most commonly explored features in daily glaucoma care. The left column shows the measurement techniques of eye pressure, visual field testing and ophthalmoscopy, respectively. The right column shows what the clinician views to assess these clinically relevant features.

Diagnosing Glaucoma in daily care

To date, there is still no technique that measures the exact nature of the disease (the death of the RGCs and their axons). All techniques developed in the past decades indirectly measure the functional or structural loss caused by the lost RGCs and axons. This means that up till now we are facing challenging glaucoma care, searching for a way to diagnose and monitor glaucoma which is most objective, patient friendly, quantitative and qualitative and highly sensitive and specific for glaucoma.

In daily glaucoma care, 3 main parameters are followed to diagnose and monitor glaucoma. Firstly, the IOP is measured. Usually an individual target pressure is determined, which is the maximal IOP that the eye can handle in order not to progress. Secondly, the function of the eyes is determined by measuring the visual field of each. Due to glaucoma, patients lose their visual field, characteristically firstly the mid-peripheral visual field², slowly increasing to the centre of the visual field. This functional loss is measured with (standard automated) perimetry. And thirdly, structural damage is assessed by measuring the optic nerve head (ONH; also referred to as optic disc). With increasing loss of retinal ganglion cells and its axons, the ONH becomes more and more excavated. The typical cupping of the ONH and the subsequent loss of thinning of the retinal nerve fiber layer are structural changes which nowadays are measured by several imaging techniques, such as optical coherence tomography, confocal scanning laser ophthalmoscopy and scanning laser polarimetry.

Because this thesis addresses the diagnosis and monitoring of glaucoma, several techniques for measuring glaucoma and its progression will be presented below further in detail.

Visual Field

Standard Visual Field Testing

The mid-peripheral visual field in glaucoma is tested by perimetry. The Humphrey Field Analyzer (HFA, Carl Zeiss Meditec, CA, USA) is the most commonly used perimeter, both clinically and scientifically. In perimetry, the visual function is assessed by determining the retinal differential light sensitivity (DLS) to white light at various locations in the central retina within 24 or 30 degrees of fixation. The DLS is most commonly assessed in 54 or 76 locations, which are compared with age-corrected normative data and summarized and translated into global indices such as the mean deviation (MD) or the visual field index (VFI). Standard automated perimetry (SAP), which employs a white stimulus on a white background, is the most commonly used visual field test in glaucoma. Glaucomatous visual field abnormalities follow a nerve fiber bundle pattern.¹⁹ Typically glaucomatous visual field defects are paracentral scotomas, arcuate (Bjerrum) scotomas, nasal steps, altitudinal defects, and temporal wedges.^{2,3;19;20} A generalized depression in sensitivity may also be caused by glaucoma, but appears more frequently due to media opacities and miosis.¹⁹ In end-stage glaucoma only a central island of vision (and a temporal remainder) is retained at the visual field.²⁰

In clinical care, visual field testing is often used for monitoring glaucoma. Several progression analysis strategies have been developed, classified into either

event- or trend-based analyses.²¹ In event-based analyses, a change that exceeds the measurement variability may be considered as progression. In trend-based progression analyses, a measurement series are analysed over time and change is defined by a significant rate of progression. Nowadays, the HFA incorporates progression analysis software (Guided Progression Analysis, GPA, HFA-II-i, Software Version 4.2, CZM, Dublin, CA, USA), providing an easy accessible progression analysis in daily glaucoma care.

Despite the typical abnormalities of a glaucomatous visual field as described before and despite many efforts towards standardizing these abnormalities, there are no generally approved and used criteria for glaucomatous visual field defects, nor for glaucomatous progression.²¹⁻²⁴ Perimetry has a number of drawbacks that preclude its use as a criterion for glaucoma. SAP is a subjective measurement, because its outcome largely depends on a patient's response to the stimulus, which varies both during and between tests.²⁵⁻²⁷ Fatigue, inability to understand the instructions and a learning effect affect the reliability of a test, limiting the reproducibility of the test.

Histopathological studies have shown that 25-50% of the RGCs have to be damaged, before visual field defects become apparent.^{3,28;29} This implies that structural damage precedes functional damage, a phenomenon which has been confirmed by several in vivo studies.^{3;30-35}

Other forms of visual field testing

Selective perimetry isolates specific retinal ganglion cell populations. There are three major subtypes of RGCs in the retina: the magnocellular cells, the parvocellular cells and the small bistratified cells. Selective perimetry is thought to identify glaucoma earlier than standard visual field testing. With *short wavelength automated perimetry (SWAP)*, the small bistratified cells are tested by employing a blue stimulus against a yellow background. The blue background saturates the medium- and long-wavelength sensitive cones, whereas the short-wavelength cones are activated by the yellow stimulus. In this setting, only the short-wavelength pathway is tested and up till now is thought to detect glaucomatous defects earlier than testing all pathways at the same time, as happens in SAP.³⁶⁻⁴⁰

Frequency-doubling technique (FDT) targets the magnocellular cells by presenting a stimulus with a high temporal frequency and a low spatial frequency.²⁰ The reason why these techniques show glaucomatous defects earlier than SAP is unknown. In daily glaucoma care, these selective perimetry tests are performed considerably less often than SAP, because of the higher measurement variability, the learning effects and because it is more demanding for the patient.⁴¹⁻⁴³

Optic nerve head assessment by ophthalmoscopy or stereophotography

The optic nerve head (ONH) is the site where structural changes are most visually apparent. Characteristic glaucomatous ONH changes are increased cupping or excavation, notching or thinning of the neuroretinal rim, disc hemorrhages, asymmetry of the amount of optic nerve cupping between the two eyes of the patient and barring of the circumlinear vessels.^{1;3;44} In daily glaucoma care, the clinician subjectively assesses the ONH by direct or indirect ophthalmoscopy, which remains a cornerstone for diagnosing and monitoring glaucoma. However, discriminating between healthy and glaucomatous ONHs has been shown to be difficult for ophthalmologists and even glaucoma specialists.⁴⁵⁻⁵¹



Figure 3 Optic nerve head and retinal nerve fiber layer assessment techniques: stereophotography (A), scanning laser polarimetry (B) and confocal scanning laser ophthalmoscopy (C), respectively.

Imaging techniques

The typical cupping of the ONH and the subsequent loss of thinning of the retinal nerve fiber layer are structural changes which can be measured by several imaging techniques, such as optical coherence tomography (OCT), confocal scanning laser ophthalmoscopy (CSLO) and scanning laser polarimetry (SLP).

Scanning Laser Polarimetry

SLP is a clinical non-invasive, noncontact technique that allows indirectly assessing the thickness of the retinal nerve fiber layer (RNFL). SLP uses the phenomenon of form birefringence, which occurs in tissue that is composed of parallel structures, each of which is of a smaller diameter than the wavelength of light used to image it.³ SLP measures the retardation (phase shift) of a polarised laser light passing through the eye onto the RNFL, of which each microtubule within the individual nerve fibers creates birefringence. The greater the number of microtubules, the greater the retardation of the polarised laser light, indicating the presence of more tissue. There are more tissues in the eye, such as the cornea, the lens and the layer of Henle in the fovea that can exhibit form birefringence.⁵²⁻⁵⁴ Since 1993, SLP

has been commercially available and since then it has evolved through several types of SLP to the currently available GDxVCC⁵⁵ and GDxECC⁵⁶ (GDx, Carl Zeiss Meditec, Dublin, CA, USA). In the currently available SLP devices, the birefringence of other structures than the RNFL is individually compensated (by the so-called variable (VCC) and enhanced (ECC) corneal compensation) per individual eye. These enhancements of the techniques were shown to have an improved ability to discriminate between healthy and glaucomatous eyes.⁵⁷⁻⁵⁹

SLP indirectly measures the thickness of the RNFL around the ONH and presents this in a 20 by 20 degrees colour-coded retardation map. The thickness of the RNFL is summarised in several parameters, which are calculated within a circular band (between 2.4mm and 3.2mm, respectively) around and centred on the ONH. The Nerve Fiber Indicator (NFI) is a support vector machine derived classifier of the entire RNFL thickness, which was trained specifically to discriminate between healthy and glaucomatous eyes. The NFI provides a single number between 0 and 100 representing the overall integrity of the RNFL, related to the likelihood that the polarimetric retinal nerve fiber layer map is abnormal.⁶⁰

Its diagnostic accuracy, reproducibility and its ability to monitor glaucoma has proven SLP to be a solid measure of structure in glaucoma, to be one of the devices most used in daily clinical care to diagnose and monitor glaucoma.^{57;61-63}

Confocal scanning laser ophthalmoscopy

CSLO allows layer-by-layer imaging to measure the topography of the ONH.⁶⁴ This technique is commercially available as the Heidelberg Retina Tomograph (HRT; Heidelberg Engineering GmbH, Dossenheim, Germany). This technique quantifies the area of the optic disc cup and neuroretinal rim, based on the reflectivity of the retinal surface. It measures the intensity of light reflected off the retinal surface at subsequent depths of focus.⁶⁵ The HRT calculates several maps (i.e. a color-coded topography map) and parameters (i.e. the retinal surface height and the neuroretinal rim area). CSLO has been shown to provide reasonable reproducibility⁶⁶ and a fairly good diagnostic accuracy^{67;68} and therefore measurements can be evaluated longitudinally to assess whether the glaucoma is stable or progressing.

Optical coherence tomography

OCT was first described in 1991 by Fujimoto and coworkers.⁶⁹ OCT enables *in vivo* visualisation of the tissue microstructure through a non-invasive, noncontact high resolution imaging technique. OCT generates a cross-sectional and three-dimensional image of the retina by measuring echo time delay of backscattered light. It uses interferometry, a phenomenon in which the time delay from light reflected from inside the tissue is measured by correlating it with light that has

travelled a known reference path. Since its introduction in daily clinical care in 1995, OCT has been increasingly used as a diagnostic tool for several retinal diseases as well as diseases of the ONH. The technique has been further developed from time-domain OCT, in which a reference mirror was mechanically moving, to spectral-domain OCT (SD-OCT), in which a fixed mirror was used and a spectrometer was introduced to decode the spectral signature in light. This development decreased the imaging time and therefore motion artefacts, and increased the axial resolution from 8-10 μm to 5-7 μm .^{70,71} Nowadays, SD-OCT is widely used in daily clinical care for diagnosing and monitoring retinal as well as glaucomatous abnormalities.

For the assessment of glaucoma, the thickness of the RNFL as well as the shape of the ONH can be determined with OCT. Software algorithms have been developed to analyse the images by segmentation of the specific retinal layers. By this, the thickness of the RNFL is calculated at, for instance, a circular band around and centred on the ONH, as is used in SLP as well. Several companies have developed their SD-OCT with their own developed hardware and software, with promising good diagnostic accuracy, but without being interchangeable. Figure 4 shows an example of one of the SD-OCT devices, currently commercially available.

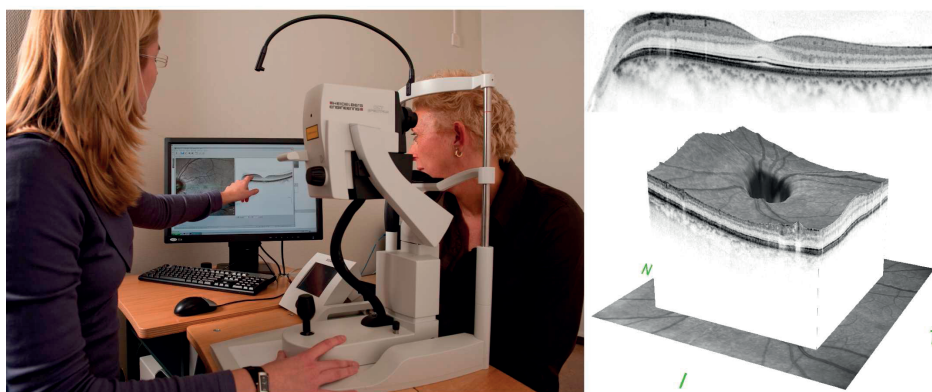


Figure 4 Example of spectral domain optical coherence tomography (OCT). The photograph presents the Spectralis OCT (Heidelberg Engineering, Dossenheim, Germany) and its (cross-sectional) images of the retina, showing the macula (upper image) and the optic nerve head (lower image).

Progression analysis

To monitor glaucoma, up till now, a clinician needed to compare several measurements by hand. Nowadays, progression analysis software has been developed for visual fields and all imaging techniques. Most analyses use both event based and trend based analyses. In event based analyses, a measurement is compared with the baseline measurement(s), assessing whether there has been any statistically

significant change. In trend based analyses, a linear regression model is most often used to detect progression, quantifying the rate of change, informing us about any potential visual disability in the future.¹⁹ Glaucoma develops in several ways, diffusely or focally, slow or fast. Therefore, these several analyses are complementary to each other to discriminate between measurement variability or progression.¹⁹ Figure 5 shows an example of progression analyses by visual field and SLP.

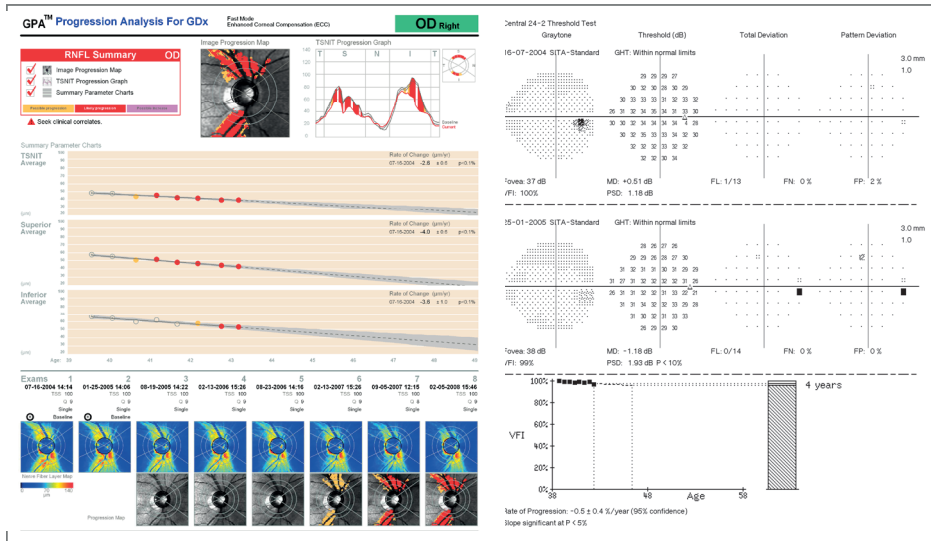


Figure 5 Progression analyses of scanning laser polarimetry (left) and visual field testing (right) of the same patient. SLP shows evident progression by all analyses, presented by the red dots above and red areas below. Visual field testing shows a minor decrease, but significant, in the visual field index (VFI).

OUTLINE OF THESIS

The objective of the research presented in this thesis was to evaluate various techniques used in daily glaucoma practice to diagnose and monitor glaucoma. This has been established by incorporating several analyses on conversion from ocular hypertension to glaucoma, using measures of function and structure. Furthermore, we also analysed (progressing) glaucomatous eyes by the techniques used most frequently in daily practice and by the newest clinically used technique, i.e. optical coherence tomography.

The first 4 chapters of this thesis present several outcomes of a large randomised controlled trial, set up at the Rotterdam Eye Hospital in Rotterdam, the Netherlands. A total of 416 subjects with ocular hypertension (OH) participated in this trial, in which they were randomly allocated to either topical IOP-lowering therapy or placebo eyedrops. Every half-year they were measured with several instruments to monitor the course of the IOP, the appearance of the optic disc and the visual field. In **chapter 2**, the outcome over time of the visual field, measured by Standard Automated Perimetry (SAP) and Short Wavelength Automated Perimetry (SWAP), is presented. The main question that will be explored/answered is which of these two visual field tests detects the conversion to glaucoma firstly.

In **chapter 3**, the use of commercially available progression analyses are incorporated to present the amount of eyes converted from OH to glaucoma. The analyses of SAP are compared to those of Scanning Laser Polarimetry (SLP), measured by the GDx with variable corneal compensation (VCC) and with enhanced corneal compensation (ECC).

Chapter 4 presents the outcome of the large randomised controlled trial into the effect of beta-blockers to prevent or delay the onset of conversion from OH to glaucoma. In this chapter, defining conversion from OH to glaucoma is based on the analyses described in Chapter 3.

In **chapter 5 & 6**, we present data on judging optic discs by various eyecare professionals by assessing stereoscopic ONH photographs in diagnosing (chapter 5) and monitoring (chapter 6) glaucoma. **Chapter 6** presents the outcome of a trial amongst glaucoma specialists of 11 European countries into matching the optic disc to a visual field. In **chapter 5**, progression analyses of glaucomatous eyes are presented, comparing the outcome of analyses of the visual field and the appearance of the optic disc, as it is monitored in daily glaucoma care.

Chapter 7 & 8 both describe new approaches to the use of optical coherence tomography (OCT). In **chapter 7**, a newly described phenomenon is presented. A temporary change in the appearance of the retinal nerve fiber layer (RNFL) in OCT is described in 7 glaucomatous eyes. In **chapter 8**, a different approach into

measuring glaucoma with OCT is presented, introducing a new parameter, the attenuation coefficient.

Finally, **chapter 9** presents a general discussion of the described research in diagnosing and monitoring glaucoma, as well as future perspectives on this matter.



REFERENCE LIST

1. European Glaucoma Society. Terminology and Guidelines for Glaucoma. 4th ed. Savona, Italy: 2014.
2. Quigley HA. Glaucoma. *Lancet* 2011;377:1367-77.
3. Weinreb RN, Khaw PT. Primary open-angle glaucoma. *Lancet* 2004;363:1711-20.
4. Jonas JB, Budde WM, Panda-Jonas S. Ophthalmoscopic evaluation of the optic nerve head. *Surv Ophthalmol* 1999;43:293-320.
5. Resnikoff S, Pascolini D, Etya'ale D, et al. Global data on visual impairment in the year 2002. *Bull World Health Organ* 2004;82:844-51.
6. Quigley HA, Broman AT. The number of people with glaucoma worldwide in 2010 and 2020. *Br J Ophthalmol* 2006;90:262-7.
7. Anton A, Andrada MT, Mujica V, et al. Prevalence of primary open-angle glaucoma in a Spanish population: the Segovia study. *J Glaucoma* 2004;13:371-6.
8. Coffey M, Reidy A, Wormald R, et al. Prevalence of glaucoma in the west of Ireland. *Br J Ophthalmol* 1993;77:17-21.
9. Dielemans I, Vingerling JR, Wolfs RC, et al. The prevalence of primary open-angle glaucoma in a population-based study in The Netherlands. The Rotterdam Study. *Ophthalmology* 1994;101:1851-5.
10. Wolfs RC, Borger PH, Ramrattan RS, et al. Changing views on open-angle glaucoma: definitions and prevalences--The Rotterdam Study. *Invest Ophthalmol Vis Sci* 2000;41:3309-21.
11. Boland MV, Quigley HA. Risk factors and open-angle glaucoma: classification and application. *J Glaucoma* 2007;16:406-18.
12. Dreyer EB, Lipton SA. New perspectives on glaucoma. *JAMA* 1999;281:306-8.
13. The Advanced Glaucoma Intervention Study (AGIS): 4. Comparison of treatment outcomes within race. Seven-year results. *Ophthalmology* 1998;105:1146-64.
14. Heijl A, Leske MC, Bengtsson B, et al. Reduction of intraocular pressure and glaucoma progression: results from the Early Manifest Glaucoma Trial. *Arch Ophthalmol* 2002;120:1268-79.
15. Klein BE, Klein R, Linton KL. Intraocular pressure in an American community. The Beaver Dam Eye Study. *Invest Ophthalmol Vis Sci* 1992;33:2224-8.
16. Gordon MO, Beiser JA, Brandt JD, et al. The Ocular Hypertension Treatment Study: baseline factors that predict the onset of primary open-angle glaucoma. *Arch Ophthalmol* 2002;120:714-20.
17. Kass MA, Heuer DK, Higginbotham EJ, et al. The Ocular Hypertension Treatment Study: a randomized trial determines that topical ocular hypotensive medication delays or prevents the onset of primary open-angle glaucoma. *Arch Ophthalmol* 2002;120:701-13.
18. Miglior S, Zeyen T, Pfeiffer N, et al. Results of the European Glaucoma Prevention Study. *Ophthalmology* 2005;112:366-75.
19. Heijl A, Patella VM, Bengtsson B. The Field Analyzer Primer: Effective Perimetry. 2012.
20. American Academy of Ophthalmology. BCSC Section 10: Glaucoma. Vol. 2014-2015. San Francisco, CA, USA: 2014.
21. Nouri-Mahdavi K, Nassiri N, Giangiacomo A, Caprioli J. Detection of visual field progression in glaucoma with standard achromatic perimetry: a review and practical implications. *Graefes Arch Clin Exp Ophthalmol* 2011;249:1593-616.

22. Johnson CA, Sample PA, Cioffi GA, et al. Structure and function evaluation (SAFE): I. criteria for glaucomatous visual field loss using standard automated perimetry (SAP) and short wavelength automated perimetry (SWAP). *Am J Ophthalmol* 2002;134:177-85.
23. Spry PG, Johnson CA. Identification of progressive glaucomatous visual field loss. *Surv Ophthalmol* 2002;47:158-73.
24. Tuulonen A, Airaksinen PJ, Erola E, et al. The Finnish evidence-based guideline for open-angle glaucoma. *Acta Ophthalmol Scand* 2003;81:3-18.
25. Heijl A, Lindgren G, Olsson J. Normal variability of static perimetric threshold values across the central visual field. *Arch Ophthalmol* 1987;105:1544-9.
26. Heijl A, Lindgren A, Lindgren G. Test-retest variability in glaucomatous visual fields. *Am J Ophthalmol* 1989;108:130-5.
27. Keltner JL, Johnson CA, Quigg JM, et al. Confirmation of visual field abnormalities in the Ocular Hypertension Treatment Study. Ocular Hypertension Treatment Study Group. *Arch Ophthalmol* 2000;118:1187-94.
28. Kerrigan-Baumrind LA, Quigley HA, Pease ME, et al. Number of ganglion cells in glaucoma eyes compared with threshold visual field tests in the same persons. *Invest Ophthalmol Vis Sci* 2000;41:741-8.
29. Quigley HA, Dunkelberger GR, Green WR. Retinal ganglion cell atrophy correlated with automated perimetry in human eyes with glaucoma. *Am J Ophthalmol* 1989;107:453-64.
30. Airaksinen PJ, Drance SM, Douglas GR, et al. Visual field and retinal nerve fiber layer comparisons in glaucoma. *Arch Ophthalmol* 1985;103:205-7.
31. Johnson CA, Sample PA, Zangwill LM, et al. Structure and function evaluation (SAFE): II. Comparison of optic disk and visual field characteristics. *Am J Ophthalmol* 2003;135:148-54.
32. Reus NJ, Lemij HG. Scanning laser polarimetry of the retinal nerve fiber layer in perimetrically unaffected eyes of glaucoma patients. *Ophthalmology* 2004;111:2199-203.
33. Sommer A, Katz J, Quigley HA, et al. Clinically detectable nerve fiber atrophy precedes the onset of glaucomatous field loss. *Arch Ophthalmol* 1991;109:77-83.
34. Tuulonen A, Airaksinen PJ. Initial glaucomatous optic disk and retinal nerve fiber layer abnormalities and their progression. *Am J Ophthalmol* 1991;111:485-90.
35. Zeyen TG, Caprioli J. Progression of disc and field damage in early glaucoma. *Arch Ophthalmol* 1993;111:62-5.
36. Demirel S, Johnson CA. Incidence and prevalence of short wavelength automated perimetry deficits in ocular hypertensive patients. *Am J Ophthalmol* 2001;131:709-15.
37. Johnson CA, Adams AJ, Casson EJ, Brandt JD. Blue-on-yellow perimetry can predict the development of glaucomatous visual field loss. *Arch Ophthalmol* 1993;111:645-50.
38. Johnson CA, Adams AJ, Casson EJ, Brandt JD. Progression of early glaucomatous visual field loss as detected by blue-on-yellow and standard white-on-white automated perimetry. *Arch Ophthalmol* 1993;111:651-6.
39. Polo V, Larrosa JM, Pinilla I, et al. Predictive value of short-wavelength automated perimetry: a 3-year follow-up study. *Ophthalmology* 2002;109:761-5.
40. Sample PA, Taylor JD, Martinez GA, et al. Short-wavelength color visual fields in glaucoma suspects at risk. *Am J Ophthalmol* 1993;115:225-33.
41. Blumenthal EZ, Sample PA, Zangwill L, et al. Comparison of long-term variability for standard and short-wavelength automated perimetry in stable glaucoma patients. *Am J Ophthalmol* 2000;129:309-13.

42. Heeg GP, Ponsioen TL, Jansonius NM. Learning effect, normal range, and test-retest variability of Frequency Doubling Perimetry as a function of age, perimetric experience, and the presence or absence of glaucoma. *Ophthalmic Physiol Opt* 2003;23:535-40.
43. Iester M, Capris P, Pandolfo A, et al. Learning effect, short-term fluctuation, and long-term fluctuation in frequency doubling technique. *Am J Ophthalmol* 2000;130:160-4.
44. Coleman AL. Glaucoma. *Lancet* 1999;354:1803-10.
45. Abrams LS, Scott IU, Spaeth GL, et al. Agreement among optometrists, ophthalmologists, and residents in evaluating the optic disc for glaucoma. *Ophthalmology* 1994;101:1662-7.
46. Andersson S, Heijl A, Bengtsson B. Optic disc classification by the Heidelberg Retina Tomograph and by physicians with varying experience of glaucoma. *Eye (Lond)* 2011;25:1401-7.
47. Girkin CA, McGwin G, Jr., Long C, et al. Subjective and objective optic nerve assessment in African Americans and whites. *Invest Ophthalmol Vis Sci* 2004;45:2272-8.
48. Reus NJ, de GM, Lemij HG. Accuracy of GDx VCC, HRT I, and clinical assessment of stereoscopic optic nerve head photographs for diagnosing glaucoma. *Br J Ophthalmol* 2007;91:313-8.
49. Reus NJ, Lemij HG, Garway-Heath DF, et al. Clinical assessment of stereoscopic optic disc photographs for glaucoma: the European Optic Disc Assessment Trial. *Ophthalmology* 2010;117:717-23.
50. Varma R, Steinmann WC, Scott IU. Expert agreement in evaluating the optic disc for glaucoma. *Ophthalmology* 1992;99:215-21.
51. Wollstein G, Garway-Heath DF, Fontana L, Hitchings RA. Identifying early glaucomatous changes. Comparison between expert clinical assessment of optic disc photographs and confocal scanning ophthalmoscopy. *Ophthalmology* 2000;107:2272-7.
52. Brink HB, van Blokland GJ. Birefringence of the human foveal area assessed in vivo with Mueller-matrix ellipsometry. *J Opt Soc Am A* 1988;5:49-57.
53. Brink HB. Birefringence of the human crystalline lens in vivo. *J Opt Soc Am A* 1991;8:1788-93.
54. van Blokland GJ, Verhelst SC. Corneal polarization in the living human eye explained with a biaxial model. *J Opt Soc Am A* 1987;4:82-90.
55. Zhou Q, Weinreb RN. Individualized compensation of anterior segment birefringence during scanning laser polarimetry. *Invest Ophthalmol Vis Sci* 2002;43:2221-8.
56. Reus NJ, Zhou Q, Lemij HG. Enhanced imaging algorithm for scanning laser polarimetry with variable corneal compensation. *Invest Ophthalmol Vis Sci* 2006;47:3870-7.
57. Mai TA, Reus NJ, Lemij HG. Diagnostic accuracy of scanning laser polarimetry with enhanced versus variable corneal compensation. *Ophthalmology* 2007;114:1988-93.
58. Tannenbaum DP, Hoffman D, Lemij HG, et al. Variable corneal compensation improves discrimination between normal and glaucomatous eyes with the scanning laser polarimeter. *Ophthalmology* 2004;111:259-64.
59. Weinreb RN, Bowd C, Zangwill LM. Glaucoma detection using scanning laser polarimetry with variable corneal polarization compensation. *Arch Ophthalmol* 2003;121:218-24.
60. Carl Zeiss Meditec. GDxPRO User Manual. 2009.
61. Medeiros FA, Zangwill LM, Bowd C, Weinreb RN. Comparison of the GDx VCC scanning laser polarimeter, HRT II confocal scanning laser ophthalmoscope, and stratus OCT optical coherence tomograph for the detection of glaucoma. *Arch Ophthalmol* 2004;122:827-37.

62. Medeiros FA, Zangwill LM, Bowd C, et al. Use of progressive glaucomatous optic disk change as the reference standard for evaluation of diagnostic tests in glaucoma. *Am J Ophthalmol* 2005;139:1010-8.
63. Reus NJ, Lemij HG. Diagnostic accuracy of the GDx VCC for glaucoma. *Ophthalmology* 2004;111:1860-5.
64. Weinreb RN. Assessment of optic disc topography for diagnosing and monitoring glaucoma. *Arch Ophthalmol* 1998;116:1229-31.
65. Weinreb RN, Dreher AW, Bille JF. Quantitative assessment of the optic nerve head with the laser tomographic scanner. *Int Ophthalmol* 1989;13:25-9.
66. Greenfield DS. Optic nerve and retinal nerve fiber layer analyzers in glaucoma. *Curr Opin Ophthalmol* 2002;13:68-76.
67. Ford BA, Artes PH, McCormick TA, et al. Comparison of data analysis tools for detection of glaucoma with the Heidelberg Retina Tomograph. *Ophthalmology* 2003;110:1145-50.
68. Reus NJ, de GM, Lemij HG. Accuracy of GDx VCC, HRT I, and clinical assessment of stereoscopic optic nerve head photographs for diagnosing glaucoma. *Br J Ophthalmol* 2007;91:313-8.
69. Huang D, Swanson EA, Lin CP, et al. Optical coherence tomography. *Science* 1991;254:1178-81.
70. Nassif N, Cense B, Park B, et al. In vivo high-resolution video-rate spectral-domain optical coherence tomography of the human retina and optic nerve. *Opt Express* 2004;12:367-76.
71. Wojtkowski M, Bajraszewski T, Gorczynska I, et al. Ophthalmic imaging by spectral optical coherence tomography. *Am J Ophthalmol* 2004;138:412-9.

2

Short wavelength automated perimetry is a poor predictor of conversion to glaucoma

Josine van der Schoot, Nicolaas J. Reus,
Thomas P. Colen, Hans G. Lemij

Ophthalmology, 2010;117(1):30-4.

ABSTRACT

Purpose. Short wavelength automated perimetry (SWAP) has been claimed to predict conversion to glaucoma 3-4 years before standard automated perimetry (SAP) defects occur. Our purpose was to compare the moment of glaucomatous conversion between SWAP and SAP.

Design. Prospective, longitudinal follow-up study.

Participants. Four hundred and sixteen subjects with ocular hypertension (intra-ocular pressure ≥ 22 and ≤ 32 mmHg and normal visual fields).

Methods. A Humphrey Field Analyser (24-2 program) was used to perform both SWAP and SAP. All participants were tested once every half year during seven to ten years or until the onset of conversion (study endpoint). The conversion to glaucoma was defined as a reproducible glaucomatous visual field defect in SAP.

Main outcome measures. The moment of onset of a reproducible defect in SAP was compared to that in SWAP.

Results. Of the 416 initial participants, 24 eyes of 21 subjects showed conversion in SAP. Of these eyes, 22 did not show earlier conversion in SWAP than in SAP. SAP even showed earlier conversion than SWAP in 15 cases. In only 2 eyes did SWAP show earlier conversion by up to 18 months.

Conclusions. Our results do not support the notion that SWAP generally predicts conversion to glaucoma in SAP. Instead, SAP appears to be at least as sensitive to conversion as SWAP in a large majority of eyes.

INTRODUCTION

Glaucoma is one of the main causes of blindness.^{1,2} Ocular hypertension (OH) has been recognized as an important risk factor in the development of primary open angle glaucoma (POAG).³ Conversion to or progression of POAG can be slowed by reducing the increased intraocular pressure.⁴⁻⁶ Follow-up of subjects with OH and POAG is usually done by a combination of tests, including standard automated perimetry (SAP), which is the current clinical standard of measuring glaucomatous functional loss. To measure early glaucomatous loss, it has been suggested that short-wavelength automated perimetry (SWAP) is more sensitive than SAP.⁷⁻¹¹

In 1993, Sample et al.¹¹ presented a small group of conversions to glaucoma, which showed substantially more prominent glaucomatous defects on SWAP than on SAP. In addition, Johnson et al.⁸ demonstrated that SWAP may predict conversion to glaucoma 3-4 years earlier than SAP, which was confirmed by other studies.^{7,10} It is unclear why SWAP shows these early glaucomatous defects prior to SAP. Because the incidence-rates of glaucomatous defects in both SAP and SWAP appear to be the same, Demirel and Johnson⁷ proposed that they monitor the same underlying disease.

Despite these reported advantages of SWAP over SAP, SWAP is relatively time-consuming, and more demanding to the subject taking it. There also is an increased variability within¹² and between¹³ subjects, as well as greater long-term fluctuations¹⁴ compared with SAP. Hutchings et al.¹⁴ therefore concluded that more sophisticated statistical procedures needed to be developed before SWAP could be used in routine follow-up. With the recently developed SITA SWAP, its manufacturer has stated that the inter-test variability has been greatly reduced, compared to the SWAP Full Threshold strategy.¹⁵ In a cross-sectional study, Bengtsson et al.¹⁶ recently found an equal diagnostic sensitivity of SAP and SWAP in early glaucoma, using three strategies (Full Threshold SWAP, SITA SWAP and SITA Fast SAP). A limitation of their study, however, was that none of the abnormal fields was confirmed by repeated testing, so it is unclear to what extent their data contained false positive fields in any of the three test strategies.

Taken together, it is unclear what the clinical role of SWAP is in the early detection of glaucomatous conversion in OH. Therefore, we have currently compared the moment of glaucomatous conversion between SWAP and SAP in a long-term follow-up study of OH.

METHODS

2

Participants

Four hundred and sixteen (416) subjects with an elevated intra-ocular pressure (IOP), recruited consecutively between November 1997 and March 2001, were tested with both SAP and SWAP. They were tested once every 6 months during seven to ten years or until the onset of conversion (study endpoint). At study entry, all participants had an IOP ≥ 22 mmHg and ≤ 32 mmHg by Goldmann applanation tonometry in both eyes and normal visual fields with SAP on at least two separate occasions. The SAP fields were undertaken either prior to the study in standard clinical care, or else within the study, in which case the participants had to undergo 2 SAP fields within one month. The second SAP was used as baseline measurement for further analysis. All visual fields were undertaken by trained, experienced technicians. A normal visual field by SAP was defined as a glaucoma hemifield test of 'Within normal limits' and no abnormalities in the total and/or pattern deviation probability plots. During inclusion, all participants were labelled as high or low risk for converting to glaucoma. To that end, we took images with the GDx-Nerve Fiber Analyzer (GDx-NFA) (Laser Diagnostic Technologies, Dublin, CA, USA) of each eye and compared it to our own normative database. If an individual's data fell below the 2nd percentile, he/she was considered as high risk, otherwise as low risk. None of the participants were stratified for other variables, including central corneal thickness and intraocular pressure. All included participants were of white ethnic origin, had a best corrected Snellen visual acuity of at least 20/40 in both eyes, and had an unremarkable slit lamp examination, including open angles on gonioscopy. The appearance of the optic disc was not a selection criterion. Subjects were excluded from participation in the presence of any significant coexisting ocular or systemic diseases known to possibly affect the visual field (e.g. diabetes mellitus), a family history of glaucoma, a history of intraocular surgery (except for uncomplicated cataract surgery), uncontrollable arterial hypertension, or any previous use of IOP-lowering agents within 3 months before the measurements.

Participants took part in a double masked placebo-controlled study on the effect of beta-blockers on the development of glaucomatous retinal nerve fiber layer defects and visual field loss in elevated IOP. In this 3-arm study, participants were randomly allocated to either Betaxolol, Timolol (Alcon Laboratories, Inc., Fort Worth, TX, USA) or placebo eyedrops. In the same session as the perimetric testing mentioned in this report, participants were tested every 6 months by several imaging techniques, including scanning laser polarimetry (GDx, Carl Zeiss Meditec, Inc., Dublin, CA, USA), scanning laser tomography (Heidelberg Retina Tomograph (HRT), Heidelberg Engineering GmbH, Dossenheim, Germany) and simultaneous

stereoscopic photos of the optic disc. The results of these structural measurements are beyond the scope of the current paper.

The methods and procedures used in this study adhered to the Declaration of Helsinki. Informed consent was obtained from all participants. This study was approved by the Medical Ethics Committee of the Erasmus Medical Centre, Rotterdam, The Netherlands.

Test strategies

SAP and SWAP were measured with the Humphrey Field Analyzer II [HFA] (Carl Zeiss Meditec, Dublin, CA, USA) by means of the 24-2 Full Threshold test paradigm. To save test-time, we decided to use SITA Standard in SAP instead of the Full Threshold strategy, as soon as SITA Standard became available. Whenever defects appeared upon SITA Standard testing, the visual field test was repeated with the Full Threshold strategy to confirm any abnormal fields. In SAP, we used a Goldmann size III white stimulus on a white background, and in SWAP a Goldmann size V blue stimulus on a yellow background. All participants were allowed to adapt to the background light for at least 5 minutes before testing. Each participant was given the same instructions for the examination, regardless of their perimetric experience, in order to minimize the effects of operator bias. The order of measurements was, per protocol, SAP OD, SAP OS, followed by SWAP OD and SWAP OS. Resting periods of 2 to 3 minutes were given prior to each examination and at 5 to 7 minutes intervals during the examination of each eye. An appropriate refractive correction was used for the viewing distance of the perimeter and the participants' age. Visual field tests for SWAP were not corrected for any possible lens transmission losses. All visual fields done by the Full Threshold strategy that were used for analysis satisfied the following reliability criteria: fixation losses $\leq 20\%$ and false-positive and false-negative responses $\leq 33\%$. In case of the use of the SITA Standard strategy, all visual fields satisfied the following, arbitrary, reliability criteria: fixation losses $\leq 10\%$, and false-positive and false-negative responses $\leq 6\%$. None of the visual fields showed a 'Generalized depression of sensitivity' on the Glaucoma Hemifield Test (GHT). Whether a test was classified as abnormal, depended on the number and probability level of abnormal points on either the total or pattern deviation plots, whichever showed the fewest abnormal points. All abnormalities had to be confirmed on a subsequent test within one year, to be classified as abnormal. Conversion to glaucoma was defined as a reproducible defect in SAP of either 1 individual point below the 0.5% probability-level, or 2 clustered points below the 1% probability-level, or 3 clustered points below the 2% probability-level, or 4 clustered points below the 5% probability-level on either the

total deviation or the pattern deviation probability plot. We used the same criteria for conversion in SWAP.

Analysis

The values of the total and pattern deviation probability plot and the GHT were derived from the standard HFA STATPAC print-out. The definitions were analysed with custom-made algorithms in Microsoft Access 2000 (Microsoft Corporation, Redmond, WA, USA).

RESULTS

Of the 416 included participants, 21 showed conversion in SAP, of whom 3 showed conversion in both eyes. The mean follow-up time of all participants was 7.1 [SD 3.4] years. Of the 21 converting participants, the mean age (at the moment of conversion) was 65.5 [SD 9.4] years. Eleven of the 21 participants (52.4%) were men. The mean age of the men was 61.6 [SD 10.9] years and 69.0 [SD 6.6] years in the women. Seven of the 24 eyes were right ones. The mean IOP in the converted eyes was 29.3 mmHg [SD 3.0]. Of the 416 included participants, 64 (15.4%) were labelled as high risk for converting to glaucoma. Of the 21 converting participants, 7 (33.3%) had been labelled as high risk.

Of the 24 eyes that converted in SAP, 22 (92%) failed to show earlier conversion in SWAP. In fact, SAP showed earlier conversion than SWAP in 15 of these 22 eyes (63%). Of the entire group, only 2 eyes (8%) showed earlier SWAP conversion than SAP conversion by up to 18 months. SAP and SWAP showed defects at the same time in 3 cases (13%). In 4 other cases (17%), when SAP showed the first defects, SWAP data turned out to be unavailable at that specific moment, which indicates either earlier SAP conversion or simultaneous conversion in the two tests. In 8 of the 832 eyes (416 participants), SWAP showed reproducible defects before completion of the study. In 6 of these 8 eyes (8 participants), SAP remained normal throughout the study. The other 2 eyes converted on SAP within the follow-up time.

The results of one participant have been presented in the figure, showing the absence of SWAP-defects prior to those in SAP, representing at least 63% of all conversions in this study.

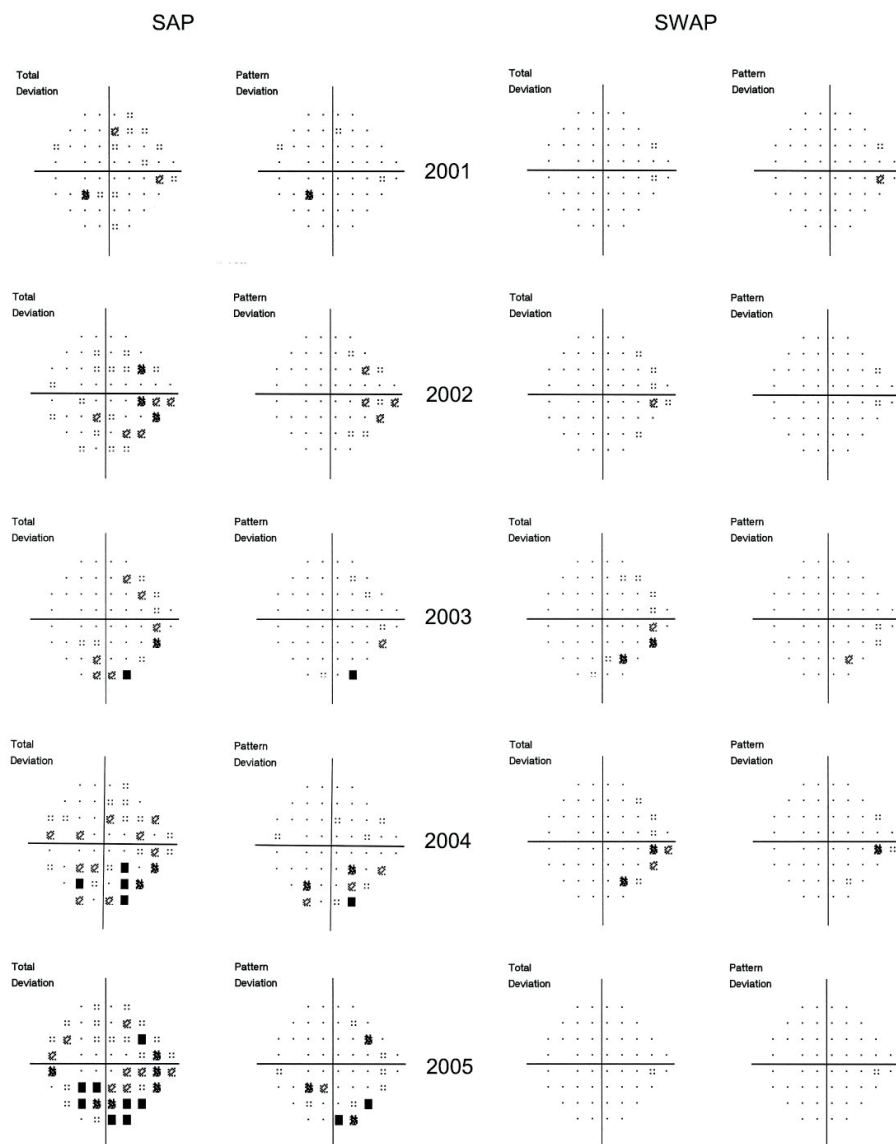


Figure Probability plots of visual fields in SAP and SWAP of a participant, presented for 5 consecutive years. Note the appearance of visual field defects in SAP prior to SWAP, representing 63% of the conversions in the present study. The second visual field of 2002 is missing. All visual fields were performed with the Full Threshold strategy. The visual fields of the fellow eye did not show any signs of conversion. The participant underwent cataract surgery prior to the last 3 visual fields. Abbreviations: SAP: standard automated perimetry; SWAP: short-wavelength automated perimetry

DISCUSSION

2

SWAP is a poor predictor of conversion to glaucoma

During long-term prospective follow-up of our large group of OH subjects (>800 eyes), the large majority of converting eyes did not show earlier reproducible perimetric conversion in SWAP than in SAP. In fact, conversion occurred more often in SAP before it occurred in SWAP. In a small minority of converted eyes did SWAP defects occur prior to those in SAP, which contrasts markedly with other studies that suggested that SWAP defects typically precede the onset of glaucomatous SAP defects.^{7;8;10;11} All these studies used different methods of SWAP, varying in, amongst others, equipment and normative database. Different study-outcomes might therefore be expected. Some methodological differences will now be discussed in greater detail.

The criteria used for a glaucomatous visual field defect in SWAP varied across studies. Reus et al.¹⁷ showed that the prevalence of abnormal SWAP defects strongly depends on the applied criteria and that it is unclear which criteria are clinically most significant. For simplicity, we have currently applied the same criteria for conversion in SWAP as in SAP, as was done in other studies.^{7;10;11} Another criterion we applied, was the reproducibility of any defects in both SAP and SWAP. Johnson et al.⁸ did not specify whether visual field defects were reproducible. Therefore, their results may in principle have contained a relatively high false positive rate. However, it has been shown that the reproducibility of early visual field defects is higher in SWAP than in SAP.⁷ Therefore, it remains unclear why Johnson et al.⁸ found such a high incidence in abnormal SWAP visual fields compared to our study.

One limitation of our study may be that, several years into the study, we changed from the Full Threshold strategy to SITA Standard in SAP, in order to save test-time. We think this change will not have significantly altered our results, because both tests have been shown to yield similar outcomes.^{18;19} Importantly, we repeated the Full Threshold strategy to confirm any abnormal SITA Standard fields.

The number of subjects with OH that converted to glaucoma in our study was perhaps smaller (5.8% in 7 to 10 years) than expected. However, this rate is somewhat comparable to the one in the OHTS trial.⁴ The OHTS trial resulted in a conversion-rate of 4.4% in the group that was treated with hypotensive medication, and 10.9% in the untreated group in 5 years.⁴ The majority of our participants was treated topically with either Betaxolol or Timolol and the rest took placebo eye drops. The use of these beta-blockers might have been protective in our patients. In addition, we only used perimetric conversion as a criterion, whereas in the OHTS trial, disc changes were also classified as conversion. It is therefore likely that we would have had a higher conversion rate if we had included disc changes as conversion.

We did not determine our own normative database for SWAP, as was done in previous studies.^{7;8;10;11} Since we used the built-in normative database, systematic differences between the normative database and our study group might have occurred, potentially yielding an underestimated number of abnormal SWAP fields in our study. On the other hand, we think that most clinicians would only consider using SWAP on a regular basis for earlier glaucoma detection, if they could rely on the built-in normative database. Our current study shows that SWAP would then probably not be useful for early conversion detection.

A potential limitation of our present study is that we did not correct for possible losses of lens transmission, as was done before.^{7;8;10;11} Losses in lens transmission due to cataract cause a generalized depression of sensitivity in SWAP, but also in SAP.²⁰ Arguably, any localized SWAP defects would have been deepened by cataract, notably in the total deviation plot, thereby probably artifactually selectively increasing the SWAP conversion rate in our study more so than in SAP. Because this conversion rate was so low compared to that in SAP, we think that correcting for lens opacities would not have supported further use of SWAP for early detection of glaucomatous visual field defects. If clinicians were required to always correct their SWAP data for lens opacities, instead of using the built-in normative database as a straight-forward reference, we think that the role of SWAP for early detection of glaucoma would, again, be *a priori* very limited. The development of the SITA SWAP strategy may have improved the applicability of SWAP, for the renewed normative database allegedly corrects for cataractous changes.¹⁵ We think this should be further explored, because Sample et al. showed that the sensitivity and specificity for detecting glaucomatous visual field loss was virtually unaffected by correcting for losses of lens transmission.²⁰ Our current study was initiated many years before SITA SWAP was released. We were therefore unable to test the newer version with its newly developed normative database. If our conclusions were largely due to the SWAP normative database that we used, the SITA SWAP strategy with its renewed normative database, might still be of use for earlier detection. This needs to be explored in future studies. However, since Bengtsson et al.¹⁶ found no significant difference in diagnostic sensitivity for early glaucoma detection between SITA SWAP and Full Threshold SWAP, we do not expect any substantial improvement in detecting early conversion of SITA SWAP over Full Threshold SWAP.

Although the design of the study by Johnson et al.⁸ was comparable to ours, we had completely different outcomes. A possible explanation of this could be that the outcome in Johnson's study⁸ (SWAP showing defects prior to SAP) is most likely attributable to chance selection of subjects that had developed a selective damage of specific subsystems. Perhaps such selective damage only occurs in a small subset of patients with OH. We therefore think that early glaucomatous dam-

age is idiosyncratic, and may become first apparent in one of different pathways, sometimes appearing first in SWAP and sometimes first in SAP. Others have shown that, with prolonged testing, the incidence-rates of visual field defects turn out to be similar for SWAP and SAP, suggesting that both tests detect the same disease (glaucoma).⁷ No single test could then become the gold standard in detecting early glaucoma. Despite its limitations, SAP has become a standard in clinical care across the world. SWAP, however, has never gained such widespread acceptance, for various reasons, some of which have been discussed earlier. It is possible that SITA SWAP will turn out to be useful for early detection of glaucomatous conversion. To date, there is insufficient evidence for that. We therefore recommend clinicians to use SAP rather than SWAP in their daily practices to detect early glaucomatous conversion in ocular hypertension.

Although early SWAP visual field defects have been suggested to typically precede those in SAP in conversion from OH to POAG, our prospective, longitudinal follow-up study does not support this suggestion. On the contrary, SAP appears to be at least as sensitive to conversion as SWAP in a large majority of eyes.



REFERENCES

1. Quigley HA, Broman AT. The number of people with glaucoma worldwide in 2010 and 2020. *Br J Ophthalmol* 2006;90:262-7.
2. Resnikoff S, Pascolini D, Etya'ale D. Global data on visual impairment in the year 2002. *Bull World Health Organ* 2004;82:844-51.
3. Leske MC, Connell AM, Wu SY, et al. Risk factors for open-angle glaucoma. The Barbados Eye Study. *Arch Ophthalmol* 1995;113:918-24.
4. Kass MA, Heuer DK, Higginbotham EJ, et al. The Ocular Hypertension Treatment Study: a randomized trial determines that topical ocular hypotensive medication delays or prevents the onset of primary open-angle glaucoma. *Arch Ophthalmol* 2002;120:701-13.
5. Miglior S, Zeyen T, Pfeiffer N, et al. Results of the European Glaucoma Prevention Study. *Ophthalmology* 2005;112:366-75.
6. Leske MC, Heijl A, Hussein M, et al. Factors for glaucoma progression and the effect of treatment: the early manifest glaucoma trial. *Arch Ophthalmol* 2003;121:48-56.
7. Demirel S, Johnson CA. Incidence and prevalence of short wavelength automated perimetry deficits in ocular hypertensive patients. *Am J Ophthalmol* 2001;131:709-15.
8. Johnson CA, Adams AJ, Casson EJ, Brandt JD. Blue-on-yellow perimetry can predict the development of glaucomatous visual field loss. *Arch Ophthalmol* 1993;111:645-50.
9. Johnson CA, Adams AJ, Casson EJ, Brandt JD. Progression of early glaucomatous visual field loss as detected by blue-on-yellow and standard white-on-white automated perimetry. *Arch Ophthalmol* 1993;111:651-6.
10. Polo V, Larrosa JM, Pinilla I, et al. Predictive value of short-wavelength automated perimetry: a 3-year follow-up study. *Ophthalmology* 2002;109:761-5.
11. Sample PA, Taylor JD, Martinez GA, et al. Short-wavelength color visual fields in glaucoma suspects at risk. *Am J Ophthalmol* 1993;115:225-33.
12. Blumenthal EZ, Sample PA, Berry CC, et al. Evaluating several sources of variability for standard and SWAP visual fields in glaucoma patients, suspects, and normals. *Ophthalmology* 2003;110:1895-902.
13. Wild JM, Moss ID, Whitaker D, O'Neill EC. The statistical interpretation of blue-on-yellow visual field loss. *Invest Ophthalmol Vis Sci* 1995;36:1398-410.
14. Hutchings N, Hosking SL, Wild JM, Flanagan JG. Long-term fluctuation in short-wavelength automated perimetry in glaucoma suspects and glaucoma patients. *Invest Ophthalmol Vis Sci* 2001;42:2332-7.
15. Carl Zeiss Meditec. SITA SWAP, Clinical Solutions; Available at: www.meditec.zeiss.com. December 29, 2008. Ref Type: Internet Communication
16. Bengtsson B, Heijl A. Diagnostic sensitivity of fast blue-yellow and standard automated perimetry in early glaucoma: a comparison between different test programs. *Ophthalmology* 2006;113:1092-7.
17. Reus NJ, Colen TP, Lemij HG. The prevalence of glaucomatous defects with short-wavelength automated perimetry in patients with elevated intraocular pressures. *J Glaucoma* 2005;14:26-9.
18. Heijl A, Bengtsson B, Patella VM. Glaucoma follow-up when converting from long to short perimetric threshold tests. *Arch Ophthalmol* 2000;118:489-93.

19. Sekhar GC, Naduvilath TJ, Lakkai M, et al. Sensitivity of Swedish interactive threshold algorithm compared with standard full threshold algorithm in Humphrey visual field testing. *Ophthalmology* 2000;107:1303-8.
20. Sample PA, Martinez GA, Weinreb RN. Short-wavelength automated perimetry without lens density testing. *Am J Ophthalmol* 1994;118:632-41.

3

Converting from ocular
hypertension to glaucoma:
Scanning laser polarimetry
or standard automated
perimetry?

Josine van der Schoot, Nicolaas J. Reus, Thomas P. Colen,
Hans G. Lemij

Submitted

ABSTRACT

Purpose. To explore the rate of conversion from ocular hypertension to glaucoma by progression analyses on visual fields and scanning laser polarimetry.

Design. Longitudinal retrospective study

Participants. Four hundred sixteen subjects with ocular hypertension (intraocular pressure (IOP) ≥ 22 and ≤ 32 mmHg and normal visual fields)

Methods. Subjects were measured every 6 months with a Humphrey Field Analyzer (HFA, 24-2 program; Carl Zeiss Meditec (CZM), Dublin, USA) and with scanning laser polarimetry (GDxVCC and GDxECC; CZM). Conversion to glaucoma was defined as a flagging by the commercially available progression software (Guided / Glaucoma Progression Analysis (GPA); HFA-II-i, Software Version 4.2, CZM; GDx Review with GPA; Software Version 6.0.1, CZM) as 'likely progression' or, in case of HFA, a negative rate of progression that was statistically significant, or in case of GDxVCC, a nerve fiber indicator (NFI) > 35 on at least 3 consecutive measurements. Two hundred and thirty-eight eyes of 134 subjects could be used for the progression analyses.

Main outcome measures. Number of eyes converting to glaucoma.

Results. 61 of the 238 eyes converted to glaucoma. 35 eyes were flagged by GDxECC, 36 by GDxVCC and 12 by standard automated perimetry (SAP). Only 3 converting eyes were flagged by all 3 techniques.

Conclusions. SLP flags conversion to glaucoma earlier than SAP in the large majority of cases, potentially leading to earlier treatment preventing further progression to moderate or severe glaucoma. However, because of little overlap in flagging conversion, we recommend the use of commercially available progression analyses of both structural and functional measurements to detect conversion to glaucoma.

INTRODUCTION

The Rotterdam Ocular Hypertension Trial (ROHT) is a randomised controlled trial into preventing ocular hypertension (OH) to convert into glaucoma. It is a double masked placebo-controlled study on the effect of beta-blockers on the development of glaucomatous retinal nerve fiber layer defects and visual field loss in eyes with elevated IOP. In this 3-arm study, patients were randomly allocated to either Betaxolol, Timolol (Alcon Laboratories, Inc., Fort Worth, TX, USA) or placebo eye drops. To be able to conclude whether topical beta-blockers protect patients with OH to convert to glaucoma, one needs to define conversion to glaucoma. In previous studies on preventing or delaying glaucoma in eyes with OH, conversion to glaucoma was usually based on changes in visual field or in the appearance of the optic disc, scored by reading centres.^{1,2} In daily practice, changes in function or structure are increasingly based on the outcome of measurements of perimetry and imaging devices, such as scanning laser polarimetry (SLP) and optical coherence tomography. In the current study, we explored the incidence of conversion to glaucoma according to the current commercially available progression analyses on standard automated perimetry (SAP) and SLP. The results of the capability of beta-blockers to prevent OH converting to glaucoma, will be reported on in chapter 4.

METHODS

Patients

Four hundred and nine subjects with an elevated intra-ocular pressure (IOP), recruited consecutively between November 1997 and March 2001, were followed up with perimetry and scanning laser polarimetry. They were tested once every half year during seven to ten years or until the onset of conversion (study endpoint). At study entry, all patients had an IOP ≥ 22 mmHg and ≤ 32 mmHg by Goldmann applanation tonometry in both eyes and normal visual fields with SAP on at least two separate occasions. A normal visual field by SAP was defined as a glaucoma hemifield test of 'Within normal limits' and no nerve fiber bundle abnormalities, as described by Keltner et al³, in the total and/or pattern deviation probability plots. All included patients were of white ethnic origin, had a corrected distance Snellen visual acuity of at least 20/40 in both eyes, and had an unremarkable slit lamp examination, including open angles on gonioscopy. The appearance of the optic disc was not a selection criterion. Our study endpoint, conversion to glaucoma, was defined as a reproducible appearance in SAP of either 1 individual point below the 0.5% probability-level, or 2 clustered points below the 1% probability-level, or 3

clustered points below the 2% probability-level, or 4 clustered points below the 5% probability-level on either the total deviation or the pattern deviation probability plot. These criteria have been used and described before⁴, not only for SAP, but also for short wavelength automated perimetry (SWAP). Patients were excluded from participation in the presence of any significant coexisting ocular or systemic diseases known to possibly affect the visual field (e.g. diabetes mellitus), a family history of glaucoma, a history of intraocular surgery (except for uncomplicated cataract surgery), uncontrollable arterial hypertension, or any previous use of IOP-lowering agents within 3 months before the measurements.

Patients took part in a double masked placebo-controlled study on the effect of beta-blockers on the development of glaucomatous retinal nerve fiber layer defects and visual field loss in elevated IOP. In this 3-arm study, patients were randomly allocated to Betaxolol, Timolol (Alcon Laboratories, Inc., Fort Worth, TX, USA) or placebo eye drops. The effects of the two beta-blockers on the conversion rate to glaucoma will be described in chapter 4.

The methods and procedures used in this study adhered to the Declaration of Helsinki. Informed consent was obtained from all participants. This study was approved by the Medical Ethics Committee of the Erasmus Medical Centre, Rotterdam, The Netherlands and registered in the Dutch Trial Register.

Test strategies

SAP was measured with the Humphrey Field Analyzer II [HFA] (Carl Zeiss Meditec (CZM), Dublin, CA, USA) by means of the 24-2 Full Threshold (FT) test paradigm. To save test-time, we decided to use SITA Standard instead of the FT strategy, after SITA Standard (SS) became available. Whenever any defects appeared upon SITA Standard testing, the visual field test was repeated with the FT strategy to confirm any abnormal fields. When no defects were present with the FT strategy, the testing was prolonged with FT measurements only. SAP test strategies and criteria have been described in detail before⁴.

SLP was measured with the GDx (CZM, Dublin, CA, USA), with both the variable corneal compensation (GDxVCC) and enhanced corneal compensation (GDxECC). For each subject, anterior segment birefringence was assessed, after which images were obtained with both VCC and ECC. All accepted scans were of high quality, i.e. with a centred optic disc, well-focused, evenly and justly illuminated throughout the image, and without any motion artefacts.

Progression analyses

For both SAP and SLP, Carl Zeiss Meditec developed progression software, the Guided (SAP) / Glaucoma (SLP) Progression Analysis (GPA). In SAP, this software

is incorporated in the HFA (HFA-II-i, Software Version 4.2, CZM, Dublin, CA, USA). The GPA parameters indicating progression result from a trend analysis, i.e. the rate of progression and its significance. This linear regression analysis is based on the visual field index (VFI). We considered an eye as converting to glaucoma in case of a negative rate of change that was statistically significant. The GPA progression analysis also includes an event analysis, in which the individual test locations of the deviation plots of each follow up measurement are compared with the baseline measurements. The result is 'no progression', if there is no change, 'possible progression' if change is detected in only one visit, or 'likely progression' if this loss is confirmed in a subsequent measurement. In case of event analysis, we considered an eye as converting to glaucoma if a follow up measurement was flagged as 'likely progressing'. For SAP, the progression analysis was based on the SS-strategy. The GPA software allowed us to include measurements performed with the FT-strategy, but only when baseline measurements were obtained through the same FT-strategy.

In case of SLP, we used GPA software that was for investigational use only (GDx Review with GPA; Software Version 6.0.1, CZM, Dublin, CA, USA). This software is comparable with the GPA software commercially available on the current GDxPRO, the successor to the GDxVCC. The parameters derived from the progression analysis include RNFL image change (Image Progression Map (IPM)), TSNIT change (TSNIT Progression Graph (TPG)), and change in summary parameters (SP) (TSNI-TAverage, SuperiorAverage, InferiorAverage). We considered an eye as converting to glaucoma in case of at least one out of the 3 parameters (IPM, TPG, SP) being flagged as likely progression. We also used the NFI change for detecting conversion. The nerve fiber indicator (NFI) is a clinically important parameter, ranging from 1 to 99. It has been trained to increase with the likelihood of glaucoma and it has been reported to have the best diagnostic accuracy among the 6 standard parameters.⁵ We defined conversion based on NFI at a value ≥ 35 , confirmed on at least 2 consecutive occasions. In case of an NFI ≥ 35 at baseline, an increase of $>30\%$, confirmed on at least 2 consecutive occasions, was also considered as progression. Our GPA software only calculated the NFI in GDxVCC data and not in GDxECC data. Therefore, we are able to only present the NFI-analyses of GDxVCC.

The selection of data for progression analyses in the current study, was based on the presence of GDxECC measurements, because GDxECC was incorporated into the study last, in 2004. During follow up of the participants, more measurements were collected than fit into the progression analyses. The GPA of the GDx operates with a maximum of 8 measurements. We therefore selected the first 3 visits in which GDxECC was performed, as well as the last 3 visits. Two additional visits were selected from the visits in between the first and last 3 visits, based on equal division

of the measurements over time. The dates of the SAP measurements that we used for the progression analyses matched those of the GDx measurements.

Data Analysis

The paired T-test was used to test for any differences between parameters at study onset and endpoint. The unpaired T-test was used to test for differences between eyes showing conversion and those not showing conversion. In the current study, a significance level of 0.05 was considered to be statistically significant. We constructed a Venn diagram to present all combinations between the converted eyes flagged by SAP, GDxECC and GDxVCC. The definitions were analysed with custom-made algorithms in Microsoft Access 2003 (Microsoft Corporation, Redmond, WA, USA) + SPSS Statistics 22 for Windows (release 22.0.0, 2013, IBM SPSS Statistics, New York, USA).

Of the 818 eyes of the 409 eligible subjects, 580 eyes were excluded from analysis for the following reasons: a cholesterol crystal that was present in a retinal artery causing a visual field defect (1), no possibility to perform GPA on all 3 measurements, i.e. GDxECC, GDxVCC and SAP, because of dropout before incorporation of the GDxECC, leading to the absence or too few measurements (454), or the measurements did not meet the software's inclusion criteria (i.e. the intermittent use of SS and FT test strategies in SAP or quality control errors in the GDx GPA software) (125). Therefore, 134 subjects (238 eyes) with elevated IOP were analyzed for the present study. The baseline characteristics of all included subjects and eyes have been shown in Table 1. The mean follow up time was 3.8 [SD 0.8] years.

RESULTS

Of the 238 included eyes, 61 eyes of 48 subjects showed conversion in one of the progression analyses with the 3 techniques, i.e. GDxECC, GDxVCC or SAP. Of these 61 converting eyes, 35 were flagged by GDxECC, 36 by GDxVCC and 12 by SAP. In the progression analysis of the GDxVCC, 15 of the 36 converting eyes were flagged as progressing by the criterion of an NFI ≥ 35 , or, in case of an NFI ≥ 35 at baseline, an increase of $>30\%$, both criteria confirmed on at least 2 consecutive occasions. In the SAP progression analyses, 6 eyes were flagged as progressing by trend analysis and another 6 eyes by event analysis. Most progression was flagged by GDx (57% by GDxECC and 59% by GDxVCC). Only 3 cases were flagged by all 3 commercially available progression analyses of GDxECC, GDxVCC and SAP. Figure 1 shows a Venn diagram of the number of converting eyes flagged by each analysis.

Table 1 Baseline characteristics of included subjects and eyes.

Subject Characteristics	units	Subjects (134)
Age	years	62.4 [9.7]
Men	N (%)	59 (44)
Eye Characteristics		Eyes (238)
CDVA	NA	1.06 [0.26]
CCT	μm	578.44 [32.41]
IOP	mmHg	26.38 [2.81]
SAP - MD	dB	0.87 [1.03]
SAP - VFI	%	99.76 [0.47]
VCC - NFI	NA	23.34 [10.24]
VCC - TSNIT Average	μm	51.21 [5.13]
ECC - TSNIT Average	μm	50.59 [4.88]

All numbers are presented as Mean [Standard Deviation]

Abbreviations: CDVA: corrected distance visual acuity [SD in Snellen letter lines]⁶; CCT: central corneal thickness; IOP: intraocular pressure; SAP: standard automated perimetry; MD: mean deviation; VFI: visual field index; VCC: GDx with variable corneal compensation; NFI: nerve fiber indicator; ECC: GDx with enhanced corneal compensation; N: number; NA: not applicable.

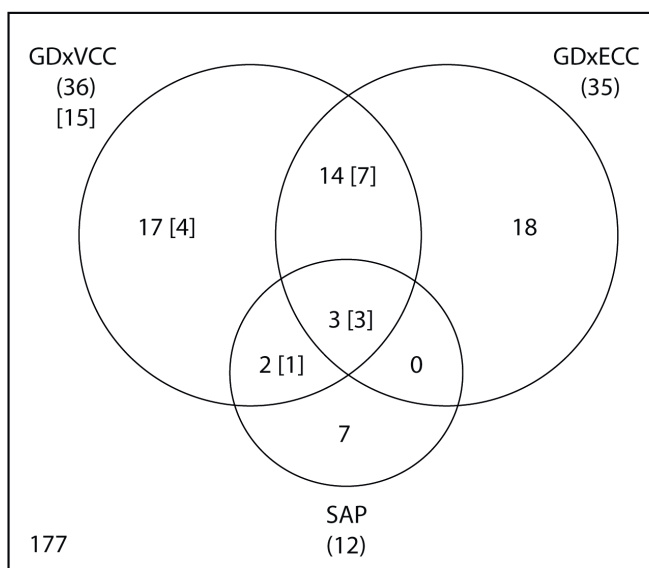


Figure 1 Venn diagram representing the number of converting eyes as detected with commercially available progression analyses for GDxECC, GDxVCC and SAP. In case of GDxVCC, the number of converting eyes based on an NFI ≥ 35 is presented between brackets. In case of an NFI ≥ 35 at baseline, an increase of $>30\%$, twice reproduced consecutively, was required to be considered as conversion.

Table 2 Characteristics of converting and non converting eyes

	units	Non-converting eyes (177)	Converting eyes (61)	Statistics
CDVA	NA	1.07 [0.26]	1.02 [0.25]	‡
CCT	µm	580.77 [31.83]	571.66 [33.35]	‡
IOP	mmHg	BASELINE * 26.26 [2.95]	BASELINE * 26.72 [2.37]	Difference 3.21 [3.56] ‡¶†
SAP - MD	dB	0.88 [1.03]	0.82 [1.03]	0.23 [0.91] * ‡†
SAP - VFI	%	99.76 [0.44]	99.74 [0.54]	0.22 [0.91] ‡¶†
VCC - NFI	NA	23.11 [10.33]	24.03 [10.03]	-9.14 [9.63] ‡¶†
VCC - TSNIT Average	µm	51.41 [4.99]	50.64 [5.52]	2.26 [2.87] ‡¶†
ECC - TSNIT Average	µm	50.78 [4.71]	50.03 [5.35]	2.46 [3.34] ‡¶†

CDVA = corrected distance visual acuity [SD in Snellen letter lines]⁶; NA = not applicable; CCT = central corneal thickness; IOP = intraocular pressure; SAP = standard automated perimetry; MD = mean deviation; dB = decibel; VFI = visual field index; NFI = nerve fiber indicator.

All numbers are presented as Mean [Standard Deviation]

Statistics (P<0.05):

- ‡ No statistically significant differences between non-converting and converting eyes at baseline (*).
- ¶ Statistically significant differences in change over time in all eyes, except for MD (*) and TSNIT Average (**).
- † Statistically significant differences in change over time between non-converting and converting eyes.

In the GDxVCC, a total of 36 eyes were flagged as converting to glaucoma. Of those eyes, only 28% (n=10) was flagged by both analyses, i.e. the progression flagged by the GPA software and an increase in NFI to ≥ 35 , or, a reproducible increase of $>30\%$ in case of an NFI ≥ 35 at baseline.

Of the 48 subjects who showed conversion, 46% (n=22) were men. The mean age of these 48 subjects was 66.2 years (SD, 9.4). The characteristics of the non-converting eyes, as well of the converting eyes have been shown in Table 2. The baseline characteristics of the converting eyes and those not converting (as described in Table 2) were not statistically significant different in CDVA, IOP and CCT ($p > 0.31$), nor in any of the parameters produced by the 3 devices ($p > 0.34$).

In all 238 included eyes, both non-converting and converting, all parameters changed statistically significantly ($p < 0.004$, paired T-test) between study onset and endpoint, except for the MD and the GDx VCC's TSNIT average. The latter changed only in the group of converting eyes. The change between study onset and endpoint was larger for all parameters in the converting eyes than for the non-converting eyes ($p < 0.02$), except for the IOP.

DISCUSSION

Twenty-six percent of the eyes with ocular hypertension in our data showed conversion to glaucoma in approximately 4 years follow-up by the criteria we adopted, using the proprietary progression analysis programmes in function and structure. Compared to the outcome of other trials, such as the OHTS and EGPS^{7,8}, this is a large proportion of converting eyes. In the OHTS and EGPS, the rate of conversion was $< 15\%$ within 5 years (treated and untreated eyes). This difference is probably mainly due to differences in methodology and criteria used to define ocular hypertension and (conversion to) glaucoma. In the OHTS and EGPS, ocular hypertension was defined by the intraocular pressure and the absence of visual field defects as well as a normal appearance of the optic disc.^{1,2} We included subjects based only on the IOP and visual field, not defining the absence of structural damage. This might have lead to including relatively more advanced preperimetric glaucomatous eyes, potentially already having structural damage. This is further supported by the fact that we had several eyes at baseline with an NFI > 35 , but without any visual field damage.

A second explanation of our relatively high rate of conversion might be the use of SLP in defining conversion to glaucoma. Apparently, structural damage often precedes functional damage in glaucomatous eyes.^{9,10} Our data confirm this phenomenon by showing a much higher conversion rate with SLP than with SAP. Only

20% of the converted eyes were flagged by the progression analysis software of SAP, while 89% were flagged by SLP. It is unclear whether all these structural conversions would also have been detected by judging the appearance of the optic disc. Judging (conversion to) glaucoma and its progression by the appearance of the optic disc¹¹⁻¹³, and also matching it with visual field progression¹⁴, has been shown to be difficult.

Our data show a relatively poor overlap between conversion on SAP and on SLP. Only 5% (3 eyes) of all converting eyes showed conversion to glaucoma in all 3 progression analyses (SAP, GDxVCC and GDxECC). In other words, there was poor agreement in conversion rates between structural and functional measurements. This agrees well with other studies into structural and functional progression and conversion in ocular hypertension and glaucoma, mainly showing a poor agreement between structure and function.¹⁵⁻²⁰ Unfortunately, an accurate comparison between our current study and other studies is not possible, mainly because a) few studies have been presented using SLP for progression analysis, and more importantly, b) our study explicitly investigated the conversion of ocular hypertension to glaucoma, a transition without any gold standard, which hampers the comparison with other trials.

The baseline characteristics of our subjects were solid, illustrated by the absence of any statistically significant differences between the converting and non-converting eyes. The small change over time in the parameters of the non-converting eyes might be due to natural aging. A similar effect of age on RNFL thickness in SLP has been reported earlier.^{21,22} The relatively small decrease over time in VFI and MD within the converting eyes might be due to the ceiling effect, described by Artes et al.²³ Apparently, when no or very little visual field damage exists, changes in VFI are much harder to detect than changes in glaucomatous visual field damage with an MD < -5dB. The VFI therefore appears to be quite insensitive to early changes in glaucomatous damage.

A methodological limitation of our study was the development of devices during the course of the trial. In SAP, we decided to use the SITA-Standard (SS) test paradigm instead of the Full-Threshold (FT) test paradigm, since it was thought to improve the quality and time of the visual fields, without compromising their outcome.²⁴⁻²⁶ Unfortunately, the GPA, which was developed later, is not capable of fully combining FT and SS strategies. This led to the exclusion of many eyes in our analyses. SLP was introduced in the current trial since its beginning by the predecessors of the GDxECC (Nerve Fiber Analyzer, Laser Diagnostics Technologies, San Diego, CA, USA). Because these earlier devices are currently no longer used, we chose to implement the measurements of GDxECC and VCC in the current analyses since they became available in 2004. Unfortunately, this has inevitably led

to a significant decrease in follow-up time. These changes over time of the commercially available devices in our trial is a reflection of an ophthalmologist's daily practice. The development of devices over the years shows a great improvement in sensitivity of diagnosing glaucoma, but complicates progression analyses, largely because the newer versions are poorly, or not at all, backwards compatible.

The progression analysis software of both SAP and SLP incorporates trend as well as event analysis. Event analysis may be more sensitive in detecting glaucoma progression than trend analysis^{27;28}, especially in a relatively short period of time. Combining both analyses is desirable in diagnosing conversion to glaucoma.²⁹ In the analysis of our SLP data, we therefore incorporated the NFI as an extra event analysis. This intuitive parameter probably reflects the use of SLP in daily care. The NFI was developed as a classifier. It therefore reflects the likelihood of glaucoma but not the severity of the disease. It has been shown to be quite accurate in discriminating between normal and glaucomatous eyes.^{30;31} Obviously the likelihood of glaucoma may go up with more advanced disease, but one should be aware that the NFI was never developed for monitoring glaucoma. The criterion of a change in NFI from below 35 to above 35 that we used had to do with a change in classification (normal versus glaucomatous). The other NFI criterion that we used (a change of >30% in case of a high NFI at baseline) therefore made less sense, and it turned out to be indeed quite insensitive, albeit more sensitive than SAP.

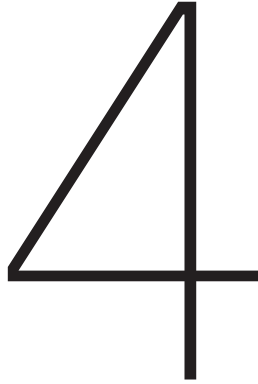
In our study, SLP flagged conversion to glaucoma earlier than SAP in the large majority of cases, potentially leading to earlier treatment preventing further progression to moderate or severe glaucoma. Based on the outcome of our study, we advise to use SLP, or another device measuring structural change in glaucoma, in daily practice to intercept conversion to glaucoma, when possible combined with SAP. SAP alone turned out to be relatively insensitive to detect conversion to glaucoma; this applied to the NFI alone as well. We recommend the use of commercially available progression software of both structural and functional measurements to detect conversion to glaucoma.



REFERENCE LIST

1. Gordon MO, Kass MA. The Ocular Hypertension Treatment Study: design and baseline description of the participants. *Arch Ophthalmol* 1999;117:573-83.
2. Miglior S, Zeyen T, Pfeiffer N, et al. The European glaucoma prevention study design and baseline description of the participants. *Ophthalmology* 2002;109:1612-21.
3. Keltner JL, Johnson CA, Cello KE, et al. Classification of visual field abnormalities in the ocular hypertension treatment study. *Arch Ophthalmol* 2003;121:643-50.
4. van der Schoot J, Reus NJ, Colen TP, Lemij HG. The ability of short-wavelength automated perimetry to predict conversion to glaucoma. *Ophthalmology* 2010;117:30-4.
5. Mai TA, Reus NJ, Lemij HG. Diagnostic accuracy of scanning laser polarimetry with enhanced versus variable corneal compensation. *Ophthalmology* 2007;114:1988-93.
6. Holladay JT. Proper method for calculating average visual acuity. *J Refract Surg* 1997;13:388-91.
7. Kass MA, Heuer DK, Higginbotham EJ, et al. The Ocular Hypertension Treatment Study: a randomized trial determines that topical ocular hypotensive medication delays or prevents the onset of primary open-angle glaucoma. *Arch Ophthalmol* 2002;120:701-13.
8. Miglior S, Zeyen T, Pfeiffer N, et al. Results of the European Glaucoma Prevention Study. *Ophthalmology* 2005;112:366-75.
9. Sommer A, Katz J, Quigley HA, et al. Clinically detectable nerve fiber atrophy precedes the onset of glaucomatous field loss. *Arch Ophthalmol* 1991;109:77-83.
10. Zeyen TG, Caprioli J. Progression of disc and field damage in early glaucoma. *Arch Ophthalmol* 1993;111:62-5.
11. Breusegem C, Fieuws S, Stalmans I, Zeyen T. Agreement and accuracy of non-expert ophthalmologists in assessing glaucomatous changes in serial stereo optic disc photographs. *Ophthalmology* 2011;118:742-6.
12. Jampel HD, Friedman D, Quigley H, et al. Agreement among glaucoma specialists in assessing progressive disc changes from photographs in open-angle glaucoma patients. *Am J Ophthalmol* 2009;147:39-44.
13. Reus NJ, Lemij HG, Garway-Heath DF, et al. Clinical assessment of stereoscopic optic disc photographs for glaucoma: the European Optic Disc Assessment Trial. *Ophthalmology* 2010;117:717-23.
14. van der Schoot J, Reus NJ, Garway-Heath DF, et al. Accuracy of matching optic discs with visual fields: the European Structure and Function Assessment Trial (ESAFAT). *Ophthalmology* 2013;120:2470-5.
15. Banegas SA, Anton A, Morilla-Grasa A, et al. Agreement among spectral-domain optical coherence tomography, standard automated perimetry, and stereophotography in the detection of glaucoma progression. *Invest Ophthalmol Vis Sci* 2015;56:1253-60.
16. Chauhan BC, McCormick TA, Nicolela MT, LeBlanc RP. Optic disc and visual field changes in a prospective longitudinal study of patients with glaucoma: comparison of scanning laser tomography with conventional perimetry and optic disc photography. *Arch Ophthalmol* 2001;119:1492-9.
17. Medeiros FA, Zangwill LM, Bowd C, et al. The structure and function relationship in glaucoma: implications for detection of progression and measurement of rates of change. *Invest Ophthalmol Vis Sci* 2012;53:6939-46.

18. Mohammadi K, Bowd C, Weinreb RN, et al. Retinal nerve fiber layer thickness measurements with scanning laser polarimetry predict glaucomatous visual field loss. *Am J Ophthalmol* 2004;138:592-601.
19. Quigley HA, Enger C, Katz J, et al. Risk factors for the development of glaucomatous visual field loss in ocular hypertension. *Arch Ophthalmol* 1994;112:644-9.
20. Schrems-Hoesl LM, Schrems WA, Laemmer R, et al. Confocal Laser Scanning Tomography to Predict Visual Field Conversion in Patients With Ocular Hypertension and Early Glaucoma. *J Glaucoma* 2014.
21. Da Pozzo S, Iacono P, Marchesan R, et al. The effect of ageing on retinal nerve fibre layer thickness: an evaluation by scanning laser polarimetry with variable corneal compensation. *Acta Ophthalmol Scand* 2006;84:375-9.
22. Rao HL, Venkatesh CR, Vidyasagar K, et al. Retinal nerve fiber layer measurements by scanning laser polarimetry with enhanced corneal compensation in healthy subjects. *J Glaucoma* 2014;23:589-93.
23. Artes PH, O'Leary N, Hutchison DM, et al. Properties of the statpac visual field index. *Invest Ophthalmol Vis Sci* 2011;52:4030-8.
24. Artes PH, Iwase A, Ohno Y, et al. Properties of perimetric threshold estimates from Full Threshold, SITA Standard, and SITA Fast strategies. *Invest Ophthalmol Vis Sci* 2002;43:2654-9.
25. Heijl A, Bengtsson B, Patella VM. Glaucoma follow-up when converting from long to short perimetric threshold tests. *Arch Ophthalmol* 2000;118:489-93.
26. Sharma AK, Goldberg I, Graham SL, Mohsin M. Comparison of the Humphrey swedish interactive thresholding algorithm (SITA) and full threshold strategies. *J Glaucoma* 2000;9:20-7.
27. Casas-Llera P, Rebolleda G, Munoz-Negrete FJ, et al. Visual field index rate and event-based glaucoma progression analysis: comparison in a glaucoma population. *Br J Ophthalmol* 2009;93:1576-9.
28. Vesti E, Johnson CA, Chauhan BC. Comparison of different methods for detecting glaucomatous visual field progression. *Invest Ophthalmol Vis Sci* 2003;44:3873-9.
29. Medeiros FA, Weinreb RN, Moore G, et al. Integrating event- and trend-based analyses to improve detection of glaucomatous visual field progression. *Ophthalmology* 2012;119:458-67.
30. Reus NJ, Lemij HG. Diagnostic accuracy of the GDx VCC for glaucoma. *Ophthalmology* 2004;111:1860-5.
31. Reus NJ, de Graaf M, Lemij HG. Accuracy of GDx VCC, HRT I, and clinical assessment of stereoscopic optic nerve head photographs for diagnosing glaucoma. *Br J Ophthalmol* 2007;91:313-8.



Does topical Betaxolol or Timolol prevent ocular hypertension from converting to glaucoma? The Rotterdam Ocular Hypertension Trial

Josine van der Schoot, Nicolaas J. Reus, Thomas P. Colen,
Hans G. Lemij

Manuscript in preparation

ABSTRACT

Purpose. To explore the effect of topical beta-blockers on the rate of conversion of ocular hypertension to glaucoma.

Design. Randomized placebo-controlled study

Participants. Four hundred sixteen subjects with ocular hypertension (intraocular pressure (IOP) ≥ 22 and ≤ 32 mmHg and normal visual fields)

Methods. Subjects were randomly allocated to either Betaxolol 0.25%, Timolol 0.25% or placebo eyedrops. Every 6 months the intraocular pressure was determined, as well as the visual field (Standard Automated Perimetry (SAP); Carl Zeiss Meditec (CZM), Dublin, USA) and scanning laser polarimetry (SLP; GDxVCC and GDxECC; CZM) was also performed. Conversion to glaucoma was defined by commercially available progression software (Guided / Glaucoma Progression Analysis (GPA); HFA-II-i, Software Version 4.2, CZM; GDx Review with GPA; Software Version 6.0.1, CZM) software of all 3 techniques. Two hundred and thirty eight eyes of 134 subjects could be used for the progression analyses.

Main outcome measures. Number of eyes converting to glaucoma and IOP for eyes using Betaxolol, Timolol and placebo eyedrops.

Results. 61 of the 238 eyes converted to glaucoma, of which 16 within the Timolol-group, 21 within the Betaxolol-group and 24 eyes that were treated with placebo eyedrops. The IOP decreased statistically significantly ($p < 0.05$) by 18% in eyes receiving Timolol, 12% in eyes receiving Betaxolol and 8% in eyes receiving placebo eyedrops.

Conclusions. In this study, we presented that beta-blockers show no advantage in preventing ocular hypertension to convert to glaucoma, as compared to placebo.

INTRODUCTION

Whether Ocular Hypertension (OH) should be medically treated to prevent the conversion to glaucoma is subject to debate. Several large studies have presented conflicting results whether or not to treat ocular hypertension. The Ocular Hypertension Treatment Study (OHTS) showed an approximately 50% reduction of the risk of developing glaucoma by topical medication.¹ The European Glaucoma Prevention Study (EGPS) showed no advantage of dorzolamide against placebo in preventing or delaying the onset of glaucoma.² The current study, The Rotterdam Ocular Hypertension Trial (ROHT), is a randomised controlled trial into preventing OH from converting to glaucoma. It is a double masked placebo-controlled study on the effect of beta-blockers (Betaxolol, Timolol (Alcon Laboratories, Inc., Fort Worth, TX, USA)) on the development of glaucomatous retinal nerve fibre layer defects and visual field loss in eyes with elevated IOP. Currently, the use of progression analyses software on diagnostic tools, such as for standard automated perimetry (SAP) and sophisticated imaging of the eye, have entered the daily care for glaucoma patients. In the current study, we have used these commercially available progression analysis software packages to detect conversion from OH to glaucoma, both for SAP and for Scanning Laser Polarimetry (SLP). More importantly, we explored the effect of beta-blockers on the conversion rates.

METHODS

Four hundred and sixteen (416) subjects with an elevated intra-ocular pressure (IOP), were included in our randomised placebo-controlled study. In this 3-arm study, patients were randomly allocated to either Betaxolol 0.25%, Timolol 0.25% (Alcon Laboratories, Inc., Fort Worth, TX, USA) or placebo eyedrops. The IOP was measured every 6 months and subjects were also tested with both SAP (Humphrey Field Analyzer II [HFA] (Carl Zeiss Meditec (CZM), Dublin, CA, USA) and SLP (GDx (CZM, Dublin, CA, USA)). SAP was measured by means of the 24-2 Full Threshold (FT) test paradigm. To save test-time, we decided to use SITA Standard instead of the FT strategy, after SITA Standard (SS) became available. SLP was measured with the GDx with both the variable corneal compensation (GDxVCC) and enhanced corneal compensation (GDxECC). For each subject, anterior segment birefringence was assessed, after which images were obtained with both VCC and ECC. Next to the SAP and SLP testing mentioned in this report, patients were tested every 6 months by several other techniques as well, including Short Wavelength Automated Perimetry (SWAP, CZM, Inc., Dublin, CA, USA), scanning laser tomog-

raphy (Heidelberg Retina Tomograph (HRT), Heidelberg Engineering GmbH, Dossenheim, Germany) and simultaneous stereoscopic photos of the optic disc. At study entry, all patients had an IOP ≥ 22 mmHg and ≤ 32 mmHg by Goldmann applanation tonometry in both eyes and normal visual fields with SAP on at least two separate occasions. A normal visual field by SAP was defined as a glaucoma hemifield test of 'Within normal limits' and no nerve fibre bundle abnormalities, as described by Keltner et al³, in the total and/or pattern deviation probability plots. The appearance of the optic disc was not a selection criterion. Detailed inclusion criteria and testing strategies have been described before.^{4,5}

We retrospectively analysed the data by performing progression analyses on the SAP and SLP data by using the commercially available software developed by CZM. For SAP, the Guided Progression Analysis (GPA) is incorporated in the HFA (HFA-II-i, Software Version 4.2, CZM, Dublin, CA, USA). In case of SLP, we used GPA software that was for investigational use only (GDx Review with GPA; Software Version 6.0.1, CZM, Dublin, CA, USA). The parameters and criteria used for this progression analysis and conversion to glaucoma have been described before.⁵ We compared the IOP and the incidence of conversion flagged by the software analyses between the subjects using Betaxolol, Timolol and placebo eyedrops.

Of the 818 eyes of the 409 eligible subjects, 580 eyes were excluded from analysis for the following reasons: a cholesterol crystal that was present in a retinal artery causing a visual field defect (1), no possibility to perform GPA on all 3 measurements, i.e. GDxECC, GDxVCC and SAP, because of dropout before incorporation of the GDxECC, leading to the absence or too few measurements (454), or the measurements did not meet the software's inclusion criteria (i.e. the intermittent use of SS and FT test strategies in SAP or quality control errors in the GDx GPA software) (125). Therefore, 134 subjects (238 eyes) with elevated IOP were analyzed for the present study.

RESULTS

Of the 238 included eyes, 61 eyes showed progression in one of the progression analyses with the 3 techniques, i.e. GDxECC, GDxVCC and SAP. The mean age of all 134 participants (at study endpoint) was 62.4 years (SD, 9.7), of whom 44% (n=59) were men. The mean follow up time was 3.8 [SD 0.8] years. The characteristics of all included eyes per treatment group have been presented in Table 1.

A total of 61 eyes (26%) converted to glaucoma, of which 16 (21%) within the Timolol-group, 21 (29%) within the Betaxolol-group and 24 (27%) eyes that were treated with placebo eyedrops. The incidence of conversion between these 3

Table 1 Characteristics per treatment group

		Timolol 0.25%		Betaxolol 0.25%		Placebo	
Subjects	n	42		41		51	
Age	yrs	62.09 [9.70]		64.98 [10.56]		60.64 [8.61]	
Gender (male)	n	20		17		22	
Eyes	n	76		73		89	
BCVA		1.10 [0.32]		1.06 [0.28]		1.03 [0.17]	
CCT	μm	577.18 [36.12]		577.59 [34.64]		580.20 [27.00]	
		START	END	START	END	START	END
IOP	mmHg	26.20 [2.79]	21.22 [3.31]	26.97 [2.44]	23.53 [2.87]	26.04 [3.07]	23.66 [3.08]
SAP - MD	dB	0.82 [0.93]	0.82 [0.98]	0.97 [1.20]	0.79 [1.26]	0.82 [0.96]	0.81 [1.02]
SAP - VFI	dB	99.76 [0.54]	99.55 [0.74]	99.79 [0.41]	99.51 [0.77]	99.72 [0.45]	99.61 [0.60]
VCC - NFI	NA	24.83 [10.71]	28.05 [13.23]	22.36 [10.49]	26.86 [13.94]	22.89 [9.58]	25.40 [12.54]

Abbreviations: BCVA = best corrected visual acuity; CCT = central corneal thickness; IOP = intraocular pressure; SAP = standard automated perimetry; MD = mean deviation; VFI = visual field index; dB = decibel; VCC = scanning laser polarimetry with variable corneal compensation; NFI = nerve fiber indicator; NA = not applicable.

All parameters presented as number (n) or mean [standard deviation].

groups did not statistically significantly differ from each other (Chi-square test, $p = 0.52$). Of the 48 subjects that showed progression, 46% ($n=22$) were men. The mean age of these 62 subjects was 66.2 years (SD, 9.4). Table 2 shows the characteristics of the converted eyes for each treatment group.

The intraocular pressure (IOP) decreased statistically significantly in all three groups (paired T-test, $p < 0.05$ for Betaxolol, Timolol and placebo). The eyes using

Table 2 Characteristics for all converted eyes per group

		Timolol 0.25%		Betaxolol 0.25%		Placebo	
Subjects	N (%)	13 (31)		18 (44)		17 (33)	
Eyes	N (%)	16 (21)		21 (29)		24 (27)	
		BASELINE	END	BASELINE	END	BASELINE	END
IOP	mmHg	26.00 [2.37]	20.37 [3.26]	27.14 [2.20]	23.81 [3.30]	26.83 [2.51]	25.33 [2.70]
SAP - MD	dB	0.68 [0.97]	0.48 [1.11]	0.97 [1.22]	0.60 [1.46]	0.78 [0.90]	0.67 [1.09]
SAP - VFI	dB	99.75 [0.77]	99.00 [1.03]	99.86 [0.36]	99.57 [0.51]	99.63 [0.49]	99.42 [0.65]
VCC - NFI		24.88 [8.53]	34.56 [15.68]	22.33 [10.69]	32.76 [15.86]	24.96 [10.56]	32.63 [17.05]

Abbreviations: N (%) = number (percentage of included eyes within group); IOP = intraocular pressure; SAP = standard automated perimetry; MD = mean deviation; VFI = visual field index; dB = decibel; VCC = scanning laser polarimetry with variable corneal compensation; NFI = nerve fiber indicator; NA = not applicable.

All parameters presented as number (n) or mean [standard deviation].

Timolol eyedrops showed the largest decrease in IOP by 18%. The IOP in eyes using Betaxolol and placebo eyedrops decreased by 12% and 8%, respectively. This difference in decrease in IOP between these 3 groups was statistically significant (Generalised Estimating Equations, $p < 0.05$). Figure 1 presents a graph with the IOP at baseline and endpoint for all three medication groups. Figure 2 presents a histogram of the decrease in IOP for converted and not converted eyes.

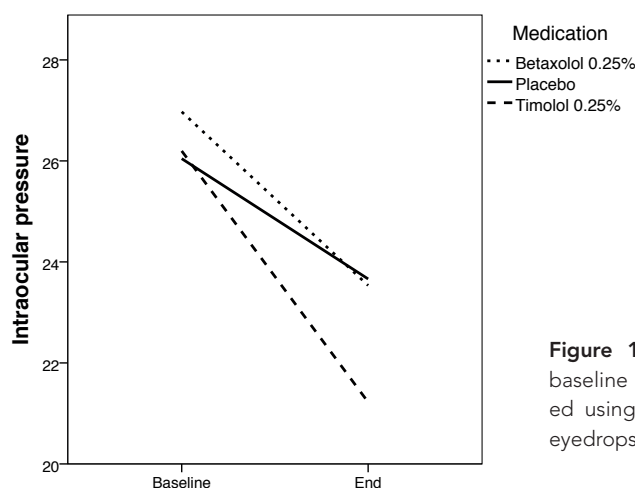


Figure 1 Mean intraocular pressure at baseline and endpoint for all eyes included using Betaxolol, Timolol or placebo eyedrops.

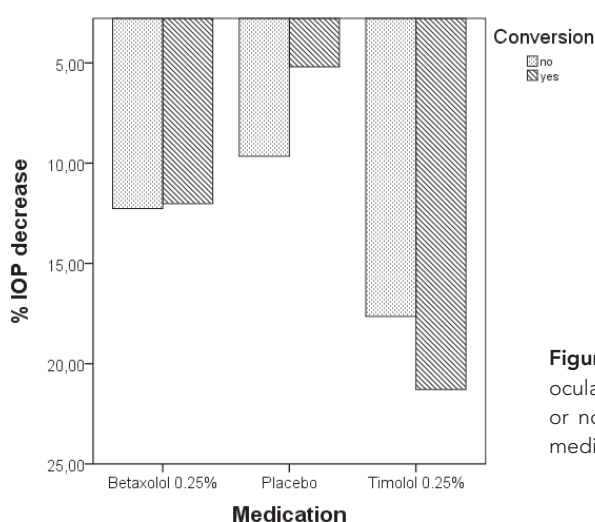


Figure 2 Percentage of decrease in intraocular pressure (IOP) in eyes converting or not converting to glaucoma for each medication group separately.

CONCLUSION

Beta-blockers induced a significant decrease in the intraocular pressure (IOP), but did not significantly reduce the conversion rates in ocular hypertensive eyes to glaucoma, compared to placebo. Timolol gave the largest decrease in IOP (18%) and lead to the fewest eyes converting to glaucoma (21%). This percentage was, however, not statistically significantly lower than the conversion rate in eyes receiving Betaxolol or placebo eyedrops. In the two largest trials in preventing ocular hypertension from converting to glaucoma, the Ocular Hypertension Treatment Study (OHTS)¹ and the European Glaucoma Prevention Study (EGPS)², a mean reduction in IOP of 22% was achieved, with topical treatment, which was more effective in preventing conversion to glaucoma. However, according to our study, a higher decrease in IOP, as Timolol elicits compared to Betaxolol and placebo eyedrops, did not significantly reduce the chance of conversion to glaucoma.

A total of 26% of the included ocular hypertensive eyes showed conversion to glaucoma within 4 years. This is a much higher conversion rate than in the OHTS and EGPS. The OHTS showed a conversion rate in 5 years of 4.4% in eyes treated with topical medication and 9% in the control group, which did not receive any treatment. The EGPS showed a higher rate of conversion in 5 years than the OHTS; 13.4% in eyes treated with dorzolamide and 14.1% in eyes receiving placebo eyedrops. This significant difference in conversion rates between the OHTS and the EGPS was probably induced by applying different criteria at inclusion and as conversion to glaucoma. We included subjects based only on the IOP and their visual fields, not taking the appearance of the optic disc into account, as the other studies did.^{6,7} This might have lead to including relatively more advanced preperimetric glaucomatous eyes, potentially already having structural damage. Also applying a different criterion for conversion to glaucoma, based on newly developed progression analyses software, might have lead to the earlier detection of conversion to glaucoma.

Initially, we included a large group of subjects with OH into this study. Due to the development of devices during the course of the trial, we were not able to analyse the data of all subjects. Due to test strategies changing over time and not being interchangeable (in case of SAP) and due to the development of newer devices during the study (in case of SLP), we were forced to exclude many subjects. The development of devices over the years shows a great improvement in sensitivity of diagnosing glaucoma, but complicates progression analyses, largely because the newer versions are poorly, or not at all, backwards compatible.

Beta-blockers are widely used in treating glaucoma. Both Timolol, a non-selective beta-adrenergic antagonist, and Betaxolol, a beta₁-selective antagonist,

reduce aqueous humor secretion and induce an increased retinal perfusion^{8,9}. Betaxolol reaches a smaller decrease in IOP than Timolol does.¹⁰ However, due to its neuroprotective effect by its calcium-channel blocking properties¹¹, Betaxolol was thought to have an equal or even better result in preventing glaucomatous progression, compared to Timolol.¹²⁻¹⁴ We therefore included both beta-blockers into this study to compare the effect of both eyedrops on the IOP and conversion of OH to glaucoma.

This study showed a higher rate of conversion to glaucoma in ocular hypertensive eyes treated with beta-blockers, as well as with placebo eye drops, than other trials have described before. We showed that, in general, beta-blockers do not prevent eyes with ocular hypertension from converting to glaucoma.



REFERENCE LIST

1. Kass MA, Heuer DK, Higginbotham EJ, et al. The Ocular Hypertension Treatment Study: a randomized trial determines that topical ocular hypotensive medication delays or prevents the onset of primary open-angle glaucoma. *Arch Ophthalmol* 2002;120:701-13.
2. Miglior S, Zeyen T, Pfeiffer N, et al. Results of the European Glaucoma Prevention Study. *Ophthalmology* 2005;112:366-75.
3. Keltner JL, Johnson CA, Cello KE, et al. Classification of visual field abnormalities in the ocular hypertension treatment study. *Arch Ophthalmol* 2003;121:643-50.
4. van der Schoot J, Reus NJ, Colen TP, Lemij HG. The ability of short-wavelength automated perimetry to predict conversion to glaucoma. *Ophthalmology* 2010;117:30-4.
5. van der Schoot J, Reus NJ, Colen TP, Lemij HG. Converting from ocular hypertension to glaucoma: Scanning laser polarimetry or standard automated perimetry? Submitted.
6. Gordon MO, Kass MA. The Ocular Hypertension Treatment Study: design and baseline description of the participants. *Arch Ophthalmol* 1999;117:573-83.
7. Miglior S, Zeyen T, Pfeiffer N, et al. The European glaucoma prevention study design and baseline description of the participants. *Ophthalmology* 2002;109:1612-21.
8. Arend O, Harris A, Arend S, et al. The acute effect of topical beta-adrenoreceptor blocking agents on retinal and optic nerve head circulation. *Acta Ophthalmol Scand* 1998;76:43-9.
9. Hester RK, Chen Z, Becker EJ, et al. The direct vascular relaxing action of betaxolol, carteolol and timolol in porcine long posterior ciliary artery. *Surv Ophthalmol* 1994;38 Suppl:S125-S134.
10. Drance SM. Vascular Risk Factors and Neuroprotection. *Glaucoma Update* 1996. Amsterdam: Kugler; 2015:221-6.
11. Osborne NN, Cazevielle C, Carvalho AL, et al. In vivo and in vitro experiments show that betaxolol is a retinal neuroprotective agent. *Brain Res* 1997;751:113-23.
12. Messmer C, Flammer J, Stumpfig D. Influence of betaxolol and timolol on the visual fields of patients with glaucoma. *Am J Ophthalmol* 1991;112:678-81.
13. Vainio-Jylha E, Vuori ML. The favorable effect of topical betaxolol and timolol on glaucomatous visual fields: a 2-year follow-up study. *Graefes Arch Clin Exp Ophthalmol* 1999;237:100-4.
14. Vainio-Jylha E, Vuori ML, Nummelin K. Progression of retinal nerve fibre layer damage in betaxolol- and timolol-treated glaucoma patients. *Acta Ophthalmol Scand* 2002;80:495-500.

5

Accuracy of matching optic discs with visual fields: the European Structure And Function Assessment Trial (ESAFAT)

Josine van der Schoot, Nicolaas J Reus, David F Garway-Heath, Ville Saarela, Alfonso Anton, Alain M Bron, Christoph Faschinger, Gábor Holló, Michele Iester, Jost B Jonas, Fotis Topouzis, Thierry G Zeyen, Hans G Lemij

Ophthalmology, 2013; 120(12):2470-5.

ABSTRACT

Purpose. To determine the ability of ophthalmologists across Europe to match stereoscopic optic disc photographs to visual fields of varying severity.

Design. Evaluation and comparison of two diagnostic tests.

Participants. A total of 109 of 260 invited ophthalmologists in 11 European countries. These had participated in the previous European Optic Disc Assessment Trial (EODAT), a trial on glaucoma diagnostic accuracy based on optic discs only.

Methods. Each participant matched stereo optic disc photographs of 40 healthy and 48 glaucomatous eyes to a visual field, chosen from 4 options per disc. The 4 presented visual fields included the corresponding one and 3 other visual fields, varying in severity. The matching accuracy and any inaccuracy per disease severity were calculated. Classification accuracy (as glaucomatous or healthy) was compared to EODAT data. Duplicate slides allowed assessing intraobserver agreement.

Main Outcome Measures. Accuracy of matching optic discs with their corresponding visual field and of classifying as healthy or glaucomatous. Intraobserver agreement (κ).

Results. The overall accuracy of ophthalmologists for correctly matching stereoscopic optic disc photographs to their visual fields was 58.7%. When incorrectly matched, the observers generally overestimated the visual field severity ($p < 0.001$), notably in eyes with early glaucoma. The intraobserver agreement was on average moderate (0.52).

Conclusions. European ophthalmologists correctly matched stereoscopic optic disc photographs to their corresponding visual field in only approximately 59% of cases. In most mismatches, the clinicians overestimated the visual field damage.

INTRODUCTION

Judgement of both the optic disc and the visual field are important mainstays in diagnosing and managing glaucoma. In a previous study, the European Optic Disc Assessment Trial (EODAT), we found that general ophthalmologists have difficulty in correctly classifying optic discs as healthy or glaucomatous (diagnostic accuracy of 80.5%).¹ More so, they were outperformed in correctly classifying eyes by structural measurements made with scanning laser polarimetry (SLP) and scanning laser tomography (SLT), with a diagnostic accuracy of 93.2% and 89.8%, respectively.¹ This confirms other, smaller, studies into the ability of ophthalmologists to discriminate between healthy and glaucomatous eyes.²⁻⁷ Typically, glaucoma diagnosis and management are currently based on a combination of functional and structural measurements. The ophthalmologist needs to be able to combine and match all clinical information, including the visual fields and optic discs. If discs and visual fields match, clinicians may confidently diagnose or stage a glaucomatous disc. On the other hand, if they don't match, the diagnosis is far from ruled out and structure analysis of the optic disc or retinal nerve fiber layer may provide further information. This study explores the ability of ophthalmologists across Europe to match stereoscopic optic disc photographs to visual fields. In addition, we compared the diagnostic accuracy of the participating ophthalmologists of the present study with their own diagnostic accuracy previously obtained in the EODAT, using the same dataset.

METHODS

In the current trial, we used the same dataset of stereoscopic photographs of optic nerve heads (ONHs) as we did in the EODAT. In the EODAT, the observers were asked to grade an ONH as normal or as glaucomatous. The same ophthalmologists who responded in the EODAT were invited to participate in this trial. In the current trial all ONH photographs were presented together with a choice of 4 visual field tests, normal or with varying amounts of glaucomatous visual field loss: mild, moderate and advanced. These 4 visual fields included the corresponding visual field of the imaged eye as well as 3 other randomly chosen visual fields. All observers were asked to choose the corresponding visual field from the 4 presented visual fields.

Ophthalmologists

We invited 260 ophthalmologists in 11 countries across Europe (the 5 bigger ones [France, Germany, Italy, Spain, and the United Kingdom] and 6 smaller ones [Aus-

tria, Belgium, Finland, Greece, Hungary, and The Netherlands)), to participate in this study. They all received letters in their native tongue, explaining the aim of the study, the estimated time their participation would take, and the anonymous nature of the study. They were also promised to receive a small gift (book) upon completion. Those who wished to participate returned a reply card. The positive respondents then received by courier mail a package consisting of 1) 110 stereoscopic optic disc slides, 2) a viewer (Asahi Pentax Stereo Viewer II, Hoya corporation, Tokyo, Japan or a similar generic viewer, because the Asahi Pentax viewers were in short supply and no longer commercially available), 3) a book with the visual fields, in which 4 fields per disc were presented half the regular size on facing pages (2 per page), 4) a score sheet, and 5) short instructions in their native tongue. All logistics were handled by a clinical research organization (MediTech Strategic Consultants B.V., Vaals, The Netherlands).

The ophthalmologists who were invited to participate were those who had taken part in the EODAT. We aimed to include approximately half of the invited ophthalmologists. In the United Kingdom, almost all ophthalmologists identify themselves by subspecialty interest, therefore we selected those with a glaucoma subspecialty interest.

Stereoscopic optic nerve head photographs

The stereoscopic photographs that we used in the present study were the same as previously described.⁵ In short, the set consisted of slides of ONHs that had been photographed with a simultaneous stereoscopic fundus camera (TRC-SS2, Topcon Medical Systems, Inc., Paramus, NJ, USA) at a 15° field of view. Only high quality images were used. We took images of 40 healthy eyes, 48 eyes with glaucoma, and also 6 with ocular hypertension. These were selected from a cohort of patients and controls who had been originally recruited for an ongoing longitudinal glaucoma study at the Rotterdam Eye Hospital. Nine photographs of glaucomatous eyes and of 7 healthy eyes were randomly selected and duplicated for assessing intraobserver agreement, totaling 110 stereophotographs. The sequence of the photographs was randomized and for each grader presented in the same order. To better estimate ONH size, reference slides of healthy, small (5th percentile), medium (50th percentile), and large (95th percentile) ONHs were provided.

Patient characteristics and in- and exclusion criteria have been described previously.¹ In short, all subjects were of white ethnic origin and had a best-corrected visual acuity of 20/40 or better. All subjects had reproducible and reliable visual fields with standard automated perimetry (SAP, Humphrey Field Analyzer II, white-on-white 24-2 program, Carl Zeiss Meditec AG, Jena, Germany). The healthy subjects all had normal visual fields, that is, a glaucoma hemifield test (GHT) within

normal limits and no nerve fiber bundle visual field defects in the total and/or pattern deviation probability plots. They had healthy-looking ONHs, as assessed by one of the glaucoma specialists at the Rotterdam Eye Hospital, and an intraocular pressure of ≤ 21 mmHg in both eyes. In the glaucomatous eyes, the disease was diagnosed by one of 4 glaucoma specialists of the Rotterdam Eye Hospital based on a glaucomatous appearance of the ONH (with notching or thinning of the neuroretinal rim, possibly with disc hemorrhages) and a matching defect with SAP. We classified the glaucoma patients by the severity of their visual field damage based on their mean deviation (MD; mild, $MD \geq -6$ dB [$n=27$]; moderate, -12 dB $\leq MD < -6$ dB [$n=13$]; severe, $MD < -12$ dB [$n=8$]).

The research adhered to the tenets of the Declaration of Helsinki. The institutional human experimentation committee had approved the research. Informed consent was obtained from the subjects after explanation of the nature and possible consequences of the study.

Visual field tests

For each presented optic disc, the participating ophthalmologists were asked to choose between 4 visual fields of which only 1 was the corresponding visual field. The visual fields were always presented in order of increasing disease severity, i.e. a normal and a mild, moderate and advanced glaucomatous visual field. The visual fields used as an alternative choice to match the ONH, were selected from the other included eyes, as follows. Firstly, the fields were divided into right and left eyes. Secondly, fields were grouped by disease severity, i.e., healthy, mild glaucoma ($MD \geq -6$ dB), moderate glaucoma (-12 dB $\leq MD < -6$ dB) and advanced glaucoma ($MD < -12$ dB). Thirdly, we randomly assigned eyes to 2 groups for difficulty of interpretation, based on the location of the defect in the visual field. One group contained eyes in which all 3 glaucomatous visual fields contained defects in the same hemifield, i.e. superior or inferior (Difficulty type 1). The second group contained 3 glaucomatous visual fields that were randomly selected, regardless of the location of the glaucomatous defect (Difficulty type 2). Because all visual fields included to this trial also served as an alternative choice for other visual fields, most of them were used several times for this purpose. There was 1 type of visual field loss that was not represented by the included glaucoma patients: mild glaucoma with an inferior scotoma. To have an alternative choice for moderate and advanced glaucomatous inferior scotomata we included such a visual field from a subject from another study at our hospital.

Data analysis

For each observer, we calculated the overall matching accuracy. Overall matching accuracy was defined as the number of correctly matched eyes divided by the total number of examined eyes. For each observer, we also calculated the matching sensitivity per group of disease severity (mild, moderate and advanced glaucoma, respectively) and the matching specificity (percentage correctly matched healthy discs). In addition, the overall matching accuracy was calculated for each country. When an optic disc was incorrectly classified, we calculated the level of mismatching. Levels were stratified by disease severity. When for instance a healthy eye was scored as an advanced glaucomatous eye, the level of mismatching was +3.

The matching intraobserver agreement in classifying disease severity was expressed as κ . The values for κ were classified as follows: ≤ 0.20 , poor; 0.21 to 0.40, fair; 0.41 to 0.60, moderate; 0.61 to 0.80, good; and ≥ 0.81 , very good.⁸

In the EODAT, all observers were asked to score every optic disc slide either as healthy or glaucomatous. We have determined this score for the current trial as well, by pooling the 3 glaucoma groups. We compared the outcome of every observer who had participated and had returned fully completed score sheets in both studies ($n=100$).

The data of eyes with ocular hypertension were not analyzed in the present study as they had merely been added to present a continuum of glaucomatous damage.

We used an analysis of variance (ANOVA) to evaluate differences in measurements between groups and countries. For differences in dichotomous variables between groups, we used the Pearson χ^2 test. We used the Kruskal-Wallis test to evaluate differences in level of mismatching. To compare the outcome of labeling as healthy or glaucoma per observer with the EODAT, we used paired t -tests. In the present study, a p -value of less than 0.05 was considered statistically significant. Statistical analyses were performed with PASW Statistics 18 for Windows (release 18.0.0, 2009, IBM SPSS Statistics, New York, USA).

The demographics of the healthy subjects and glaucoma patients have been presented in table 1.

RESULTS

Of the 260 ophthalmologists that were invited, 109 (39.5%) agreed to participate. Figure 1 shows the number of those invited per country and the number of participating ophthalmologists. All participants returned completed score sheets. The rate of responders varied considerably between countries. The highest response rate was in Greece (72.7%). Italy showed the lowest response rate of 16.7%.

Table 1 Demographics of Healthy Subjects and Glaucoma Patients

	Unit	Healthy subjects (n=40)	Glaucoma Patients (n=48)			P
			Mild (n=27)	Moderate (n=13)	Advanced (n=8)	
Age (SD; range)	yrs	59 (12;30-82)	63 (10;46-82)	63 (10;45-81)	54 (12;30-68)	0.16
Gender (male) (%)	NA	19 (48)	14 (52)	7 (54)	5 (63)	0.88
MD (SD; range)	dB	0.07 (0.92; -1.55 to 2.04)	-2.14 (1.72; -5.94 to 2.26)	-8.72 (1.42; -10.99 to -6.70)	-18.26 (4.01; -22.26 to -12.55)	<0.001
Randomized eye (right) (%)	NA	21 (53)	6 (22)	7 (54)	5 (63)	0.05

dB = decibel; MD = mean deviation; NA = not applicable; SD = standard deviation

Differences between the groups were tested for statistical significance with an analysis of variance for continuous variables and the Pearson chi-square test for dichotomous variables.

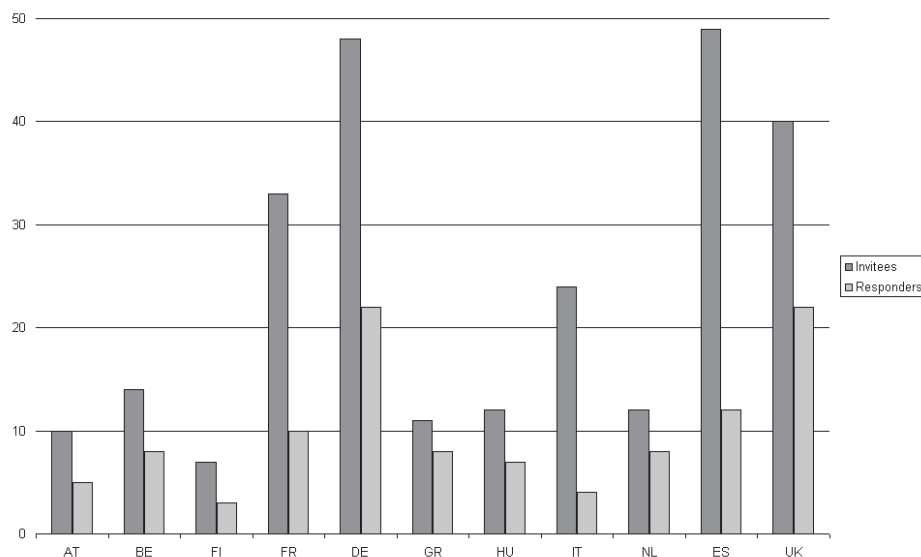


Figure 1 Histogram of the number of invited (*left*) and participating (*right*) ophthalmologists per country. AT: Austria; BE: Belgium; FI: Finland; FR: France; DE: Germany; GR: Greece; HU: Hungary; IT: Italy; NL: The Netherlands; ES: Spain; UK: United Kingdom.

Matching Accuracy

The overall matching accuracy of the 109 participating ophthalmologists for correctly matching stereoscopic optic disc photographs to their visual fields was 58.7%. The matching sensitivity for glaucomatous eyes was 30.9%, 51.4% and 75.8% for mild, moderate and advanced glaucoma, respectively. The matching specificity was 76.4%. None of the ONH stereo-slides was matched correctly by all observers. One mild

glaucomatous ONH was correctly scored by only 3 observers (2.8%). An analysis of variance showed that there were statistically significant differences in the matching accuracy between the various countries ($p<0.05$), except for the matching sensitivity for advanced glaucomatous eyes ($p=0.192$). The participants of the United Kingdom (glaucoma subspecialist group) performed better than the general ophthalmologists of the other countries. This was statistically significant for 7 other countries ($p<0.05$), except for Austria, Finland and The Netherlands. The results of correctly matching ONHs to their appropriate visual field have been presented in Table 2.

Table 2 Matching Accuracy for correctly matching stereoscopic optic disc photographs to their visual field by ophthalmologists from various countries, presented for each disease severity.

	Observers (n)	Overall matching accuracy (%)	Matching Specificity (%)	Matching Sensitivity (%)		
			Healthy (n=40)	Mild (n=27)	Moderate (n=13)	Advanced (n=8)
Overall	109	58.7 (51.6)	76.4 (30.6)	30.9 (8.3)	51.4 (6.7)	75.8 (6.1)
Austria	5	63.9 (56.2)	83.5 (33.4)	33.3 (9.0)	53.8 (7.0)	85.0 (6.8)
Belgium	8	57.5 (50.6)	73.4 (29.3)	30.1 (8.1)	52.9 (6.9)	78.1 (6.3)
Finland	3	62.9 (55.3)	90.0 (36.0)	22.2 (6.0)	53.8 (7.0)	79.2 (6.3)
France	10	50.6 (44.5)	68.8 (27.5)	21.9 (5.9)	41.5 (5.4)	71.3 (5.7)
Germany	22	57.6 (50.7)	75.9 (30.4)	32.0 (8.6)	49.3 (6.4)	66.4 (5.3)
Greece	8	54.7 (48.1)	67.8 (27.1)	33.8 (9.1)	44.2 (5.8)	76.6 (6.1)
Hungary	7	53.4 (47.0)	70.4 (28.1)	30.2 (8.1)	42.9 (5.6)	64.3 (5.1)
Italy	4	54.0 (47.5)	68.8 (27.5)	34.3 (9.3)	38.5 (5.0)	71.9 (5.8)
The Netherlands	8	61.4 (54.0)	80.3 (32.1)	33.3 (9.0)	50.0 (6.5)	79.7 (6.4)
Spain	12	53.7 (47.3)	67.5 (27.0)	25.3 (6.8)	50.0 (6.5)	86.5 (6.9)
United Kingdom	22	67.8 (59.7)	87.8 (35.1)	35.4 (9.6)	65.7 (8.6)	80.7 (6.5)

Overall matching accuracy, matching specificity and matching sensitivity are presented as mean (number).

Mismatching

When the observers incorrectly matched the ONH to the visual field, they tended to overestimate the severity of visual field damage (Kruskal-Wallis test, $p<0.001$). Figure 2 shows the amount of under- and overestimation of the incorrectly scored stereo slides.

The incorrectly scored healthy eyes were, on average, overestimated by 1.33 (SD 0.60) classes. Mild glaucomatous eyes were overestimated by, on average, 0.65 (SD 1.22; $p<0.001$) classes, while moderate and advanced glaucomatous eyes were underestimated, by, on average, -0.05 (SD 1.15; $p<0.001$) and -1.26 (SD 0.54) classes, respectively. We found statistically significant differences in the level of mismatching between the various countries (Kruskal-Wallis test, $p<0.001$).

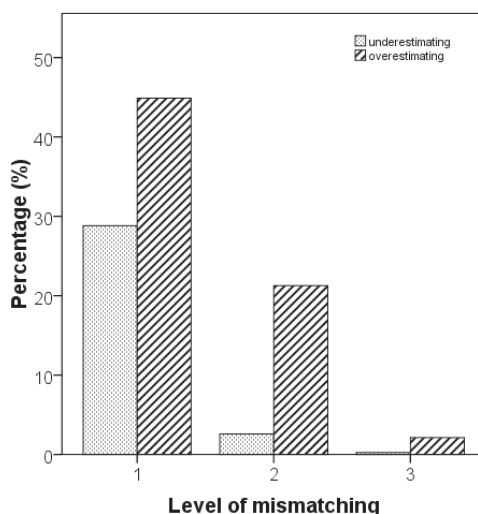


Figure 2 Histogram of the percentage of mismatched optic disc stereo slides to their corresponding visual field. The level of mismatching represents the under- or overestimation of the visual field damage stratified per disease severity.

Difficulty

The ophthalmologists had somewhat more trouble in correctly matching the ONH to the appropriate visual field when the alternative choices all showed a glaucomatous defect in the same hemifield (Difficulty Type 1) than when the location of the alternative scotomata had been randomized (Difficulty Type 2; $p=0.04$). The overall matching accuracy was 57.0% and 60.4%, respectively, for Difficulty Types 1 and 2. Within Difficulty group Type 1, any mismatches were equally balanced for over- and underestimating the severity of glaucoma ($p=0.09$).

Matching intraobserver agreement

The matching intraobserver agreement within the ESAFAT data, expressed as κ , was on average moderate (0.52; SD 0.23), ranging between -0.04 and 1.00.

Comparison of ESAFAT with EODAT

We compared the accuracy of classifying optic discs as healthy or glaucomatous for every individual ophthalmologist participating fully in both the current trial and the EODAT ($n=100$); for each, we also determined the intraobserver agreement.

Diagnostic accuracy

The overall accuracy and the specificity of the participating ophthalmologists were statistically significantly higher in the EODAT than in the ESAFAT ($p \leq 0.009$). Their

Table 3 Diagnostic accuracy for discriminating between healthy and glaucomatous eyes on the basis of clinical assessment of stereoscopic optic disc photographs for diagnosis glaucoma by ophthalmologists, presented for the current ESAFAT and the corresponding EODAT.

	Observers (n)	Sensitivity (%)			Specificity (%)			Overall Accuracy (%)		
		ESAFAT	EODAT	p-value	ESAFAT	EODAT	p-value	ESAFAT	EODAT	p-value
Overall	100	85.6 ± 8.0	76.3 ± 10.0	<0.001	77.1 ± 16.9	89.7 ± 9.1	<0.001	80.7 ± 6.9	82.4 ± 6.3	0.009
United Kingdom	21	85.8 ± 5.8	81.0 ± 9.7	0.026	88.3 ± 6.8	94.4 ± 5.1	0.001	86.0 ± 2.7	87.1 ± 4.9	0.290

ESAFAT: European Structure And Function Trial; EODAT: European Optic Disc Assessment Trial

Sensitivity, specificity and overall accuracy are presented as mean ± standard deviation.

Differences between groups were tested for statistical significance with a paired t-test.

sensitivity for glaucomatous discs was higher in the ESAFAT ($p < 0.001$). The participants of the United Kingdom (glaucoma subspecialist group) performed better than the general ophthalmologists of the other countries in both the ESAFAT and EODAT ($p < 0.023$ in all countries, except for Austria, Finland and The Netherlands in the ESAFAT and Austria, Finland and Spain in the EODAT). The overall diagnostic accuracy of all ophthalmologists together and that of the participants of the United Kingdom has been presented in Table 3.

Intraobserver agreement

The intraobserver agreement of optic disc classification in the ESAFAT, expressed as κ , was on average moderate (0.57; SD 0.25), and worse than in the EODAT, which was good (0.71; SD 0.23; paired t-test; $p < 0.001$).

DISCUSSION

Ophthalmologists across Europe correctly matched stereoscopic photographs of healthy and glaucomatous optic discs of various stages of the disease to their corresponding visual field in only approximately 59% of cases. In misclassifications of early glaucomatous ONHs, the severity of glaucomatous visual field damage was more often overestimated than underestimated.

The conditions of our current trial were almost ideal. The ophthalmologists were asked to grade stereo-photographs of good quality and match them to reliable visual fields with no artifacts. This contrasts markedly with assessing optic discs and visual fields in everyday clinical care, in which both the visual fields and the stereoscopic visibility of the optic discs may be suboptimal. In addition, we presented the observers four visual fields per optic disc photograph to choose from, in arbitrarily selected classes, and selected only perimetric glaucoma cases. These experimental conditions may have yielded an overestimation of the performance of general ophthalmologists in Europe under real life circumstances.

In the current investigation we re-targeted our previous (EODAT) ophthalmologist population¹, to see whether their classification performance was improved. Despite the statistically significant, but small differences between the two trials, it remains somewhat speculative whether the presence of visual fields weakens or strengthens general ophthalmologists' ability to diagnose glaucoma. Though classification accuracies were statistically significantly different in the two investigations, the outcome of the current trial confirms the outcome of EODAT¹, i.e. that general ophthalmologists classify optic discs only moderately well for detecting glaucoma, especially in the early stage of the disease. It is likely that whenever

clinical classification of visual fields and optic discs correspond, clinicians will feel more confident about their judgment than in cases when structure and function are thought to disagree. Visual fields that may look relatively good, compared to the optic discs, may even put the clinician off guard. However, it is unclear to what extent these presumed effects might impact on clinical decision making.

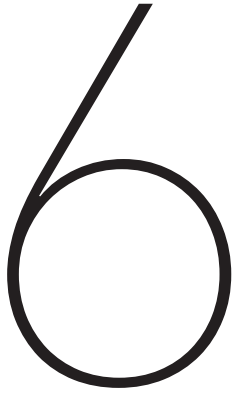
Another interpretation of our findings is that the participating ophthalmologists were suboptimally trained. Years of training leads to an improved judgment of optic discs (Zeyen T et al., *Invest Ophthalmol Vis Sci* 2011,43:4169)^{9,10}, as was also illustrated by the modest difference between the diagnostic accuracy of the trained UK glaucoma specialists and the general ophthalmologists in our current study, as well as in the EODAT trial. On the other hand, even glaucoma specialists may have difficulties in judging optic discs.^{6,7,11} Perhaps both general ophthalmologists and glaucoma specialists require better or more training. Several glaucoma associations worldwide have been taking effort to improve the ability of (general) ophthalmologists and residents to judge optic discs and visual fields by organizing various educational programs. Education and training of ONH judgment (Zeyen T et al., *Invest Ophthalmol Vis Sci* 2011,43:4169)^{9,10,12,13} as well as of visual field testing at an appropriate re-test frequency¹⁴ are most likely to yield optimal monitoring of glaucoma. Our findings do not necessarily apply to other parts of the world, where training programs may be quite different from those in Europe, which already happen to be quite heterogenic.

In conclusion, we think that both clinical ONH judgment and evaluation of visual field test results remain important mainstays in daily clinical care. Continuous education of general ophthalmologists in both areas is therefore particularly important.



REFERENCES

1. Reus NJ, Lemij HG, Garway-Heath DF, et al. Clinical assessment of stereoscopic optic disc photographs for glaucoma: the European Optic Disc Assessment Trial. *Ophthalmology* 2010;117:717-23.
2. Abrams LS, Scott IU, Spaeth GL, et al. Agreement among optometrists, ophthalmologists, and residents in evaluating the optic disc for glaucoma. *Ophthalmology* 1994;101:1662-7.
3. Andersson S, Heijl A, Bengtsson B. Optic disc classification by the Heidelberg Retina Tomograph and by physicians with varying experience of glaucoma. *Eye (Lond)* 2011;25:1401-7.
4. Girkin CA, McGwin G Jr, Long C, et al. Subjective and objective optic nerve assessment in African Americans and whites. *Invest Ophthalmol Vis Sci* 2004;45:2272-8.
5. Reus NJ, de Graaf M, Lemij HG. Accuracy of GDx VCC, HRT I, and clinical assessment of stereoscopic optic nerve head photographs for diagnosing glaucoma. *Br J Ophthalmol* 2007;91:313-8.
6. Varma R, Steinmann WC, Scott IU. Expert agreement in evaluating the optic disc for glaucoma. *Ophthalmology* 1992;99:215-21.
7. Wollstein G, Garway-Heath DF, Fontana L, Hitchings RA. Identifying early glaucomatous changes. Comparison between expert clinical assessment of optic disc photographs and confocal scanning ophthalmoscopy. *Ophthalmology* 2000;107:2272-7.
8. Altman DG. *Practical Statistics for Medical Research*. London: Chapman and Hall; 1991:406-7.
9. Andersson S, Heijl A, Boehm AG, Bengtsson B. The effect of education on the assessment of optic nerve head photographs for the glaucoma diagnosis. *BMC Ophthalmol* [serial online] 2011;11:12. Available at: <http://www.biomedcentral.com/1471-2415/11/12>. Accessed April 21, 2013.
10. Law SK, Tamboli DA, Ou Y, et al. Development of a resident training module for systematic optic disc evaluation in glaucoma. *J Glaucoma* 2012;21(9):601-7.
11. Jampel HD, Friedman D, Quigley H, et al. Agreement among glaucoma specialists in assessing progressive disc changes from photographs in open-angle glaucoma patients. *Am J Ophthalmol* 2009;147:39-44.
12. World Glaucoma Association; Available at: <http://www.worldglaucoma.org> . Accessed at May 21st, 2013.
13. European Glaucoma Society. Available at: <http://www.eugs.org> . Accessed at May 21st, 2013.
14. Jansonius NM. Progression detection in glaucoma can be made more efficient by using a variable interval between successive visual field tests. *Graefes Arch Clin Exp Ophthalmol* 2007;45:1647-51.



Detecting progression in
glaucoma; a comparison
between visual fields and
stereoscopic photographs of
the optic nerve head.

Josine van der Schoot, Robine Donken, Hans G Lemij

Submitted

ABSTRACT

Purpose. Progression of glaucoma can be monitored by assessment of functional changes in visual fields and structural changes of the optic nerve head (ONH) and retinal nerve fibre layer. This study determines the association between those techniques used most in daily glaucoma care for detecting glaucoma progression; i.e. standard automated perimetry (SAP) and clinical assessment of the ONH; to explore the latter, we use stereoscopic photographs. It also investigates any differences among various eye-care professionals in their ability to detect progression on sequential stereoscopic ONH photographs.

Methods. Stereoscopic ONH photographs of 67 glaucomatous eyes were assessed by 4 optometrists, 4 ophthalmology residents, 4 general ophthalmologists and 4 glaucoma specialists. Their scores were compared with the outcome of progression analysis software on SAP (Guided Progression Analysis (GPA); Humphrey Field Analyzer II-i, Carl Zeiss Meditec, Dublin, USA).

Results. There were no statistically significant differences between the progression detected by the GPA and that by the professionals, but there was no association found ($p=0.096$). Inter observer agreement was fair in all professions and highest among glaucoma specialists (intra class correlation coefficient = 0.302). The intra observer agreement ranged between κ -0.333 and 1.0 (average 0.474).

Conclusions. In this study on glaucomatous progression, there was poor agreement between visual fields and ONH changes scored by eye care professionals. The overall accuracy for the use of stereoscopic photographs in detecting glaucomatous progression was poor.

INTRODUCTION

In daily glaucoma practice, the appearance of the optic nerve head (ONH) is one of the first aspects a clinician judges, next to the intraocular pressure (IOP) and the visual field. Although most ophthalmic clinicians assess multiple ONHs per day, general ophthalmologists poorly judge an ONH as healthy or glaucomatous.¹ They are even outperformed in correctly classifying eyes by devices measuring structural glaucomatous change, such as scanning laser polarimetry (SLP) and scanning laser tomography (SLT).¹ The assessment of an ONH for making a diagnosis is sensitive to subjective judgment, and judging it for progression detection probably also.¹⁻⁴

None of the various methods for detecting structural glaucomatous progression, such as SLP, SLT and optical coherence tomography, is generally accepted as a gold standard.⁵ In a study comparing two structural methods to detect progression, stereoscopic ONH photography and SLT, there was poor agreement between the two.⁶ Substantial variability in the interpretation of glaucomatous progression in ONH photographs exists.^{7,8} Arguably, assessment of the ONH by stereo-photographs most closely reflects the clinical setting.⁹

Glaucomatous progression detected by visual fields is usually seen as the gold standard. However, the agreement between expert clinicians using serial printouts of the Humphrey Field Analyzer (HFA) to detect progression turns out to be poor.¹⁰ Since the introduction of progression analysis software, such as the Glaucoma Progression Analysis on the Humphrey Field Analyzer, a more sophisticated way of detecting progression is introduced, leading to a higher interobserver agreement.⁵

In monitoring glaucoma, determining whether structural or functional progression has occurred is an important challenge.^{11,12} The exact relationship between structure and function in glaucoma has not yet been clarified.¹³⁻¹⁶ Apparently, structural progression often precedes functional progression.^{11,15,17-20} On the other hand, one of the largest trials in measuring conversion from ocular hypertension into glaucoma, the Ocular Hypertension Treatment Study, found that conversion to glaucoma was first detected in ONH photography in around 50% and by visual field testing in approximately 40%.²¹ In earlier studies on progression detection on visual fields, progression was detected by means of extensive, complicated or nowadays outdated analyses of the visual fields.^{17,18,21-24} In this study, we therefore implemented the latest progression analyses in standard automated perimetry and explored their ability to detect glaucomatous progression in visual fields. Because ONH assessment and visual field testing is performed most often in daily glaucoma care, we explored both the progression detection in visual fields and the clinical assessment of glaucomatous progression in ONH stereo-photographs. This study also explores any differences among various Dutch eye-care professionals in judging progression on these ONH stereo-photographs.

METHODS

Subjects

Seventy-two glaucomatous eyes were selected from a cohort of patients in an ongoing prospective, longitudinal imaging study at the Rotterdam Eye Hospital (REH) that adheres to the tenets of the Declaration of Helsinki and that was approved by the Medical Ethics Committee of the Erasmus Medical Centre, Rotterdam, The Netherlands. Informed consent was obtained from all subjects. All subjects were Caucasian and had a best-corrected visual acuity of 20/40 or better. None of them had a history of intraocular surgery (except for uncomplicated cataract or glaucoma surgery) or of coexisting ocular disease. Their treatment for glaucoma was part of standard clinical care. Glaucoma had been diagnosed by a glaucoma specialist based on the appearance of the ONH and a corresponding reproducible visual field defect with SAP.

For the current study, only those subjects from the cohort were selected with at least a five year interval between the first and last stereo ONH photographs, leading to the amount of 72 eligible eyes. Stereo ONH photographs were taken once or twice yearly and SAP visual fields were taken every 6 months. Baseline ONH stereo-photographs as well as the last ones were taken at the same visit as the visual field tests.

Stereoscopic ONH photographs

The ONHs were photographed with a simultaneous stereoscopic fundus camera (TRC-SS2, Topcon Medical Systems Inc., Paramus, NJ, USA) with a 15 degree field of view. A total of 8 eyes was randomly selected and included twice to test the intra observer agreement. In all, we had a set of 80 pairs of stereoscopic ONH slides.

Clinical assessment of stereoscopic ONH photographs

The stereoscopic ONH slides were evaluated by a total of 16 observers: 4 optometrists, 4 senior residents in ophthalmology, 4 general ophthalmologists and 4 glaucoma specialists, who all worked at the REH. The observers received the ONH slides and 2 viewers (Asahi Pentax Stereo Viewer II, Hoya Corporation, Tokyo, Japan). The observers also received a score sheet that briefly explained which signs of progression to look for: any narrowing of the neuroretinal rim, changes in defects of the RNFL, generalised thinning of the RNFL, the presence of disc haemorrhages, changes to the position of the blood vessels, as well as changes in any peripapillary atrophy. The observers individually classified the pairs of ONH slides as either progressing or stable. The slide-pairs were presented in chronological order, and the observers were informed as such. This chronological order of slides was used to mimic the clinical setting as much as possible.

Standard Automated Perimetry (SAP)

SAP was obtained by HFA (Humphrey Field Analyzer II, Carl Zeiss Meditec AG, Jena, Germany) by either using the 24-2 Full Threshold (FT) or the 24-2 Swedish Interactive Thresholding Algorithm (SITA) strategies or a combination of both. During the course of this trial, we decided to use the Sita-Standard (SS) test paradigm instead of the Full-Threshold (FT) test paradigm, since it was thought to improve the quality and shorten the test-time of the visual fields, without compromising their outcome.^{25,26} All subjects had reproducible VF defects. Only reliable tests were included. To that end, all of the following criteria had to be met: fixation losses $FT \leq 20\%$, $SITA \leq 7\%$; false positive and negative rate $FT \leq 33\%$, $SITA \leq 7\%$.

Glaucomatous progression of the VF was determined by using the visual field index (VFI) trend analysis of the Glaucoma Progression Analysis (GPA) software on the HFA (HFA-II-i, Software Version 4.2, CZM, Dublin, CA, USA), expressed in %/year. We randomly selected 14 VFs for the GPA whenever more tests were eligible, because 14 is the maximum for the GPA. The 2 baseline exams, as well as the final one were always included. The eyes were classified as progressing if the slope of the VFI was negative and statistically significant over time ($p < 0.05$).

Data analysis

The statistical analyses were performed with SPSS for Windows (release 15.0, 2005, SPSS inc., Chicago, IL, USA). McNemar's tests were used to calculate if there were statistically significant ($p < 0.05$) differences between the progression determined by GPA or by assessment of eye-care professionals. The qualification of progression during the assessment by the professionals, was measured by a census of 75% of the professionals. Spearman's Rho was used to measure if there was a linear relation between the rate of progression and the number of eye-care professionals who detected progression. The intra observer agreement was expressed as κ . The values for κ were classified as follows: ≤ 0.20 , poor; 0.21 to 0.40, fair; 0.41 to 0.60, moderate; 0.61 to 0.80, good; and ≥ 0.81 , very good.²⁷ The inter observer agreement was expressed as an intra class correlation coefficient (ICC). The values for ICC were classified as described earlier for κ . The ICC was calculated for the overall group and per group of eye-care professionals. Sensitivities and specificities were calculated for each individual observer, with the GPA outcome as a reference.

The ONH photographs of 5 subjects were deemed to be of too poor quality by at least 6 of the observers. These photographs were therefore excluded from further analysis, so that a total of 67 eyes remained.

RESULTS

More than half (52.2%) of our cohort of 67 glaucomatous eyes showed progression based on the GPA of the visual fields, using the visual field index (VFI in %/year). The rate of progression of progressing eyes was significantly higher than that of non-progressing eyes ($p<0.0001$). The demographics of the glaucomatous patients are shown in Table 1. In addition, we explored the correlation between the rate of progression and the number of professionals who detected progression in the ONH stereo-photographs (Fig. 1).

Table 1 Demographics of glaucomatous eyes (n=67)

		Unit	Subjects
Age at inclusion		Years (SD;range)	59 (10; 29-77)
Gender		% male	63
			Glaucomatous eyes
Time between photos		Months (SD;range)	88 (8; 62-119)
MD t(0)		dB (SD)	-8.22 (5.7)
MD t(end)		dB (SD)	-9.94 (5.6)
GPA - Progression (negative slope significant $p<0.05$)		Number (%)	35 (52.2)
Rate of progression	Overall	(Mean %/year) (\pm 95% CI)	-0.7 (\pm 0.8)
	Progressing eyes	(Mean %/year) (\pm 95% CI)	-1.3 (\pm 1.2)
	Non-progressing eyes	(Mean %/year) (\pm 95% CI)	-0.1 (\pm 0.4)

Abbreviations: dB = decibel, MD = mean deviation, SD = standard deviation, GPA = Glaucoma Progression Analysis; CI = confidence interval

The correlation between the rate of field progression and the number of observers that detected ONH progression was tested by using Spearman's Rho and turned out to be statistically non-significant (-0.286 , $p=0.096$).

Observer agreement

The overall intra class correlation (ICC) for inter observer agreement was 0.168, indicating poor agreement among all observers. Each of the various professionals scored a fair agreement within their respective groups (Table 2). The intra observer agreement was on average moderate ($\kappa = 0.474$; Table 2). Nevertheless there was a great range between the different professions and professionals. Some observers mentioned that there were slides duplicated. It is possible they, and others as well, therefore purposely reassessed these photographs, thereby checking what they had previously answered, to be more consistent. This might have adversely affected the reliability of the intra observer reproducibility. Nevertheless, it was generally quite poor. It may, however, possibly explain why some observers reached a perfect intra-observer agreement with a κ of 1.0.

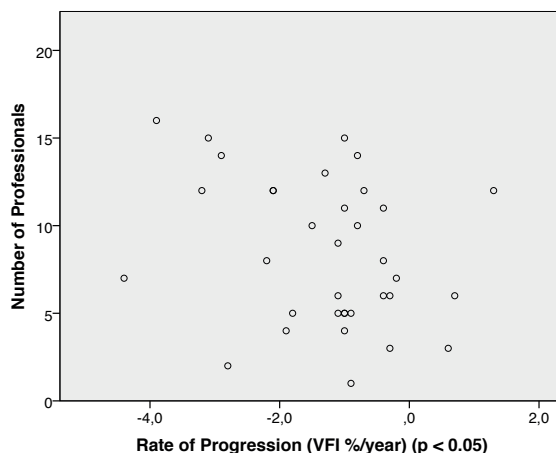


Figure 1 The rate of progression of the visual field index (VFI, statistically significant) as scored by the glaucoma progression analysis (GPA) software on visual fields versus the number of professionals who detected progression based on optic nerve head stereo photographs.

Table 2 Observer agreement for the various professions in assessing stereoscopic ONH photographs

	Inter observer agreement	Intra observer agreement	
	ICC	Mean κ	Range
Optometrists	0.252	0.750	0.500 - 1.000
Residents in Ophthalmology	0.264	-0.008	-0.250 - 0.467
Ophthalmologists	0.246	0.319	-0.333 - 1.000
Glaucoma Specialists	0.302	0.835	0.588 - 1.000
Overall	0.168	0.474	-0.333 - 1.000

Abbreviations: ICC = intra class correlation

Sensitivity and specificity

The mean sensitivity for the observers in detecting progression on ONH photographs compared to the GPA II was 0.531 [SD 0.13]. The mean specificity was 0.604 [SD 0.10]. The sensitivity and specificity of all individual observers have been shown in Table 3.

DISCUSSION

We found no correlation between the rate of progression and the number of professionals that detected progression on sequential stereoscopic ONH photographs. This may not be very surprising, because several studies have shown that

Table 3 Sensitivity and specificity for different observers in assessing stereoscopic ONH photographs

	Sensitivity	Specificity	Overall accuracy
Optometrist 1	0.343	0.531	0.437
Optometrist 2	0.486	0.594	0.540
Optometrist 3	0.571	0.500	0.536
Optometrist 4	0.371	0.719	0.545
Resident 1	0.543	0.688	0.615
Resident 2	0.571	0.375	0.473
Resident 3	0.686	0.750	0.718
Resident 4	0.600	0.594	0.597
Ophthalmologist 1	0.400	0.594	0.497
Ophthalmologist 2	0.486	0.688	0.587
Ophthalmologist 3	0.706	0.469	0.587
Ophthalmologist 4	0.571	0.656	0.614
Glaucoma Specialist 1	0.771	0.594	0.683
Glaucoma Specialist 2	0.364	0.710	0.537
Glaucoma Specialist 3	0.429	0.625	0.527
Glaucoma Specialist 4	0.600	0.581	0.590

the correlation between structure and function in glaucoma is generally weak, and also in glaucomatous progression.^{13-15;20;28;29} In our study, the progression seen on the ONH stereo-photographs did not match the progression scored by the GPA. In fact, there was no relation at all. For instance, there was a case with an ROP of -4.0, which only half of the observers scored as structural ONH progression. On the other end of the scale, there was a case in which about 75% of the professionals scored ONH progression and the GPA didn't show any progression. This outcome confirms other studies, suggesting that structural and functional progression are independent indicators of progressive disease.¹³ Therefore, it is probably wise to use both structural and functional measurements clinically, to avoid missing any progressing cases.

Because we used the GPA progression criterion as a reference standard, the sensitivity and specificity of ONH photographs progression assessments were, not surprisingly, disappointing, given the poor correlation between structural and functional progression. The poor sensitivity and specificity of ONH assessments might therefore probably be seen as indicators of a poor correlation between structural and functional progression^{28;29}, rather than as poor performance of the observers. Nevertheless, a possibly poor performance should also be taken into account. Friedman et al. found that 40 percent of all stereoscopic ONH photographs that were classified as progressing, were in fact replicates of baseline photographs,

which indicates that the judgment of such photographs is quite poor, even by glaucoma specialists.⁸ Clinically using both structural and functional methods of progression detection runs the risk of overcalling, since both methods show significant measurement variability; this may be avoided by setting high specificity criteria for each, which may in part be achieved by requiring progression to be reproducible.

We found a fair agreement in detecting progression in sequential ONH photographs between eye care professionals within their various groups. Jampel et al., in a group of glaucoma specialists, found somewhat worse results, which may perhaps be explained by differences in methods; one such difference was that they used stereoscopic ONH photographs that were taken sequentially, instead of simultaneously (as in our study).⁸ In our group as a whole, the inter observer agreement for ONH progression detection was poor. We decided to present the photographs in chronological order and inform the observers about the sequence. The chronological order might have affected the results.³⁰ The group of glaucoma specialists in our study had a slightly better inter observer agreement than the other groups of observers. For making a diagnosis of glaucoma on stereoscopic ONH photographs, it was also observed that glaucoma specialists generally did better than other eye care professionals with less training and experience.³¹ This may suggest that training and experience improve the consistency of detecting both structural damage and progression in stereoscopic ONH photographs.

Although we had a small sample size for calculating the intra observer agreement, we found that the intra observer agreement of detecting glaucomatous progression varied widely across observers, which confirms other studies.^{4,9} This means that some observers are very consistent and others are not. We think that few clinicians are aware of their own consistency in judging glaucomatous ONH progression. Perhaps training could improve that consistency. We found that the optometrists and glaucoma specialists did better than the other groups of observers, perhaps because they were more experienced. We think, however, that clinicians that do not regularly assess simultaneous stereoscopic ONH photographs will be even less likely to consistently detect structural glaucomatous progression, when they resort to less accurate methods, e.g., descriptions or drawings of the ONH in the medical records. This probably calls for objective structural measures for detecting glaucomatous progression. Although we are unaware how many clinicians use stereoscopic ONH photographs for follow-up in their glaucoma management, we think this number is relatively small. Probably many more make descriptions or (annotated) drawings, or simply write down cup-to-disc (C/D) ratios. To our knowledge, the accuracy of these methods for detecting glaucoma progression

has never been formally assessed, although baseline C/D ratios have been shown to be predictive of future visual field loss.^{32,33}

In daily care, next to the IOP, the appearance of the ONH and the visual field are the standard means to monitor glaucoma. This study confirms earlier evidence of the generally poor performance of eye care professionals to properly judge an ONH as progressing or not, let alone determining the rate of progression. By applying the latest commercially available progression algorithms on visual fields, we used the analyses resembling standard basic, modern daily glaucoma care. Even with the latest visual field progression algorithms, the correlation with ONH assessment was strikingly poor. The use of optical coherence tomography (OCT), a structural measurement technique currently implemented more often in daily glaucoma practice, may be promising. Several studies have shown OCT to predict progression on visual fields.³⁴⁻³⁶ The thickness of the RNFL^{35,36} as well as the thickness of the macular ganglion cell complex³⁴ predicts visual field loss in the following years. Taken together, these results suggest the potentially important clinical role of OCT measurements in glaucoma care; they appear to hold considerably greater promise than the clinical assessment of the ONH by an ophthalmologist.

In conclusion, our results confirm earlier work that there is a poor agreement between structural and functional progression detection in the clinical assessment of serial stereoscopic ONH photographs and visual fields in glaucoma. To our dismay, the latest version of the GPA did not markedly improve this correlation. In addition, we observed that the inter observer agreement was poor to fair for judging ONH photographs. The intra observer agreement for ONH photographs was also highly variable and sometimes alarmingly poor. In general, glaucoma specialists judged ONH photographs for progression detection slightly more consistently than did less experienced eye care professionals.

ACKNOWLEDGMENTS

We would like to thank the participating glaucoma specialists, general ophthalmologists, ophthalmology residents and optometrists of the Rotterdam Eye Hospital.



REFERENCE LIST

1. Reus NJ, Lemij HG, Garway-Heath DF, et al. Clinical assessment of stereoscopic optic disc photographs for glaucoma: the European Optic Disc Assessment Trial. *Ophthalmology* 2010;117:717-23.
2. Abrams LS, Scott IU, Spaeth GL, et al. Agreement among optometrists, ophthalmologists, and residents in evaluating the optic disc for glaucoma. *Ophthalmology* 1994;101:1662-7.
3. Wollstein G, Garway-Heath DF, Fontana L, Hitchings RA. Identifying early glaucomatous changes. Comparison between expert clinical assessment of optic disc photographs and confocal scanning ophthalmoscopy. *Ophthalmology* 2000;107:2272-7.
4. Zeyen T, Miglior S, Pfeiffer N, et al. Reproducibility of evaluation of optic disc change for glaucoma with stereo optic disc photographs. *Ophthalmology* 2003;110:340-4.
5. Viswanathan AC, Crabb DP, McNaught AI, et al. Interobserver agreement on visual field progression in glaucoma: a comparison of methods. *Br J Ophthalmol* 2003;87:726-30.
6. O'Leary N, Crabb DP, Mansberger SL, et al. Glaucomatous progression in series of stereoscopic photographs and Heidelberg retina tomograph images. *Arch Ophthalmol* 2010;128:560-8.
7. Chauhan BC, Hutchison DM, Artes PH, et al. Optic disc progression in glaucoma: comparison of confocal scanning laser tomography to optic disc photographs in a prospective study. *Invest Ophthalmol Vis Sci* 2009;50:1682-91.
8. Jampel HD, Friedman D, Quigley H, et al. Agreement among glaucoma specialists in assessing progressive disc changes from photographs in open-angle glaucoma patients. *Am J Ophthalmol* 2009;147:39-44.
9. Azuara-Blanco A, Katz LJ, Spaeth GL, et al. Clinical agreement among glaucoma experts in the detection of glaucomatous changes of the optic disk using simultaneous stereoscopic photographs. *Am J Ophthalmol* 2003;136:949-50.
10. Alencar LM, Zangwill LM, Weinreb RN, et al. Agreement for detecting glaucoma progression with the GDx guided progression analysis, automated perimetry, and optic disc photography. *Ophthalmology* 2010;117:462-70.
11. Breusegem C, Fieuws S, Stalmans I, Zeyen T. Agreement and accuracy of non-expert ophthalmologists in assessing glaucomatous changes in serial stereo optic disc photographs. *Ophthalmology* 2011;118:742-6.
12. Kourkoutas D, Buys YM, Flanagan JG, et al. Comparison of glaucoma progression evaluated with Heidelberg retina tomograph II versus optic nerve head stereophotographs. *Can J Ophthalmol* 2007;42:82-8.
13. Artes PH, Chauhan BC. Longitudinal changes in the visual field and optic disc in glaucoma. *Prog Retin Eye Res* 2005;24:333-54.
14. Garway-Heath DF, Poinoosawmy D, Fitzke FW, Hitchings RA. Mapping the visual field to the optic disc in normal tension glaucoma eyes. *Ophthalmology* 2000;107:1809-15.
15. Girkin CA. Relationship between structure of optic nerve/nerve fiber layer and functional measurements in glaucoma. *Curr Opin Ophthalmol* 2004;15:96-101.
16. Strouthidis NG, Scott A, Peter NM, Garway-Heath DF. Optic disc and visual field progression in ocular hypertensive subjects: detection rates, specificity, and agreement. *Invest Ophthalmol Vis Sci* 2006;47:2904-10.

17. Mohammadi K, Bowd C, Weinreb RN, et al. Retinal nerve fiber layer thickness measurements with scanning laser polarimetry predict glaucomatous visual field loss. *Am J Ophthalmol* 2004;138:592-601.
18. Schrems-Hoesl LM, Schrems WA, Laemmer R, et al. Confocal Laser Scanning Tomography to Predict Visual Field Conversion in Patients With Ocular Hypertension and Early Glaucoma. *J Glaucoma* 2014.
19. Sommer A, Katz J, Quigley HA, et al. Clinically detectable nerve fiber atrophy precedes the onset of glaucomatous field loss. *Arch Ophthalmol* 1991;109:77-83.
20. Zeyen TG, Caprioli J. Progression of disc and field damage in early glaucoma. *Arch Ophthalmol* 1993;111:62-5.
21. Keltner JL, Johnson CA, Anderson DR, et al. The association between glaucomatous visual fields and optic nerve head features in the Ocular Hypertension Treatment Study. *Ophthalmology* 2006;113:1603-12.
22. Johnson CA, Sample PA, Cioffi GA, et al. Structure and function evaluation (SAFE): I. criteria for glaucomatous visual field loss using standard automated perimetry (SAP) and short wavelength automated perimetry (SWAP). *Am J Ophthalmol* 2002;134:177-85.
23. Leske MC, Heijl A, Hyman L, Bengtsson B. Early Manifest Glaucoma Trial: design and baseline data. *Ophthalmology* 1999;106:2144-53.
24. Miglior S, Zeyen T, Pfeiffer N, et al. The European glaucoma prevention study design and baseline description of the participants. *Ophthalmology* 2002;109:1612-21.
25. Artes PH, Iwase A, Ohno Y, et al. Properties of perimetric threshold estimates from Full Threshold, SITA Standard, and SITA Fast strategies. *Invest Ophthalmol Vis Sci* 2002;43:2654-9.
26. Heijl A, Bengtsson B, Patella VM. Glaucoma follow-up when converting from long to short perimetric threshold tests. *Arch Ophthalmol* 2000;118:489-93.
27. Altman DG. *Practical Statistics for Medical Research*. London: Chapman and Hall; 1991:406-7.
28. Chauhan BC, Nicolela MT, Artes PH. Incidence and rates of visual field progression after longitudinally measured optic disc change in glaucoma. *Ophthalmology* 2009;116:2110-8.
29. Kass MA, Gordon MO, Kymes SM. Incorporating the results of the Ocular Hypertension Treatment Study into clinical practice. *Arch Ophthalmol* 2005;123:1021-2.
30. Altangerel U, Bayer A, Henderer JD, et al. Knowledge of chronology of optic disc stereophotographs influences the determination of glaucomatous change. *Ophthalmology* 2005;112:40-3.
31. Reus NJ, de GM, Lemij HG. Accuracy of GDx VCC, HRT I, and clinical assessment of stereoscopic optic nerve head photographs for diagnosing glaucoma. *Br J Ophthalmol* 2007;91:313-8.
32. Araie M, Sekine M, Suzuki Y, Koseki N. Factors contributing to the progression of visual field damage in eyes with normal-tension glaucoma. *Ophthalmology* 1994;101:1440-4.
33. Quigley HA, Katz J, Derick RJ, et al. An evaluation of optic disc and nerve fiber layer examinations in monitoring progression of early glaucoma damage. *Ophthalmology* 1992;99:19-28.
34. Anraku A, Enomoto N, Takeyama A, et al. Baseline thickness of macular ganglion cell complex predicts progression of visual field loss. *Graefes Arch Clin Exp Ophthalmol* 2014;252:109-15.

35. Kuang TM, Zhang C, Zangwill LM, et al. Estimating Lead Time Gained by Optical Coherence Tomography in Detecting Glaucoma before Development of Visual Field Defects. *Ophthalmology* 2015;122:2002-9.
36. Sung KR, Kim S, Lee Y, et al. Retinal nerve fiber layer normative classification by optical coherence tomography for prediction of future visual field loss. *Invest Ophthalmol Vis Sci* 2011;52:2634-9.

7

Transient Peripapillary Retinoschisis in Glaucomatous Eyes

Josine van der Schoot, Koenraad A. Vermeer,
Hans G. Lemij

J Ophthalmol. 2017;2017:1536030.

ABSTRACT

Purpose. To investigate transient focal microcystic retinoschisis in glaucomatous eyes in images obtained with several imaging techniques used in daily glaucoma care.

Methods. Images of 117 glaucoma patients and 91 healthy subjects participating in a large prospective follow up study into glaucoma imaging were reviewed. Participants were measured with spectral domain optical coherence tomography (SD-OCT), scanning laser polarimetry (SLP), scanning laser tomography (SLT) and standard automated perimetry (SAP). The presence of a focal retinoschisis in SD-OCT was observed and correlated to SLP, SLT and SAP measurements, both cross-sectionally and longitudinally.

Results. Seven out of 117 glaucoma patients showed a transient, localised, peripapillary, heterogeneous microcystic schisis of the retinal nerve fiber layer (RNFL) and sometimes other retinal layers as well, in SD-OCT. None of the healthy eyes showed this phenomenon, nor did any of the other imaging techniques display it as detailed and consistently as did the SD-OCT. SAP showed a temporarily decreased focal retinal sensitivity during the retinoschisis and we found no signs of glaucomatous progression related to the retinoschisis.

Conclusions. Transient microcystic retinoschisis appears to be associated with glaucomatous wedge defects in the RNFL. It was best observed with SD-OCT and it was absent in healthy eyes. We found no evidence that the retinoschisis predicted glaucomatous progression.

INTRODUCTION

In glaucoma, retinal nerve fibers are damaged and lost, leading to thinning of the retinal nerve fiber layer (RNFL).^{1,2} The thinning of the RNFL can be measured by different imaging techniques, such as scanning laser polarimetry (SLP), scanning laser tomography (SLT) and optical coherence tomography (OCT).³ The current generation OCT, i.e. spectral domain OCT (SD-OCT)⁴⁻⁷, shows a more detailed image of all layers of the retina compared to time domain OCT, which potentially leads to new insights.

Several recent studies presented cases with peripapillary retinoschisis, imaged with SD-OCT.⁸⁻¹³ All studies showed a relation of the retinoschisis with the presence of glaucoma. Kahook et al.¹¹ and Lee et al.¹² related the retinoschisis also with high or fluctuating intraocular pressures. Following a large population for several years, Lee et al. were able to observe spontaneous resolution of the retinoschisis. Recently, Lee et al. presented alterations of the lamina cribrosa to be associated with peripapillary retinoschisis.¹³ To date, several insights in this newly described phenomenon have been presented, but the pathogenesis and the course of the retinoschisis remains uncertain. Also, whether the retinoschisis is related to glaucoma progression and whether it can also be imaged by other techniques used in daily glaucoma care, still is unknown.

In the current study, we describe the appearance of this peripapillary retinoschisis over time that we observed in SD-OCT images of a subset of subjects participating in a large, prospective longitudinal study on glaucoma imaging. We also explore the effects of the retinoschisis on the measurements of various other, commonly used functional and structural techniques in glaucoma care. In addition, we assess a potential correlation between the appearance or disappearance of the retinoschisis and glaucomatous progression, measured by several techniques.

METHODS

Participants

This report presents the outcome of reviewing a study cohort of 117 glaucoma patients and 91 subjects with healthy eyes on the presence of a peripapillary retinoschisis. All subjects participated in a longitudinal prospective follow-up study into glaucoma imaging. All acquired images that had been taken in 4 successive years, were retrospectively reviewed for the presence of any peripapillary retinoschisis.

To be qualified as healthy, a subject was required to have a normal visual field and an intraocular pressure of 22 mmHg or less. A normal visual field had, by definition,

a Glaucoma Hemifield Test within normal limits and a Mean Deviation (MD) and Pattern Standard Deviation (PSD) within their respective 95% confidence intervals. Visual fields were considered as glaucomatous if at least two of the following findings were confirmed on the successive visual field: a PSD significant at the 5% probability level, a Glaucoma Hemifield Test outside normal limits and a cluster of 3 or more points below the 5% probability level or 1 individual point below the 1% probability level.

Subjects were excluded from participation in the presence of any significant coexisting ocular or systemic disease known to possibly affect the visual field (e.g., diabetes mellitus), a history of intraocular surgery (except for uncomplicated cataract surgery and glaucoma surgery in glaucoma patients), uncontrollable arterial hypertension and secondary glaucoma.

All participants had a best-corrected Snellen visual acuity of at least 20/40 in both eyes, a spherical equivalent refractive error between -10.0D and +5.0D, and unremarkable findings upon slit-lamp examination, including open angles on gonioscopy.

All glaucoma patients were recruited at the Glaucoma Service at the Rotterdam Eye Hospital. The healthy subjects were mainly friends and spouses of the glaucoma patients who volunteered to participate in the longitudinal study. The methods and procedures used in this study adhered to the Declaration of Helsinki. Informed consent was obtained from all participants. This study was approved by the Medical Ethics Committee of the Erasmus Medical Centre, Rotterdam, The Netherlands.

Image Acquisition

All participants were measured with the Spectralis OCT (Heidelberg Engineering GmbH, Dossenheim, Germany), an imaging device that features SD-OCT. With SD-OCT, the peripapillary areas of both eyes were scanned by means of a volume scan of 20 by 20 degrees.

In the same session, all participants were measured with several other imaging techniques as well, including SLP (GDxECC [GDx]; Carl Zeiss Meditec inc., Dublin, CA, USA) and SLT (Heidelberg Retina Tomograph III [HRT], Heidelberg Engineering GmbH, Dossenheim, Germany). All participants also underwent visual field testing (Humphrey Field Analyzer [HFA], Carl Zeiss Meditec Inc., Dublin, CA, USA). All measurements were repeated every six months in glaucomatous cases and every 12 months in healthy cases.

Analysis

Cross-sectional

Because we incidentally noticed a focal schisis of the RNFL, and sometimes of other retinal layers as well, in some of the SD-OCT images, we systematically reviewed all images of all participants in the longitudinal study to detect a similar schisis in other eyes. The cases that showed the focal retinoschisis were followed over time, to evaluate its course. We also explored whether any of the other imaging devices allowed us to image the schisis. In addition, we compared the area of schisis, measured with SD-OCT, to the corresponding sectors of the visual field, using the method introduced by Garway-Heath et al.¹⁴ To indicate the presence and size of a glaucomatous defect, we counted the number of points below the 0.5% probability level within the corresponding sector in either the total or the pattern deviation probability plot, whichever showed the fewest abnormal points. In the GDx, we examined the retardation map. The HRT has no specific parameters to quantify RNFL thickness around the optic nerve head (ONH). Therefore, the three-dimensional topography image (HRT-3D) was the only way in the HRT to quantitatively determine the surface height around the ONH.

To explore whether our observation might be related to retinal disease, such as posterior vitreous detachment (PVD), we retrospectively reviewed all SD-OCT images containing the RNFL schisis. Peripapillary vitreoretinal traction syndrome, with retinal thickening next to the ONH is associated with PVD.^{15,16} We therefore explored the presence of other retinal diseases by careful scrutiny of all SD-OCT B-scans at large magnification.

Longitudinal

When possible, we compared the images during the focal retinoschisis with the outcome either before or after the schisis. In the VF, we calculated the mean retinal sensitivity (MRS) of all individual points in the corresponding sector, as presented on the printout. We used the paired Student's t-test to evaluate differences between the MRS of the measurements during and before / after the disturbed area. In the HRT, Topographic Change Analysis (HRT-TCA) was used to determine any changes in height of the RNFL.

One hundred and eighty-nine eyes of 117 glaucoma patients (66 men, 51 women), as well as 182 eyes of 91 healthy subjects (36 men, 55 women) were measured at least once, with a maximum follow up time of 34 months. The mean age of the healthy subjects was 57 years (SD 13) and of glaucoma patients 69 years (SD 10).

RESULTS

Seven out of 189 glaucomatous eyes showed a transient, localised, peripapillary schisis of the RNFL and sometimes of other retinal layers as well. This phenomenon was not observed in any of the 182 healthy eyes ($p=0.0089$, χ^2 -test). All 7 subjects were women. Their mean age was 70.7 years (SD 8.3). The subject and scan characteristics have been presented in Tables 1 & 2.

Table 1 Subject characteristics.

Case	Eye	Age (years)	IOP (mmHg)	Severity Glaucoma*	Glaucoma treatment	Surgical interventions
#1	OD	61.5	14	Moderate	None	Trabeculectomy (2007)
#2	OD	63.2	15	Advanced	None	Trabeculectomy (1995)
#3	OD	76.2	12	Mild	Dorzolamide/ Timolol; Latanoprost	None
#4	OD	72.8	14	Advanced	Dorzolamide/ Timolol; Carteolol	None
#5	OD	61.8	12	Moderate	Timolol; Bimatoprost	Trabeculectomy (2000)
#6	OD	80.6	21	Mild	Timolol	YAG PI (1996), Trabeculectomy (1999)
#7	OS	78.6	12	Mild	Timolol	YAG PI (1996)

* Mild glaucoma: MD >-6 dB; Moderate glaucoma -12 dB $>$ MD >-6 dB; Advanced glaucoma <-12 dB
Abbreviations: IOP: Intra-ocular pressure; YAG PI: yttrium-aluminium-garnet (YAG) laser peripheral iridotomy; MD: Mean Deviation (of visual field)

Table 2 Characteristics of SD-OCT and visual field of each case.

Case	SD-OCT		VF
	Location RNFL schisis	Layers involved	# abnormal points
#1	Superotemporal (ST)	RNFL, GCL	10 (10) (ST)
#2	Superotemporal (ST)	RNFL, GCL	7 (10) (ST)
#3	Nasal (N)	RNFL, GCL, ONL	1 (4) (N)
#4	Temporal (T+IT)	RNFL	17 (19) (T/IT)
#5	Inferotemporal (T+IT)	RNFL, GCL, INL	7 (16) (T/IT)
#6	Inferotemporal (IT)	RNFL, GCL	8 (13) (IT)
#7	Superotemporal (ST)	RNFL	0 (10) (ST)

An abnormal point was an individual point below the 0.5% probability level in either the total or the pattern deviation plot. The number of abnormal points (+ total amount of points) were counted per sector corresponding with the location of the schisis of the RNFL in SD-OCT.¹⁴

Abbreviations: SD-OCT: spectral domain optical coherence tomography; RNFL: retinal nerve fiber layer; GCL: ganglion cell layer; ONL: outer nuclear layer; INL: inner nuclear layer; VF: visual field.

Scan images

The SD-OCT scans of all 7 cases showed an area of schisis of the RNFL. This area was well demarcated on the en-face infrared image and it verged on the ONH. In all cases, the schisis appeared as a localised, heterogeneous microcystic mass within the RNFL and sometimes also partially on top of it (cases 4 and 5). In most cases, other layers under the RNFL were involved as well, such as the ganglion cell layer (cases 1, 4, 6), or even deeper retinal layers, like the inner and outer nuclear layer (cases 3 and 5). None of the SD-OCT scans of these cases showed any signs of other ONH- or retinal abnormalities, such as posterior vitreous detachment or a macular pucker. An overview with images of three cases is presented in Figure 1.

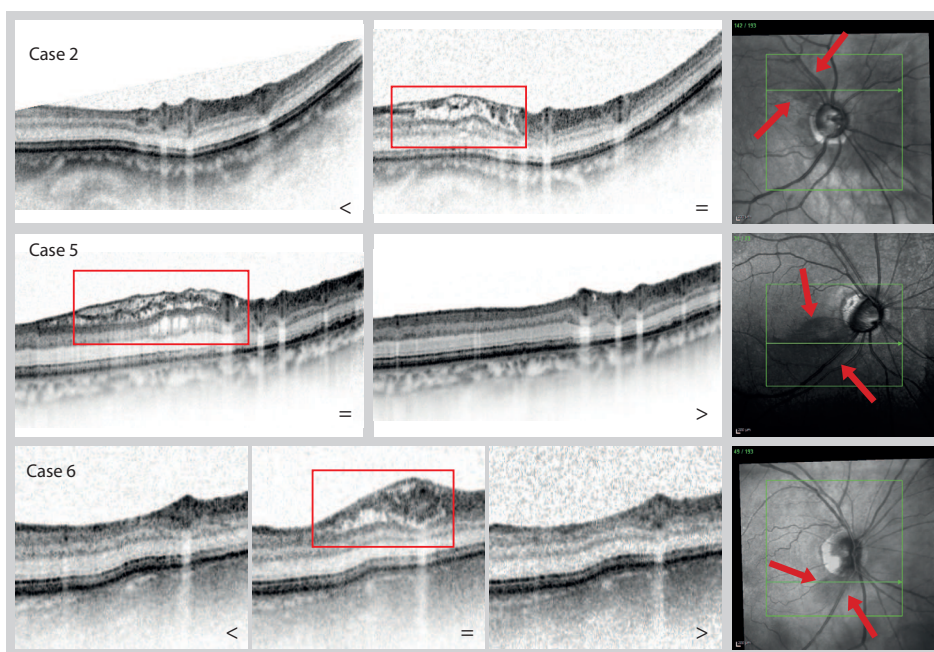


Figure 1 IR (right) and SD-OCT images of 3 cases, representing cases with measurements before (<) and during (=) the retinoschisis (Case 2); and representing cases with measurements during and after (>) the retinoschisis (Case 5). Case 6 was the only case imaged before (<), during (=) and after (>) the presence of the retinoschisis. The detail inside the red boxes represents the retinoschisis. Between the red arrows in the IR fundus images is the area of the focal retinoschisis.

Abbreviations: IR: infrared image; SD-OCT: spectral domain optical coherence tomography

Outcome other imaging devices

No other imaging device captured this localised retinoschisis as clearly as the SD-OCT did. In 6 cases, the visual field showed a glaucomatous defect in the sectors corresponding with the location of the schisis in the SD-OCT images. In the case

without a glaucomatous visual field defect in the corresponding sector (case 7), the thickening was located in a very small wedge defect. In none of the cases was the RNFL schisis detectable by SLP (GDx); its image only showed a localised RNFL wedge at the same location. In three cases, the retinoschisis was displayed also by SLT (HRT-3D), presented as a slightly elevated surface in the three-dimensional image. In one case, we performed fluorescence angiography during the retinoschisis to seek for any signs of a pathophysiological mechanism. Besides some atherosclerotic arteries, the angiogram showed no pathological patterns, such as leakage or other signs of inflammation.

The disagreements between the various imaging techniques in the ability to capture the transient, focal retinoschisis have been illustrated by Figure 2.

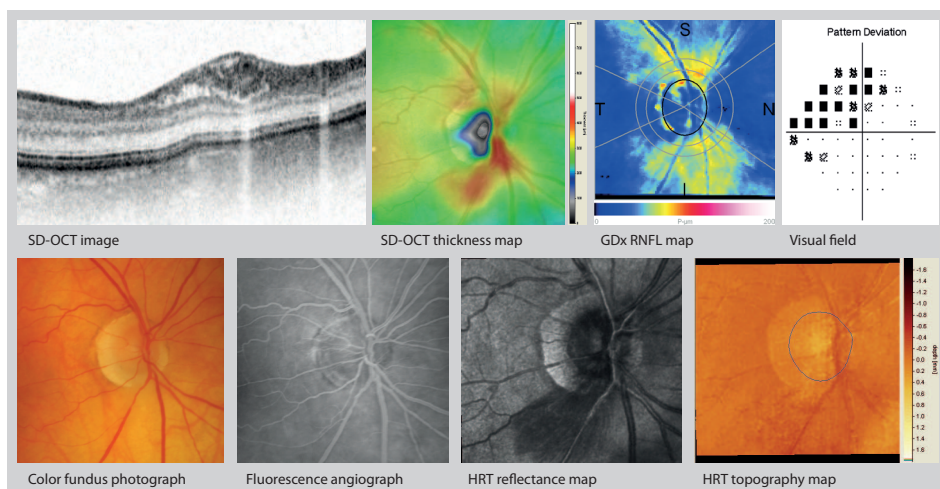


Figure 2 SD-OCT, Scanning Laser Polarimetry (GDx), visual field, color fundus photograph, fluorescence angiograph and Scanning Laser Tomography (HRT) images during the presence of the focal retinoschisis in Case 6. The SD-OCT image shows the retinoschisis inferotemporally (see thickness map). The thickness map shows the total retinal thickness. The GDx shows no increased RNFL thickness. The color fundus photograph as well as the fluorescein angiography show no clear signs of the retinoschisis, except for atherosclerotic arteries inferiorly to the ONH. The HRT shows a darker area at the thickened location in the reflectance map, as well as a slight increased height in the topography map.

Abbreviations: SD-OCT: Spectral Domain Optical Coherence Tomography; RNFL: retinal nerve fiber layer.

Outcome over time

All 7 subjects were measured at least four times with SD-OCT at 6-monthly intervals. In case 6 we saw that the retinoschisis was present at the fourth measurement and that it had disappeared after 13 months. In cases 4 and 5, the retinoschisis

disappeared, and in cases 2 & 3, the schisis occurred within the time frame of these measurements. In cases 1 and 7, we observed the retinoschisis in all measurements, suggesting it can last for at least 27 months. The images taken with and without the schisis, in the same location, have been presented in Figure 1.

Of the 5 eyes imaged both with and without the presence of retinoschisis, 4 eyes were imaged with other devices as well. As presented in Table 3, the defect in the visual field, expressed by the MRS, appeared to be worse during the time of retinoschisis. In 3 of these 4 eyes, the MRS decreased by at least 2.5 dB during the retinoschisis, statistically non-significantly however. In none of these 4 eyes did the GDx and HRT-TCA show any change in height. The HRT-3D image did reveal a focally elevated surface when the schisis was present.

Table 3 Measurement characteristics of visual field of four cases of measurements with and without the focal retinoschisis.

Case	Visual field				
	MRS during retinoschisis	Moment without retinoschisis	MRS without retinoschisis	Difference	p-value*
#3	24.3 [SD 5.1]	<	21.3 [SD 3.3]	3.0	0.19
#4	5.5 [SD 9.1]	>	8.2 [SD 10.9]	-2.7	0.04
#5	17.6 [SD 9.4]	>	20.1 [SD 9.5]	-2.5	0.14
#6	17.3 [SD 7.0]	< & >	20.9 [SD 6.6]	-3.5	0.04

The MRS was calculated in the sector corresponding with the location of the RNFL schisis on spectral-domain optical coherence tomography.¹⁴ The moment without retinoschisis is presented as before (<) or after (>) the retinoschisis.

* paired Student's t-test

Abbreviations: MRS: mean retinal sensitivity; RNFL: retinal nerve fiber layer

DISCUSSION

This study presents a focal schisis of the retinal nerve fiber layer (RNFL) and sometimes deeper retinal layers in glaucomatous eyes. None of the healthy eyes showed this phenomenon. In all cases, the retinoschisis was located in an area of a pre-existing glaucomatous RNFL defect, which suggests that this phenomenon is associated with glaucomatous wedge defects of the RNFL.

Several recent studies presented cases with peripapillary retinoschisis, imaged with SD-OCT.⁸⁻¹³ All studies showed a relation of the retinoschisis with the presence of glaucoma. We also observed the retinoschisis in glaucomatous eyes only, all verging on a glaucomatous (wedge) defect. Kahook et al.¹¹ presented two cases with retinal schisis cavities in the presence of narrow occludable angles and increased intraocular pressure, suggesting a tight relation, which has been confirmed

by Lee et al.¹² Our data did not confirm this finding, but we found the retinoschisis in open angles and with low intraocular pressures as well, suggesting a different pathophysiology. Because they followed a large population for several years, Lee et al. were able to observe spontaneous resolution of the retinoschisis.¹² We also observed that the retinoschisis appeared and disappeared with various time spans between eyes, ranging from less than six months up to over 27 months.

None of the previously mentioned studies adopted other techniques commonly used for monitoring glaucoma to investigate their ability to detect this retinoschisis or to relate it to glaucomatous loss or potential progression. We followed all participants longitudinally with visual field testing, SLP, SLT and SD-OCT. All these techniques measured a glaucomatous (wedge) defect at the location of the retinoschisis. Interestingly, the schisis itself of the RNFL and sometimes other deeper retinal layers could hardly be detected by any of the other imaging devices. SLP (GDx) did not detect this schisis at all. This is not very surprising, because the GDx measures retardation. Without any change to the number of nerve fibers and without any substantial change in their course, we would not have expected any changes in retardation. The apparent accumulation of fluid within the schisis area would not have led to a change in retardation, similar to the lack of change in case of disc edema.¹⁷ SLT (HRT) did capture the thickening in the three-dimensional surface display, but it failed to detect any schisis by the HRT parameters.

In the eyes in which the retinoschisis appeared between measurements or disappeared over time, a corresponding difference in RNFL-thickness on SD-OCT was observed. The HRT and GDx did not appear to measure any differences in RNFL thickness between measurements prior to or after the RNFL schisis nor during its presence. The visual field, however, showed a, statistically not significant, decreased mean retinal sensitivity (MRS) of at least 2.5dB during the retinoschisis at the exact location corresponding with the schisis¹⁴, compared to the visual field before or after the retinoschisis. This suggests a temporary decreased function due to the retinoschisis, fortunately not leading to permanent progression of the glaucomatous defect.

The pathophysiological mechanism of this schisis is unclear. Most likely, the schisis contains fluid, since its reflectivity is lower than the surrounding tissues and it absorbs or scatters part of the incident light. The origin of the fluid remains unclear. Potentially, thickening and fluid accumulation might be characteristic of inflammation. The absence of other signs of inflammation, including the fully normal fluorescence angiography in our study, suggests another cause. As suggested by others^{8,11,12}, the fluid might be of vitreous origin. The fluid might enter the RNFL through microscopic interconnections, leading to the schisis. Kahook et al. hypothesize that pressure peaks lead to changes in axial length, which might

lead to vitreous traction.¹¹ Whenever the vitreous detaches from the inner limiting membrane, this might lead to peripapillary vitreoretinal traction syndrome with retinal thickening next to the ONH.^{15,16,18} Our SD-OCT scans, combined with retrospective medical chart search for any PVD observations, showed no signs of other ONH- or retinal abnormalities potentially causing thickening and edema inside the retina. Since all cases differed somewhat in their treatment, we do not think the retinoschisis was therapy related.

The focal retinoschisis always verged on the ONH, suggesting it follows the pattern of loss of nerve fibers. In addition, the RNFL schisis seems to follow the nerve fibers into the lamina cribrosa, suggesting that the fluid might enter the RNFL from the subarachnoidal space through the lamina cribrosa along the tiny canals created by the pathological absence of previously present nerve fibers. Recently, Lee et al. strengthened this hypothesis by presenting the relationship between retinoschisis and damage to the lamina cribrosa.¹³ They found that the location of the lamina cribrosa abnormalities, found on OCT with enhanced depth imaging, appeared to be associated with the involved retinal layers. Lee et al. related this hypothesis to the presence of an optic pit, which was found in 36% of their cases.¹² The eyes in our study did not show any optic pits. Interestingly, cerebrospinal fluid contains proteins, which in SD-OCT potentially lead to shadowing effects, causing relatively lower reflectivity of the retinal layers underneath. This matches our findings such as illustrated in Figure 1, strengthening this hypothesis. Whether proteins would remain between or in the retinal layers after the resolution of the fluid remains unclear. Our data did not show any visible signs of differences in reflectivity of the retinal layer at the location of the former schisis and its surrounding area, suggesting that the proteins dissolve completely.

Our study was subject to some limitations. First, this study was based on a review of images obtained from a large prospective longitudinal study into glaucoma imaging, which was not specifically designed for investigating the clinical course of retinoschisis. Second, the sample size was small. We therefore think that the only remarkable finding in the patient characteristics, i.e. that all subjects that showed the retinoschisis were women, is probably coincidental and due to this small sample size. On the other hand, a large group of subjects with glaucoma were included in our long term follow up study on glaucoma imaging, while only few showed the retinoschisis. In fact, only about 4% of the 189 eyes measured for many years showed the retinoschisis. Further longitudinal follow-up of a larger population is necessary to address the exact course of the retinoschisis and its potential relation to glaucomatous progression.

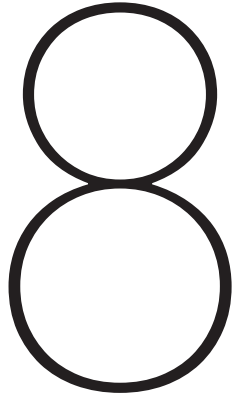
In conclusion, our data suggest that transient, localised, peripapillary schisis of the RNFL, and sometimes other deeper retinal layers, is associated with glauco-

matous RNFL wedge defects. Of all techniques used to monitor glaucoma in daily practice, the retinoschisis was best observed with SD-OCT. The visual field showed a temporary focally decreased sensitivity during the retinoschisis. We found no evidence that the retinoschisis predicts glaucomatous progression.



REFERENCE LIST

1. Quigley HA, Nickells RW, Kerrigan LA, et al. Retinal ganglion cell death in experimental glaucoma and after axotomy occurs by apoptosis. *Invest Ophthalmol Vis Sci* 1995;36:774-86.
2. Ritch R, Shields M.B., Krupin Th. *Anatomy and Pathophysiology of the Retina and Optic Nerve. The Glaucomas; Basic Sciences*. St. Louis, Missouri, USA: Anne Patterson; 1996:139-76.
3. Lin SC, Singh K, Jampel HD, et al. Optic nerve head and retinal nerve fiber layer analysis: a report by the American Academy of Ophthalmology. *Ophthalmology* 2007;114:1937-49.
4. Cense B, Nassif N, Chen T, et al. Ultrahigh-resolution high-speed retinal imaging using spectral-domain optical coherence tomography. *Opt Express* 2004;12:2435-47.
5. Nassif N, Cense B, Park B, et al. In vivo high-resolution video-rate spectral-domain optical coherence tomography of the human retina and optic nerve. *Opt Express* 2004;12:367-76.
6. Nassif N, Cense B, Park BH, et al. In vivo human retinal imaging by ultrahigh-speed spectral domain optical coherence tomography. *Opt Lett* 2004;29:480-2.
7. Wojtkowski M, Leitgeb R, Kowalczyk A, et al. In vivo human retinal imaging by Fourier domain optical coherence tomography. *J Biomed Opt* 2002;7:457-63.
8. Bayraktar S, Cebeci Z, Kabaalioglu M, et al. Peripapillary Retinoschisis in Glaucoma Patients. *J Ophthalmol* 2016;2016:1612720.
9. Farjad H, Besada E, Frauens BJ. Peripapillary schisis with serous detachment in advanced glaucoma. *Optom Vis Sci* 2010;87:E205-E217.
10. Hwang YH, Kim YY, Kim HK, Sohn YH. Effect of peripapillary retinoschisis on retinal nerve fibre layer thickness measurement in glaucomatous eyes. *Br J Ophthalmol* 2014;98:669-74.
11. Kahook MY, Noecker RJ, Ishikawa H, et al. Peripapillary schisis in glaucoma patients with narrow angles and increased intraocular pressure. *Am J Ophthalmol* 2007;143:697-9.
12. Lee EJ, Kim TW, Kim M, Choi YJ. Peripapillary retinoschisis in glaucomatous eyes. *PLoS One* 2014;9:e90129.
13. Lee JH, Park HL, Baek J, Lee WK. Alterations of the Lamina Cribrosa Are Associated with Peripapillary Retinoschisis in Glaucoma and Pachychoroid Spectrum Disease. *Ophthalmology* 2016.
14. Garway-Heath DF, Poinoosawmy D, Fitzke FW, Hitchings RA. Mapping the visual field to the optic disc in normal tension glaucoma eyes. *Ophthalmology* 2000;107:1809-15.
15. Hedges TR, III, Flattem NL, Bagga A. Vitreopapillary traction confirmed by optical coherence tomography. *Arch Ophthalmol* 2006;124:279-81.
16. Hixson A, Reynolds S. Peripapillary vitreoretinal traction. *Optometry* 2011;82:602-6.
17. Banks MC, Robe-Collignon NJ, Rizzo JF, III, Pasquale LR. Scanning laser polarimetry of edematous and atrophic optic nerve heads. *Arch Ophthalmol* 2003;121:484-90.
18. Kroll P, Wiegand W, Schmidt J. Vitreopapillary traction in proliferative diabetic vitreoretinopathy. *Br J Ophthalmol* 1999;83:261-4.



The Effect of Glaucoma on the Optical Attenuation Coefficient of the Retinal Nerve Fiber Layer in Spectral Domain Optical Coherence Tomography Images

Josine van der Schoot, Koenraad A. Vermeer,
Johannes F. de Boer, Hans G. Lemij

Invest Ophthalmol Vis Sci. 2012;53(4):2424-30.

ABSTRACT

Purpose. To demonstrate the effect of glaucoma on the optical attenuation coefficient of the retinal nerve fiber layer (RNFL) in Spectral Domain Optical Coherence Tomography (SD-OCT) images.

Methods. We analyzed images of the peripapillary areas in 10 healthy and 30 glaucomatous eyes (mild, moderate and advanced glaucoma, 10 eyes each), scanned with the Spectralis OCT (Heidelberg Engineering GmbH, Dossenheim, Germany). To calculate the RNFL attenuation coefficient (μ_{att}), determined by the scattering properties of the RNFL, we used a model that normalized the reflectivity of the RNFL by the retinal pigment epithelium. The analysis was performed at 4 preset locations around the optic nerve head (ONH) (i.e. temporally, superiorly, nasally and inferiorly) and on averages per eye. To assess the structure-function relationship, we correlated the μ_{att} to the Mean Deviation (MD) in standard automated perimetry (SAP).

Results. The μ_{att} of the RNFL decreased up to 40% with increasing disease severity, on average as well as in each location around the ONH (Jonckheere-Terpstra test, $P < 0.001$ in all tests). The μ_{att} of the RNFL depended significantly on the location around the ONH in all eyes (Kruskal-Wallis test, $P < 0.001$) and was lowest nasally from the ONH. The μ_{att} correlated significantly with the MD in SAP ($R^2 = 0.337$, $p < 0.001$).

Conclusion. The measurements clearly demonstrated that the μ_{att} of the RNFL decreased with increasing disease severity. The RNFL attenuation coefficient may serve as a new method to quantify glaucoma in SD-OCT images.

INTRODUCTION

In glaucoma, retinal nerve fibers are damaged and lost, leading to thinning of the retinal nerve fiber layer (RNFL)^{1, 2}. Optical coherence tomography (OCT), a technique used e.g. for *in vivo* retinal imaging, can measure the thickness of retinal layers, such as the RNFL. Since its development^{3, 4} for ophthalmology, this technology has been predominantly used for imaging the macula and macular diseases, and, to a lesser extent, glaucoma. Time Domain OCT (TD-OCT) yielded a gradually improving reproducibility of measurements over the past decade⁵⁻⁹. Nevertheless, it never exceeded the diagnostic capabilities of other structural measurement techniques for glaucoma, such as scanning laser polarimetry (SLP) and confocal scanning laser ophthalmoscopy (CSLO)⁹⁻¹². Since the recent development of Spectral Domain Optical Coherence Tomography (SD-OCT)¹³⁻¹⁶, OCT is increasingly used in glaucoma assessment because of its high image resolution, high reproducibility of measurements¹⁷⁻²³ and diagnostic accuracy²⁴⁻²⁶.

The local signal strength of the OCT is used to measure thickness of retinal layers. Optical scattering properties of each retinal layer are closely related to the tissue properties. Pons et al.²⁷ reported a decreased reflectivity of the RNFL in glaucoma measured with TD-OCT. In a recent study, we confirmed the diminished reflectivity of the RNFL in glaucomatous eyes compared to healthy eyes in SD-OCT images [Van der Schoot, IOVS, 2010, 51, ARVO E-Abstract, 212]. Even focal defects are detected by this method (Vermeer, IOVS, 2011, 52, ARVO E-abstract, 3666). Figure 1 illustrates the difference in reflectivity of the RNFL between a healthy and a glaucomatous eye. These findings suggest that glaucomatous damage is not only reflected by the thickness of the RNFL, but also by changes in its optical scattering properties. The latter may potentially lead to a new method to diagnose or follow glaucoma.

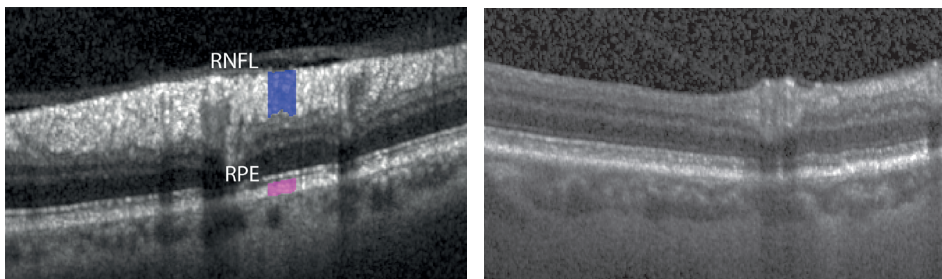


Figure 1 SD-OCT image of a healthy eye (left) and of an advanced glaucomatous eye (right). The two coloured areas represent the manual segmentation of the areas of the RNFL (blue) and RPE (purple), used for analysis. Note the reduced brightness of the retinal nerve fiber layer (RNFL) in the glaucomatous eye compared to the healthy eye, representing the diminished RNFL reflectivity in the glaucomatous eye.

To determine the optical scattering properties of a retinal layer, it is not sufficient to measure its reflectivity. The measured reflectivity of a layer is sensitive to e.g., media opacities and light collection geometry. Therefore, a relative measurement is necessary to extract quantitative scattering properties from OCT images. In this article we present a method to quantify the attenuation coefficient (μ_{att}) of the RNFL in SD-OCT images, by taking the scattering properties of the retinal pigment epithelium (RPE) as a reference. To investigate the μ_{att} of the RNFL as a clinical diagnostic parameter, we measured the μ_{att} of the RNFL in healthy and glaucomatous eyes.

PATIENTS AND METHODS

Participants

Datasets of 10 healthy subjects and 30 subjects with glaucoma were randomly selected from a larger population, participating in a longitudinal prospective follow-up study into glaucoma imaging. The selection of the 30 glaucomatous subjects was based on the severity of their glaucoma per eye, stratified by the Mean Deviation (MD) of the visual field test (determined with the standard 24-2 W/W SITA test programme of the Humphrey Field Analyzer, Carl Zeiss Meditec, Dossenheim, Germany). The severity of glaucoma was defined as an MD between 0 dB and -6 dB, between -6 dB and -12 dB and worse than -12 dB, for mild, moderate and advanced glaucoma, respectively. Of each group, 10 eyes of different subjects were randomly selected.

For inclusion, a healthy subject needed to have a normal visual field and an intraocular pressure below 22 mmHg. A normal visual field had, by definition, a Glaucoma Hemifield Test within normal limits and an MD and PSD within the 95% confidence intervals. Visual fields were considered as glaucomatous if they had at least 2 of the following on at least 2 separate occasions: a PSD significant at the 5% probability level, a Glaucoma Hemifield Test outside normal limits and a cluster of more than 2 points below the 5% probability level or 1 individual point below the 1% probability level. All patients were recruited from the population treated for glaucoma at the Rotterdam Eye Hospital.

Subjects were excluded from participation in the presence of any coexisting ocular or systemic disease known to possibly affect the visual field (e.g. diabetes mellitus), a history of intraocular surgery (except for uncomplicated cataract surgery or glaucoma surgery in glaucoma patients), uncontrollable arterial hypertension, and secondary glaucoma in case of glaucoma.

All participants had a best-corrected Snellen visual acuity of at least 20/40 in both eyes, a spherical equivalent refractive error between -10.0D and +5.0D, and had unremarkable findings upon slit-lamp examination, including open angles on gonioscopy.

The methods and procedures used in this study adhered to the Declaration of Helsinki. Informed consent was obtained from all participants. This study was approved by the Medical Ethics Committee of the Erasmus Medical Centre, Rotterdam, The Netherlands.

All participants were scanned once with the Spectralis OCT (Heidelberg Engineering, Dossenheim, Germany) between January and September 2009. The optic disc and peripapillary area were scanned by means of a volume scan of 20 by 20 degrees. This scan contained 193 B-scans, each consisting of 512 A-scans. Each B-scan was an average of 5 scans on the same location (made possible by the built-in eye-tracking system on the Spectralis OCT with ART value 5). The lateral distance between adjacent B-scans was 30 μm . To minimize the decrease in sensitivity as a function of depth, all retinal cross sections were placed in the upper one third of the scan depth. A volume scan was excluded, if the proprietary overall quality score provided by the Spectralis was below 15 dB or if the volume scan was incomplete due to the built-in maximum acquisition time of 300 seconds.

Image Processing and Model

We used the exported raw data of optic nerve head (ONH) scans for all analyses. To determine the reflectivity, we exported the raw data which represents the measured intensity on a linear scale between 0 and 1. The device displays these intensities in a grayscale image after applying the following formula: $Y=4\sqrt{X}$; where X represents the raw data values; $Y=0$ represents no reflectivity and $Y=1$ maximum reflectivity²⁸.

The model we developed, is based on two different scattering layers: the RNFL and the RPE. Assuming that the backscatter properties of the RPE are constant, we used it to normalize the RNFL OCT signal. The model can be summarized as follows: The amount of light that is backscattered from the RNFL is proportional to the incident intensity and the amount by which the incident beam on the eye is attenuated due to scattering. The incident light that is not scattered by the RNFL propagates to the RPE, and is partially backscattered by the RPE. The ratio of total light backscattered by the RNFL (RNFL reflectivity) and the RPE (RPE reflectivity) is now related to the μ_{att} of the RNFL according to the following formula:

$$\mu_{\text{att}} = \frac{\log\left(\frac{R}{2.3} + 1\right)}{2 \cdot d},$$

in which μ_{att} represents the attenuation coefficient in mm^{-1} , R is the ratio between the reflectivity of the RNFL and RPE, and d is the thickness of the RNFL in mm. The model is derived in the Appendix.

The analysis of the μ_{att} was performed in all 4 quadrants around the optic nerve head (ONH) at fixed locations. The centre of the ONH was manually selected, taking the border of the RPE as a reference. From this centre of the ONH, the areas of interest were selected 1.3 mm superiorly, inferiorly, temporally and nasally. To correct for any failed B-scans, the best out of 3 B-scans closest to the selected distance was selected for analysis. Per B-scan, we selected an area for analysis of 20 pixels wide. If the selected area of 20 pixels contained any blood vessels, the 20 pixels wide window was shifted along the B-scan toward an area without blood vessels, to avoid any scatter caused by the blood vessel. We determined the μ_{att} in all 4 peripapillary locations separately and calculated the mean μ_{att} per patient by averaging μ_{att} of these 4 locations. The error of the mean μ_{att} was calculated over the patient population.

To obtain the reflectivity of each retinal layer separately, the layers were manually segmented and color coded by a manual segmentation tool, called ITKSNAP²⁹. The color coding was manually performed by a trained physician. The reflectivity of the RNFL and the RPE were used for analysis. An example of this color coding is presented in Figure 1.

Of the 3 selected B-scans (one superiorly, one inferiorly and one running from nasally to temporally to the ONH, containing the nasal and the temporal 20 pixel wide area of interest), the quality scores (as given by the device) were reported, ranging from 0 dB to 40 dB.

To correlate the measure of structure (μ_{att}) with a measure of function, we noted the MD of the visual field test, which was performed by all participants in the same visit as the Spectralis measurement.

Statistics

We used an analysis of Generalized Estimating Equations (GEE) to test for differences in the demographics. The Jonckheere-Terpstra test for trend was used for comparison between the μ_{att} of healthy eyes and of the 3 groups of glaucomatous eyes and to test for a trend in the μ_{att} between the various locations around the ONH. We used the Kruskal-Wallis test to test for the presence of an effect of location on μ_{att} . We calculated the coefficient of determination (R^2) of exponential regression analysis between MD and μ_{att} . A significance level of 0.05 was considered to be statistically significant.

RESULTS

Between the 4 groups of randomly selected subjects, there were no statistically significant differences in age and scan quality (Table 1). The MD showed a statistically significant difference between the 4 groups, decreasing with increasing disease severity (Table 1). No patients were excluded because of bad scan quality (<15dB) or incomplete scans. Examples of an SD-OCT image of a healthy eye and of a glaucomatous eye are shown in Figure 1.

Table 1 Patient Demographics and Scan Quality

	Healthy	Mild glaucoma	Moderate glaucoma	Advanced glaucoma	p-value
Mean age (years)	63.7 [SD 9.9]	65.3 [SD 1.4]	66.1 [SD 7.1]	71.8 [SD 9.3]	0.18
MD (dB)	0.15 [SD 1.10]	-2.80 [SD 1.39]	-9.05 [SD 3.64]	-17.65 [SD 4.31]	<0.001
Scan quality (dB)	26.5 [SD 3.6]	24.0 [SD 3.9]	24.4 [SD 2.9]	24.5 [SD 3.8]	0.2

Analysis of Generalized Estimating Equations for differences between age, Mean Deviation (MD) and scan quality in healthy, mild, moderate and advanced glaucomatous eyes.

The mean attenuation coefficient (μ_{att}) of the healthy and the mild, moderate and advanced glaucomatous eyes, as well as for each location, have been presented in table 2. The average μ_{att} of the RNFL showed a statistically significant trend for decreasing μ_{att} with increasing disease severity (Jonckheere-Terpstra test, $P < 0.001$). Figure 2 shows the trend of decreasing average μ_{att} of healthy and glaucomatous eyes, increasing in severity.

Table 2 Mean (\pm standard error) Attenuation Coefficient μ_{att} in healthy and glaucomatous eyes [mm^{-1}]

	Attenuation Coefficient of the Retinal Nerve Fiber Layer				
	Average	Temporal	Superior	Nasal	Inferior
Healthy	4.78 \pm 0.27	5.25 \pm 0.59	5.31 \pm 0.53	3.60 \pm 0.53	4.96 \pm 0.42
Mild Glaucoma	4.09 \pm 0.28	4.72 \pm 0.72	4.41 \pm 0.47	2.73 \pm 0.46	4.51 \pm 0.38
Moderate Glaucoma	3.14 \pm 0.25	3.33 \pm 0.49	3.99 \pm 0.49	1.74 \pm 0.20	3.51 \pm 0.46
Advanced Glaucoma	2.93 \pm 0.24	3.54 \pm 0.54	3.67 \pm 0.46	2.02 \pm 0.26	2.48 \pm 0.42

The location significantly affected the μ_{att} of the RNFL in all 4 groups (Kruskal-Wallis test, $P < 0.001$). In these eyes, the μ_{att} of the RNFL was lower nasally than in the other locations. All locations showed a statistically significant trend for decreasing μ_{att} with increasing disease severity (Jonckheere-Terpstra test, $P < 0.001$ for temporal, superior, nasal and inferior). These findings are illustrated by Figure 3.

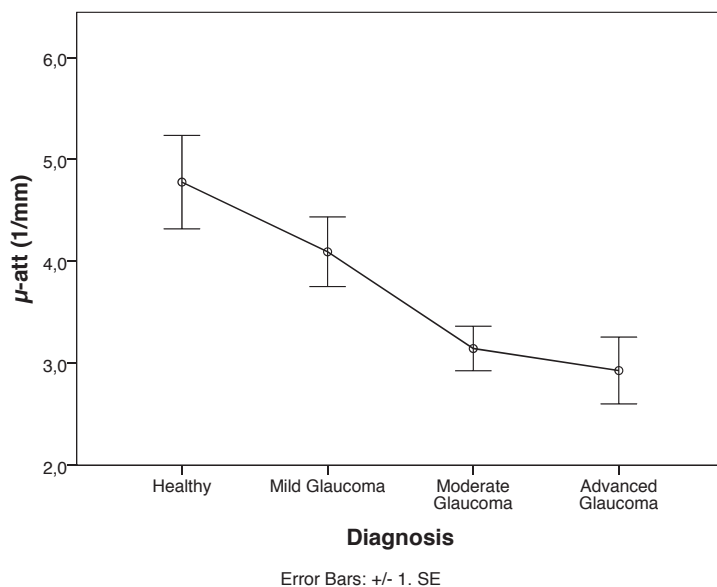


Figure 2 Box plot of the average attenuation coefficient μ_{att} [mm^{-1}] in healthy and glaucomatous eyes.

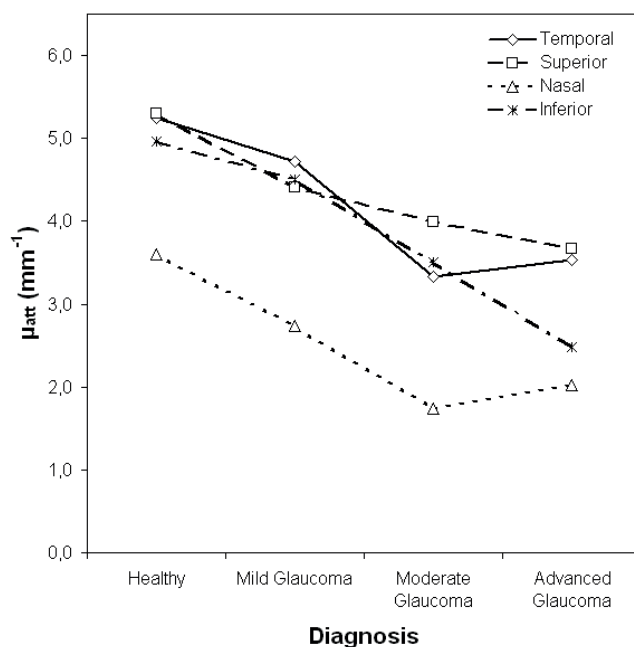


Figure 3 Plot presenting the trend of decreasing attenuation coefficient μ_{att} (mm^{-1}) with increasing disease severity for all locations separately. Note the difference in μ_{att} between the nasal and the other locations.

We also found a significant relationship between MD and μ_{att} ($R^2 = 0.337$, $p < 0.001$). The plot of this correlation is presented in Figure 4.

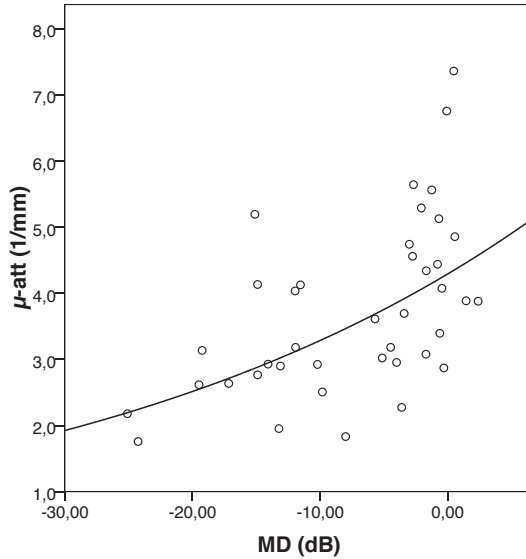


Figure 4 Plot presenting the correlation between the attenuation coefficient μ_{att} (mm^{-1}) and the Mean Deviation MD (dB), from the visual field test. The coefficient of determination (R^2) of exponential regression analysis between MD and μ_{att} is 0.337 ($P < 0.001$).

DISCUSSION

The attenuation coefficient (μ_{att}) of the RNFL decreased with increasing disease severity in SD-OCT images of healthy and glaucomatous eyes. We created a model to quantify the optical scattering properties from OCT data by calculating μ_{att} . The model was based on the reflectivity of the RNFL and the RPE, on interaction between light and the tissue and on the thickness of the RNFL. This novel analysis confirms earlier conclusions, i.e. that the optical scattering properties of the RNFL change in glaucoma²⁷ [Van der Schoot, IOVS, 2010, 51, ARVO E-Abstract, 212]. In our current study we looked at the attenuation coefficient, because it is based on relative measurements of the reflectivity. Absolute measurements of reflectivity might be affected by a number of factors, such as the particular alignment of the OCT beam on the cornea, and media opacities. Relative measurements are less sensitive to these factors and thus provide a more reliable measure of change related to pathological processes in glaucoma.

The model we developed incorporated the backscatter signal of the RNFL and the RPE and not of the layers in between. These layers have a relatively low backscatter signal, compared to the RNFL and RPE³⁰, and they attenuate only a relatively small part of the incident light. Moreover, the attenuation of these layers is uncorrelated with disease severity and was therefore not incorporated in our model. We also assumed the backscatter properties of the RPE to be constant. This assumption does not hold in case of peripapillary atrophy (PPA). In glaucoma, the RPE near the ONH can be affected by PPA, an important cause of irregular RPE around the ONH. PPA can be divided into 2 zones, the alpha and beta zone. The alpha zone is characterized by pigmentary irregularities in the RPE, while the beta zone, which is nearest to the ONH, correlates with a complete loss of RPE cells³¹. The alpha zone is nearest to the location of our analyses, which was 1.3 mm from the centre of the ONH. It is sometimes difficult to exactly delineate the peripheral border of alpha zone PPA. In retrospect, only 1.9% of the regions of analysis of our included eyes potentially contained some alpha zone PPA. Therefore, we feel confident that the PPA did not significantly affect our dataset.

We hypothesize that μ_{att} indirectly measures the nerve fiber density of the RNFL. Evidently, there is loss of nerve fibers due to glaucoma². In a histology study, Quigley et al.¹ measured a decrease of the fiber density in glaucomatous eyes compared to healthy eyes. A structural change due to glaucoma, i.e. the decreased density of the nerve fibers, is also thought to be associated with a decrease in birefringence of the RNFL^{32, 33}. A decreased nerve fiber density will also have its effect on the optical scattering properties of the RNFL. The denser the tissue is, the more the incident light is attenuated by the RNFL. We found that the μ_{att} of the RNFL diminished with increasing disease severity. A reduction of μ_{att} could be an early sign of glaucomatous damage. This hypothesis is supported by the findings of Huang and others. Firstly, they found that 50% of the RNFL reflectance is caused by microtubules³⁴ and secondly they found a change in reflectance of the RNFL to precede thinning of the RNFL³⁵. Future studies are needed to elucidate the relation between μ_{att} , reflectance, and glaucomatous damage.

The location significantly affected the μ_{att} of the RNFL. μ_{att} was lower nasally from the ONH, compared to the other locations (temporally, superiorly and inferiorly) in both healthy and in glaucomatous eyes. These differences in μ_{att} appear to be unrelated to glaucoma, because they occurred in both glaucomatous and healthy eyes. The difference between the retina nasally from the ONH and the other locations, is that the RNFL is usually thinner nasally. More importantly, the incident light being reflected by the RNFL nasally is probably less compared to the other locations because of a different angle of this part of the retina. The nasal side of the ONH is more towards the periphery, leading to a higher retinal curvature

perpendicular on the light beam. The less perpendicular the RNFL is to the light beam and consequently, the larger the scan angle is, the smaller the reflectance of the cylindrical nerve fibers will be.³⁶ This might explain the lower μ_{att} nasally compared to the other locations.

We also assessed a structure-function relationship by correlating μ_{att} to the MD. In previously published studies, in which the average RNFL thickness was used as a structural measure, and an index of visual fields as the functional measure, the structure-function relationship was generally quite weak and variable (R^2 from 0.08 to 0.55³⁷⁻⁴⁰). In our current study, the structure-function relationship between μ_{att} and MD showed a correlation well within the same range ($R^2 = 0.337$). Compared to earlier structure-function studies³⁷⁻⁴⁰, this result is promising, since our model is a first attempt of characterizing RNFL scattering properties in SD-OCT images. Further development in modeling the relationship between the μ_{att} and an index of visual fields is needed to explore the use of μ_{att} as a measure for structure in characterizing a structure-function relationship.

To our knowledge, SD-OCT currently does not consistently outperform several other available techniques in their diagnostic accuracy, such as SLP and CSLO⁹⁻¹². With every available imaging technique, it is notably difficult to detect early glaucoma, because of the large biological variation between healthy eyes and the inherent overlap with glaucomatous eyes. We have currently created a model for SD-OCT to quantify the attenuation of light, which is related to the optical scattering properties of the RNFL. With our method, we found a clear effect of glaucoma on the μ_{att} of the RNFL. The correlation of μ_{att} with standard automated perimetry (SAP) is comparable to that of SLP and CSLO with SAP³⁷⁻⁴⁰. We speculate that the reduced μ_{att} of the RNFL in SD-OCT images in glaucomatous eyes might serve as a discriminating feature for structural changes. Future studies are needed to clarify the role of the μ_{att} of the RNFL in diagnosing and following glaucoma with SD-OCT, potentially leading to a new method to quantify glaucoma in SD-OCT images.



REFERENCES

1. Quigley HA, Addicks EM, Green WR. Optic nerve damage in human glaucoma. III. Quantitative correlation of nerve fiber loss and visual field defect in glaucoma, ischemic neuropathy, papilledema, and toxic neuropathy. *Arch Ophthalmol*. 1982;100:135-146.
2. Ritch R, Shields M.B., Krupin Th. Anatomy and Pathophysiology of the Retina and Optic Nerve. In: *The Glaucomas; Basic Sciences*. 2nd ed. St. Louis, Missouri, USA: Anne Patterson; 1996:139-176.
3. Fercher AF, Hitzengerger CK, Drexler W, Kamp G, Sattmann H. In vivo optical coherence tomography. *Am J Ophthalmol*. 1993;116:113-114.
4. Huang D, Swanson EA, Lin CP, et al. Optical coherence tomography. *Science*. 1991;254:1178-1181.
5. Blumenthal EZ, Williams JM, Weinreb RN, Girkin CA, Berry CC, Zangwill LM. Reproducibility of nerve fiber layer thickness measurements by use of optical coherence tomography. *Ophthalmology*. 2000;107:2278-2282.
6. Budenz DL, Chang RT, Huang X, Knighton RW, Tielsch JM. Reproducibility of retinal nerve fiber thickness measurements using the stratus OCT in normal and glaucomatous eyes. *Invest Ophthalmol Vis Sci*. 2005;46:2440-2443.
7. Budenz DL, Fredette MJ, Feuer WJ, Anderson DR. Reproducibility of peripapillary retinal nerve fiber thickness measurements with stratus OCT in glaucomatous eyes. *Ophthalmology*. 2008;115:661-666.
8. Paunescu LA, Schuman JS, Price LL, et al. Reproducibility of nerve fiber thickness, macular thickness, and optic nerve head measurements using StratusOCT. *Invest Ophthalmol Vis Sci*. 2004;45:1716-1724.
9. Schuman JS, Pedut-Kloizman T, Hertzmark E, et al. Reproducibility of nerve fiber layer thickness measurements using optical coherence tomography. *Ophthalmology*. 1996;103:1889-1898.
10. Leon Ortega JE, Sakata LM, Kakati B, et al. Effect of glaucomatous damage on repeatability of confocal scanning laser ophthalmoscope, scanning laser polarimetry, and optical coherence tomography. *Invest Ophthalmol Vis Sci*. 2007;48:1156-1163.
11. Leung CK, Cheung CY, Lin D, Pang CP, Lam DS, Weinreb RN. Longitudinal variability of optic disc and retinal nerve fiber layer measurements. *Invest Ophthalmol Vis Sci*. 2008;49:4886-4892.
12. Lin D, Leung CK, Weinreb RN, Cheung CY, Li H, Lam DS. Longitudinal evaluation of optic disc measurement variability with optical coherence tomography and confocal scanning laser ophthalmoscopy. *J Glaucoma*. 2009;18:101-106.
13. Cense B, Nassif N, Chen T, et al. Ultrahigh-resolution high-speed retinal imaging using spectral-domain optical coherence tomography. *Opt Express*. 2004;12:2435-2447.
14. Nassif N, Cense B, Park B, et al. In vivo high-resolution video-rate spectral-domain optical coherence tomography of the human retina and optic nerve. *Opt Express*. 2004;12:367-376.
15. Nassif N, Cense B, Park BH, et al. In vivo human retinal imaging by ultrahigh-speed spectral domain optical coherence tomography. *Opt Lett*. 2004;29:480-482.
16. Wojtkowski M, Leitgeb R, Kowalczyk A, Bajraszewski T, Fercher AF. In vivo human retinal imaging by Fourier domain optical coherence tomography. *J Biomed Opt*. 2002;7:457-463.

17. Garas A, Vargha P, Hollo G. Reproducibility of retinal nerve fiber layer and macular thickness measurement with the RTVue-100 optical coherence tomograph. *Ophthalmology*. 2010;117:738-746.
18. Gonzalez-Garcia AO, Vizzeri G, Bowd C, Medeiros FA, Zangwill LM, Weinreb RN. Reproducibility of RTVue retinal nerve fiber layer thickness and optic disc measurements and agreement with Stratus optical coherence tomography measurements. *Am J Ophthalmol*. 2009;147:1067-74, 1074.
19. Kim JS, Ishikawa H, Sung KR, et al. Retinal nerve fibre layer thickness measurement reproducibility improved with spectral domain optical coherence tomography. *Br J Ophthalmol*. 2009;93:1057-1063.
20. Lee SH, Kim SH, Kim TW, Park KH, Kim DM. Reproducibility of Retinal Nerve Fiber Thickness Measurements Using the Test-retest Function of Spectral OCT/SLO in Normal and Glaucomatous Eyes. *J Glaucoma*. 2010.
21. Leung CK, Cheung CY, Weinreb RN, et al. Retinal nerve fiber layer imaging with spectral-domain optical coherence tomography: a variability and diagnostic performance study. *Ophthalmology*. 2009;116:1257-63, 1263.
22. Menke MN, Knecht P, Sturm V, Dabov S, Funk J. Reproducibility of nerve fiber layer thickness measurements using 3D fourier-domain OCT. *Invest Ophthalmol Vis Sci*. 2008;49:5386-5391.
23. Wu H, de Boer JF, Chen TC. Reproducibility of Retinal Nerve Fiber Layer Thickness Measurements Using Spectral Domain Optical Coherence Tomography. *J Glaucoma*. 2010.
24. Chang RT, Knight OJ, Feuer WJ, Budenz DL. Sensitivity and specificity of time-domain versus spectral-domain optical coherence tomography in diagnosing early to moderate glaucoma. *Ophthalmology*. 2009;116:2294-2299.
25. Park SB, Sung KR, Kang SY, Kim KR, Kook MS. Comparison of glaucoma diagnostic Capabilities of Cirrus HD and Stratus optical coherence tomography. *Arch Ophthalmol*. 2009;127:1603-1609.
26. Rao HL, Zangwill LM, Weinreb RN, Sample PA, Alencar LM, Medeiros FA. Comparison of different spectral domain optical coherence tomography scanning areas for glaucoma diagnosis. *Ophthalmology*. 2010;117:1692-9, 1699.
27. Pons ME, Ishikawa H, Gurses-Ozden R, Liebmann JM, Dou HL, Ritch R. Assessment of retinal nerve fiber layer internal reflectivity in eyes with and without glaucoma using optical coherence tomography. *Arch Ophthalmol*. 2000;118:1044-1047.
28. Heidelberg Engineering GmbH. Spectralis Viewing Module, Software Version 4.0, Special Function: Exporting Raw Data. 11 ed. Dossenheim, Germany; 2008.
29. Yushkevich PA, Piven J, Hazlett HC, et al. User-guided 3D active contour segmentation of anatomical structures: significantly improved efficiency and reliability. *Neuroimage*. 2006;31:1116-1128.
30. Chen Y, Burnes DL, de BM, Mujat M, de Boer JF. Three-dimensional pointwise comparison of human retinal optical property at 845 and 1060 nm using optical frequency domain imaging. *J Biomed Opt*. 2009;14:024016.
31. Jonas JB. Clinical implications of peripapillary atrophy in glaucoma. *Curr Opin Ophthalmol*. 2005;16:84-88.
32. Cense B, Chen TC, Park BH, Pierce MC, de Boer JF. Thickness and birefringence of healthy retinal nerve fiber layer tissue measured with polarization-sensitive optical coherence tomography. *Invest Ophthalmol Vis Sci*. 2004;45:2606-2612.

33. Huang XR, Bagga H, Greenfield DS, Knighton RW. Variation of peripapillary retinal nerve fiber layer birefringence in normal human subjects. *Invest Ophthalmol Vis Sci.* 2004;45:3073-3080.
34. Huang XR, Knighton RW, Cavuoto LN. Microtubule contribution to the reflectance of the retinal nerve fiber layer. *Invest Ophthalmol Vis Sci.* 2006;47:5363-5367.
35. Huang XR, Zhou Y, Kong W, Knighton RW. Reflectance Decrease Prior to Thickness Change of the Retinal Nerve Fiber Layer in Glaucomatous Retinas. *Invest Ophthalmol Vis Sci.* 2011.
36. Knighton RW, Huang XR. Directional and spectral reflectance of the rat retinal nerve fiber layer. *Invest Ophthalmol Vis Sci.* 1999;40:639-647.
37. Bowd C, Zangwill LM, Medeiros FA, et al. Structure-function relationships using confocal scanning laser ophthalmoscopy, optical coherence tomography, and scanning laser polarimetry. *Invest Ophthalmol Vis Sci.* 2006;47:2889-2895.
38. Mai TA, Reus NJ, Lemij HG. Structure-function relationship is stronger with enhanced corneal compensation than with variable corneal compensation in scanning laser polarimetry. *Invest Ophthalmol Vis Sci.* 2007;48:1651-1658.
39. Rao HL, Zangwill LM, Weinreb RN, Leite MT, Sample PA, Medeiros FA. Structure-function relationship in glaucoma using spectral-domain optical coherence tomography. *Arch Ophthalmol.* 2011;129:864-871.
40. Reus NJ, Lemij HG. Relationships between standard automated perimetry, HRT confocal scanning laser ophthalmoscopy, and GDx VCC scanning laser polarimetry. *Invest Ophthalmol Vis Sci.* 2005;46:4182-4188.

APPENDIX - MODEL

The proposed model is based on two different scattering layers: the RNFL and the RPE. The former is the layer of interest, while the latter will serve as an internal calibration layer. These layers are also the two most scattering layers in the retina. Other, weakly scattering retinal layers are not included. Assuming constant RPE backscatter properties, this layer is used to normalize the OCT signal from the RNFL. First, a model of the interaction between light and tissue is described. This model is then applied to the RNFL and the RPE, producing a method to determine the RNFL attenuation coefficient.

Attenuation and scattering of a homogeneous layer

The incoming beam, with a power of I_0 when it arrives at the front surface of the tissue, is attenuated by the tissue according to $\frac{dI}{dx} = -\mu_{att} \cdot I(x)$.

The power of the beam at depth x is then given by $I(x) = I_0 e^{-\mu_{att} x}$, where μ_{att} is the attenuation coefficient of the tissue. Combining these equations produces the attenuation of the light at depth x : $\mu_{att} \cdot I(x) = \mu_{att} \cdot I_0 e^{-\mu_{att} x}$. A fraction of the attenuated light, given by α , is backscattered. Before reaching the detector, this light is again attenuated by the tissue. The power of the light at the detector that was backscattered at depth x is then given by $\alpha \cdot \mu_{att} \cdot I_0 e^{-2\mu_{att} x}$. Integrating over a depth range d results in the total power of the backscattered signal at the detector

$$T = \int_{x=0}^d \alpha \cdot \mu_{att} \cdot I_0 e^{-2\mu_{att} x} dx = \frac{\alpha \cdot I_0}{2} (1 - e^{-2\mu_{att} d}). \quad (1)$$

RNFL

The RNFL is the first retinal layer that the incident light beam interacts with. The total backscattered signal for the RNFL is given by

$$T_{RNFL} = \frac{\alpha_{RNFL} \cdot I_0}{2} (1 - e^{-2\mu_{RNFL} d_{RNFL}}), \quad (3)$$

RPE

Light that reaches the RPE is first attenuated by the RNFL. After interacting with the RPE, the backscattered light is again attenuated by the RNFL. The total backscattered signal for the RPE is therefore given by

$$T_{RPE} = \frac{\alpha_{RPE} I_0}{2} (1 - e^{-2\mu_{RPE} d_{RPE}}) \cdot e^{-2\mu_{RNFL} d_{RNFL}}. \quad (5)$$

Deriving μ

Calculating the ratio of the total OCT signal of the RNFL and the RPE yields

$$\begin{aligned} R &= \frac{T_{RNFL}}{T_{RPE}} \\ &= \frac{\frac{\alpha_{RNFL} I_0}{2} (1 - e^{-2\mu_{RNFL} d_{RNFL}})}{\frac{\alpha_{RPE} I_0}{2} (1 - e^{-2\mu_{RPE} d_{RPE}}) \cdot e^{-2\mu_{RNFL} d_{RNFL}}} \\ &= \frac{\alpha_{RNFL} (e^{2\mu_{RNFL} d_{RNFL}} - 1)}{\alpha_{RPE} (1 - e^{-2\mu_{RPE} d_{RPE}})} \end{aligned} \quad (7)$$

Assuming that α_{RNFL} and α_{RPE} are constant, and that the attenuation of the RPE is constant (i.e., μ_{RPE} and d_{RPE} are constant), this equation reduces to

$$R = \beta (e^{2\mu_{att} d} - 1). \quad (8)$$

Solving this equation for μ_{att} results in

$$\mu_{att} = \frac{\log(R / \beta + 1)}{2d}. \quad (9)$$

Calculating β

In equation 9, μ can be calculated if R , d and β are known. Both R and d can be determined from a segmented OCT scan. Given that β is a constant in our model, it may be estimated from the data. For estimating β , equation 8 was used. The data set contained R and d determined from OCT data of healthy eyes, and μ and β were fitted to the model by minimizing the error

$$\sum_i \left(\log \frac{\beta (e^{2\mu_{att} d_i} - 1)}{R_i} \right)^2. \quad (10)$$

The result is shown in the Figure and the optimal fit was found for $\beta = 2.3$ (and $\mu_{att} = 4.6 \text{ mm}^{-1}$).

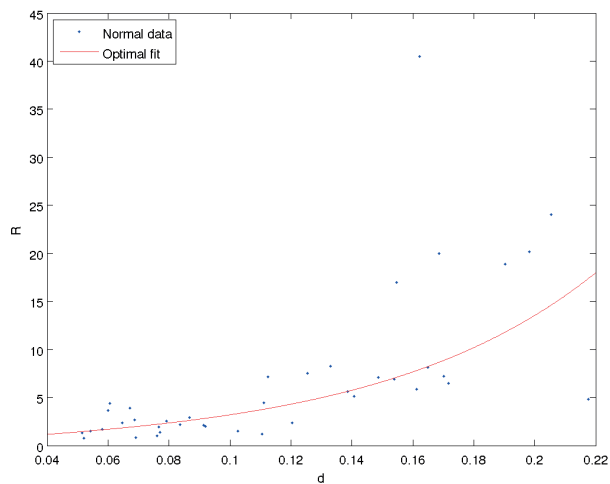


Figure Scatter plot of the ratio (R) between the reflectivity of the RNFL and RPE against the RNFL thickness (d) for healthy eyes.

9

General Discussion & Future Perspectives

GENERAL DISCUSSION

In this thesis we investigated various techniques used for diagnosing and monitoring glaucoma. The first difficulty in this matter is defining glaucoma. Glaucoma is defined as 'a heterogeneous group of progressive optic neuropathies characterised by an accelerated degeneration of retinal ganglion cells (RGCs) and their axons, resulting in a typical appearance of the optic nerve head (ONH) and a matching pattern of irreversible visual field loss'.¹⁻³

Judging the optic nerve head

In this definition of glaucoma, the terms '*heterogeneous*' group and '*typical appearance*' of the ONH both lead to a mystification of glaucoma. What is a typical appearance of the ONH? Apparently, this is one of the hardest aspects an ophthalmologist encounters in glaucoma care. Several studies described how hard it is to distinguish a healthy ONH from a glaucomatous one.⁴⁻¹⁰ In *Chapter 5 & 6* we describe two different aspects of judging the ONH. In daily glaucoma care, an ophthalmologist often needs to correlate an ONH he/she judges by the slitlamp, with a corresponding visual field. Based on this information, plus the intraocular pressure (IOP), the ophthalmologist decides to start therapy or to alter or continue the current therapy. In the ESAFAT (*Chapter 5*), a trial across Europe in matching stereoscopic optic disc photographs to its corresponding visual fields of varying severity, we found that European ophthalmologists tended to overestimate the visual field damage. In *Chapter 6*, we describe how hard it is to find progression solely based on the appearance of the ONH. There was poor agreement between eyecare professionals judging an ONH as progressing and progression based on visual fields. Apparently, in judging the ONH as having glaucoma or as progressing by glaucoma, this 'typical' appearance of the ONH does not seem to be so typical for an ophthalmologist.

Functional loss

If we, as humans, have so much difficulty in judging ONHs, how good are the commercially available structural and functional tests in diagnosing and monitoring glaucoma? To date, there is still no clinically applicable technique that measures the exact nature of the disease (the death of the RGCs and their axons). All techniques developed in the past decades indirectly measure the functional and structural loss. The function of the eye is determined by measuring the visual field by perimetry. Several types of perimetry have been developed to measure the functional glaucomatous loss. Standard automated perimetry is the visual field testing used most often and it is currently seen as the gold standard in measuring

functional glaucomatous loss. Other types of perimetry, such as frequency-doubling technique (FDT) or short wavelength automated perimetry (SWAP), currently play a minor role in the daily management of glaucoma. Despite the many years of SWAP development, we found that it does not outperform SAP in monitoring ocular hypertension and detecting conversion to glaucoma (*Chapter 2*). Our study shows conflicting results compared to earlier studies.¹¹⁻¹⁵ We therefore think that early glaucomatous damage is idiosyncratic, and may become first apparent in one of different pathways, sometimes appearing first in SWAP and sometimes first in SAP. Then, no specific perimetric test can be the gold standard in detecting early glaucoma. Fortunately, these conflicting results of our and other trials lead to a general advice of, for instance, the European Glaucoma Society to initially perform SAP, whereas other types of visual field testing have insufficient evidence to offer any advantage over SAP.¹

Structural loss

Other techniques developed for measuring glaucoma are based on measuring the *structural* glaucomatous loss by assessing the optic nerve head (ONH) and the loss of RGCs and their axons, leading to the typical cupping of the ONH and the subsequent loss or thinning of the retinal nerve fiber layer (RNFL). These structural changes are currently measured by several imaging techniques, such as optical coherence tomography (OCT), confocal scanning laser ophthalmoscopy (CSLO) and scanning laser polarimetry (SLP). OCT is in an ongoing promising development, whereas CSLO and SLP are currently the two structural techniques that have (almost) reached the end of their development. Both techniques yield a diagnostic accuracy of more than 90% and 86% for SLP and CSLO respectively.^{7,16-20} It therefore exceeds the ability of ophthalmologists to judge an ONH, with a diagnostic accuracy of 80.5%.⁸ Currently, most studies conclude a poor agreement between structure and function²¹⁻²⁷ instead of one preceding the other. This phenomenon leads to an individual approach in monitoring glaucoma, sometimes following a patient with measurements of structure, and sometimes with measurements of function. We have shown that SLP is especially an essential tool in diagnosing glaucoma in eyes converting from ocular hypertension (*Chapter 3*). Apparently, SLP is more sensitive in diagnosing early glaucoma in eyes converting from ocular hypertension than SAP. This is confirmed by older studies in the early nineties.^{28,29} We therefore advise an ophthalmologist to consider to implement SLP, or another measurement of structure, in this individual approach in daily care to monitor eyes with ocular hypertension to diagnose early glaucoma.

Glaucoma with only structural defects and no functional defects (yet) is known as preperimetric glaucoma. This group of glaucoma will enlarge when monitoring is

more and more done by structural measurements, such as SLP or OCT. But in the long term, compared to waiting for it to become perimetric glaucoma, this earlier detection and proper treatment of preperimetric glaucoma, will ideally lead to less severe glaucoma and therefore to less visual disability.

Optical coherence tomography

Spectral domain OCT (SD-OCT) is commercially available since 2006. Since then, it is increasingly used in daily glaucoma care. Especially now that SLP technology is no longer commercially manufactured, SD-OCT becomes more and more the standard technique to measure structural glaucomatous loss. Interestingly, to our knowledge, measuring the RNFL thickness around the ONH by SD-OCT currently does not consistently outperform other available techniques in their diagnostic accuracy, such as SLP and CSLO.^{20,30-33} On the other hand, newer technologies lead to new insights. In this thesis, we presented two new insights in glaucoma due to the use of SD-OCT. Firstly, we presented a newly described phenomenon: a focal microcystic schisis of the RNFL in glaucomatous eyes, located in an area of a pre-existing glaucomatous RNFL defect, suggesting that this phenomenon is associated with glaucomatous wedge defects of the RNFL (*Chapter 7*). Several recent studies presented cases with peripapillary retinoschisis, imaged with SD-OCT.³⁴⁻³⁹ All studies showed a relation between the retinoschisis and the presence of glaucoma. The pathophysiological mechanism is still speculated on: most agree on the presence of fluid in or between the retinal layers. The origin of this fluid remains unclear. It might be of vitreous origin, as Kahook et al. suggested³⁷, or the fluid might be cerebrospinal fluid, entering the retina through the lamina cribrosa along the tiny canals created by the pathological absence of the nerve fibers. Evidently, this interesting phenomenon needs further study to analyse its underlying pathophysiological mechanisms and its relation to glaucoma.

The second new observation that we made with the SD-OCT was not only that the RNFL thins in glaucoma, but also that the optical scattering properties of the RNFL change due to glaucoma. We presented a newly described parameter, the attenuation coefficient (μ_{att}), which quantifies the optical scattering properties of retinal layers. Up till now, the only parameter related to the RNFL was its thickness. The model we described, is based on the reflectivity of the RNFL and the RPE, as well as on the interaction between light and the tissue and also on the thickness of the RNFL. We hypothesized that μ_{att} indirectly measures the nerve fiber density of the RNFL. The attenuation coefficient of the RNFL in SD-OCT images was lower in glaucomatous eyes than in healthy eyes and it decreased with increasing disease severity. Additionally, we found that the correlation of μ_{att} with standard automated perimetry (SAP) was comparable to that of SLP and CSLO with SAP.⁴⁰⁻⁴³

We speculate that the reduced μ_{att} of the RNFL in SD-OCT images in glaucomatous eyes might serve as a discriminating feature for structural changes. Further analyses of this parameter might also potentially lead to new scientific insights in the pathophysiological mechanism of the development of glaucoma. Future studies are needed to clarify the role of the μ_{att} of the RNFL in diagnosing and following glaucoma with SD-OCT, potentially leading to a new method to quantify glaucoma in SD-OCT images in daily practice.

Progression analysis

Currently, every commercially available device measuring functional or structural glaucomatous damage, provides analyses of progression. These progression analyses are helpful to diagnose conversion to glaucoma in eyes with ocular hypertension, as is described in *Chapter 3*. In our study, measurements of structure (SLP) showed conversion to glaucoma earlier than measurements of function (SAP) did. On the other hand, in progressing glaucomatous eyes, SAP flagged glaucomatous progression much more often than ophthalmologists did, when observing structural change based on the ONH, as described in *Chapter 6*. Because of this poor agreement between structure and function²¹⁻²⁶ in monitoring and detecting glaucomatous progression, as in diagnosing glaucoma, up till now no gold standard has been determined. In daily practice, determining the rate of progression (RoP) is an important part of monitoring glaucoma, usually based on SAP. The RoP is the loss of RGCs and visual function compared to the decay based on aging alone and, amongst other parameters, one of the pillars of glaucoma management. The conflicting results on detecting glaucomatous progression by different techniques hampers the justified use of RoP in daily practice.

FUTURE PERSPECTIVES

Currently, the future in diagnosing and monitoring glaucoma is directed to SD-OCT, or even its successors. SLP and CSLO are both still used in daily glaucoma practice. Nevertheless, nowadays the focus has increasingly been shifted towards SD-OCT. The main advantage of SD-OCT is its multifunctional use in ophthalmology. Not only glaucoma, but also many other retinal abnormalities are currently detected and followed by SD-OCT. Also the ongoing development of the technique promises increased quality of images and analyses in the near future.

Development of new analyses

Until recently, the main structural parameter in measuring glaucoma was the thickness of the peripapillary RNFL. Nowadays, also the thickness of the macular ganglion cell layer & inner plexiform layer together combined with the RNFL, called the ganglion cell complex (GCC), is incorporated in commercially available analyses. This analysis is based on the knowledge that up to 50% of the RGCs are located in the macular region.⁴⁴ These layers are potentially easier to image, because the RGC body has a larger diameter than its axons and the macular area is characterised by less intersubject variability.⁴⁵ Analyses of the GCC therefore potentially detect thinning more easily than by measuring the peripapillary RNFL thickness.⁴⁶ Various studies have shown a comparable diagnostic sensitivity between these 2 mentioned parameters.⁴⁵ Currently, these macular parameters do not seem to outperform the RNFL thickness, but they might be of additional value in patients with anatomical variations leading to erroneous peripapillary RNFL measurements, such as high myopia, peripapillary atrophy or a tilted disc.⁴⁵

Another newly developed analysis in SD-OCT is a neuroretinal rim analysis, measuring the minimal rim width, defined as the shortest distance between the Bruchs membrane opening and the inner limiting membrane, averaged around the optic disc.^{47;48} With further developing techniques, both approaches are promising. These analyses have already been implemented in some commercially available devices.

Development of new OCT techniques

Swept-source OCT provides higher resolution images with enhanced depth imaging due to the use of a 1050nm light source and a higher scanning speed. Currently, the first commercial device (DRI-OCT1 Atlantis system, Topcon, Tokyo, Japan) has become available. Studies have shown SS-OCT not to outperform SD-OCT in diagnosing glaucoma by measuring RNFL thickness⁴⁹ and the thickness of the GCC⁵⁰. On the other hand, SS-OCT shows promising results in measuring other

parameters in glaucoma, such as anatomical changes of the lamina cribrosa⁵¹⁻⁵³ and the anterior chamber angle^{54,55}, because of its enhanced depth imaging.

Polarisation sensitive OCT combines measuring the birefringence of the RNFL with measuring the RNFL thickness by OCT.⁵⁶⁻⁵⁸ A third development in the technique of OCT, is the introduction of *adaptive optics* (AO). AO increases imaging resolution and sensitivity. It has been incorporated into CSLO, and also into OCT. This AO-OCT provides analyses of the individual retinal nerve fiber bundles, enabling more detailed analysis of the loss of these bundles due to glaucoma.⁵⁹

Pitfalls of OCT and technical development

A worrisome aspect of the current development of SD-OCT is the many commercial developers creating an SD-OCT device. To date, more than 10 different SD-OCTs are commercially available, all with their own hardware and software. The differences between these devices, with their own hardware and software algorithms, makes it impossible to interchange data. Every company creates their own analyses, image processing and scan protocols, as well as the earlier described new analyses. No standardisation has been achieved between these different SD-OCTs. Therefore, scans and their interpretations are not comparable to each other.

The quick development in the past few years and most probably also in the upcoming years leads to the question whether the measurements of a current device still are useful and backward compatible in the near future, when newer software, scan protocols, image processing and analyses have been developed. This question is often asked by general ophthalmologists in case of several ophthalmologic devices, used in daily care, but is a very essential question in chronic diseases such as glaucoma. Long term analyses measuring progression need to be backward compatible and stable for several years. Also long term follow up trials are severely hampered by this problem of development and (absence of) backward compatibility of devices, as illustrated by the data presented in Chapter 3 & 4, which has led to a severe decline of useful data. It is an important challenge for the developers of these devices to implement innovation in the current devices used for follow up without hampering accessibility of the already collected data to newly developed analyses.

Challenges

With every currently available imaging technique, it remains a challenge to detect and follow glaucoma. Firstly in *diagnosing glaucoma*, one needs to combine the outcome of several measurements in order to decide whether or not glaucoma is present. This is a challenge, because of the large biological variation within healthy eyes and the inherent overlap with glaucomatous eyes. Between trials,

glaucoma or its progression are defined differently, hampering comparison of the outcomes of these trials. But it even makes it harder for any clinician to translate these outcomes to the daily care of glaucoma patients. Also choosing the type of measurements in daily practice to diagnose glaucoma, is a challenging task for an ophthalmologist. Should you just measure IOP, look at the ONH and do visual field testing? Or does imaging indeed lead to an earlier diagnosis of glaucoma? Based on our studies, we advise to combine functional and structural measurements in diagnosing early glaucoma. On the other hand, in daily practice this might not always be possible due to practical and financial reasons. Up till now, no strict consensus has been achieved on how exactly to diagnose and monitor glaucoma. This encourages ophthalmologists to diagnose and treat every individual patient by an individual approach.

In *monitoring glaucoma*, the most challenging issue is implementing the ongoing development of techniques into the follow-up measurements over many years, without losing information. This chronic and usually slowly progressing disease requires techniques that are robust over time, as well as sensitive and specific. Whether or not to speak of progressing glaucoma is also an everyday challenge, depending on the types of measurements and the prudence or awareness of the ophthalmologist.

The absence of a strict consensus in diagnosing and monitoring glaucoma encourages an ophthalmologist to create an individual approach based on scientifically-based protocols, experience and gut feeling. Diagnosing and monitoring glaucoma is an everyday complex challenge!



REFERENCE LIST

1. European Glaucoma Society. Terminology and Guidelines for Glaucoma. 4th ed. Savona, Italy: 2014.
2. Quigley HA. Glaucoma. *Lancet* 2011;377:1367-77.
3. Weinreb RN, Khaw PT. Primary open-angle glaucoma. *Lancet* 2004;363:1711-20.
4. Abrams LS, Scott IU, Spaeth GL, et al. Agreement among optometrists, ophthalmologists, and residents in evaluating the optic disc for glaucoma. *Ophthalmology* 1994;101:1662-7.
5. Andersson S, Heijl A, Bengtsson B. Optic disc classification by the Heidelberg Retina Tomograph and by physicians with varying experience of glaucoma. *Eye (Lond)* 2011.
6. Girkin CA, McGwin G, Jr., Long C, et al. Subjective and objective optic nerve assessment in African Americans and whites. *Invest Ophthalmol Vis Sci* 2004;45:2272-8.
7. Reus NJ, deGraaf M, Lemij HG. Accuracy of GDx VCC, HRT I, and clinical assessment of stereoscopic optic nerve head photographs for diagnosing glaucoma. *Br J Ophthalmol* 2007;91:313-8.
8. Reus NJ, Lemij HG, Garway-Heath DF, et al. Clinical assessment of stereoscopic optic disc photographs for glaucoma: the European Optic Disc Assessment Trial. *Ophthalmology* 2010;117:717-23.
9. Varma R, Steinmann WC, Scott IU. Expert agreement in evaluating the optic disc for glaucoma. *Ophthalmology* 1992;99:215-21.
10. Wollstein G, Garway-Heath DF, Fontana L, Hitchings RA. Identifying early glaucomatous changes. Comparison between expert clinical assessment of optic disc photographs and confocal scanning ophthalmoscopy. *Ophthalmology* 2000;107:2272-7.
11. Demirel S, Johnson CA. Incidence and prevalence of short wavelength automated perimetry deficits in ocular hypertensive patients. *Am J Ophthalmol* 2001;131:709-15.
12. Johnson CA, Adams AJ, Casson EJ, Brandt JD. Blue-on-yellow perimetry can predict the development of glaucomatous visual field loss. *Arch Ophthalmol* 1993;111:645-50.
13. Johnson CA, Adams AJ, Casson EJ, Brandt JD. Progression of early glaucomatous visual field loss as detected by blue-on-yellow and standard white-on-white automated perimetry. *Arch Ophthalmol* 1993;111:651-6.
14. Polo V, Larrosa JM, Pinilla I, et al. Predictive value of short-wavelength automated perimetry: a 3-year follow-up study. *Ophthalmology* 2002;109:761-5.
15. Sample PA, Taylor JD, Martinez GA, et al. Short-wavelength color visual fields in glaucoma suspects at risk. *Am J Ophthalmol* 1993;115:225-33.
16. Mai TA, Reus NJ, Lemij HG. Diagnostic accuracy of scanning laser polarimetry with enhanced versus variable corneal compensation. *Ophthalmology* 2007;114:1988-93.
17. Medeiros FA, Zangwill LM, Bowd C, Weinreb RN. Comparison of the GDx VCC scanning laser polarimeter, HRT II confocal scanning laser ophthalmoscope, and stratus OCT optical coherence tomograph for the detection of glaucoma. *Arch Ophthalmol* 2004;122:827-37.
18. Medeiros FA, Zangwill LM, Bowd C, et al. Use of progressive glaucomatous optic disk change as the reference standard for evaluation of diagnostic tests in glaucoma. *Am J Ophthalmol* 2005;139:1010-8.
19. Reus NJ, Lemij HG. Diagnostic accuracy of the GDx VCC for glaucoma. *Ophthalmology* 2004;111:1860-5.
20. Michelessi M, Lucenteforte E, Oddone F, et al. Optic nerve head and fibre layer imaging for diagnosing glaucoma. *Cochrane Database Syst Rev* 2015;11:CD008803.

21. Banegas SA, Anton A, Morilla-Grasa A, et al. Agreement among spectral-domain optical coherence tomography, standard automated perimetry, and stereophotography in the detection of glaucoma progression. *Invest Ophthalmol Vis Sci* 2015;56:1253-60.
22. Chauhan BC, McCormick TA, Nicoleta MT, LeBlanc RP. Optic disc and visual field changes in a prospective longitudinal study of patients with glaucoma: comparison of scanning laser tomography with conventional perimetry and optic disc photography. *Arch Ophthalmol* 2001;119:1492-9.
23. Medeiros FA, Zangwill LM, Bowd C, et al. The structure and function relationship in glaucoma: implications for detection of progression and measurement of rates of change. *Invest Ophthalmol Vis Sci* 2012;53:6939-46.
24. Mohammadi K, Bowd C, Weinreb RN, et al. Retinal nerve fiber layer thickness measurements with scanning laser polarimetry predict glaucomatous visual field loss. *Am J Ophthalmol* 2004;138:592-601.
25. Quigley HA, Enger C, Katz J, et al. Risk factors for the development of glaucomatous visual field loss in ocular hypertension. *Arch Ophthalmol* 1994;112:644-9.
26. Schrems-Hoesl LM, Schrems WA, Laemmer R, et al. Confocal Laser Scanning Tomography to Predict Visual Field Conversion in Patients With Ocular Hypertension and Early Glaucoma. *J Glaucoma* 2014.
27. Crabb DP. Modelling measurement variation and noise is a potential source of the poor agreement between structure and function. 1-5-2016. Ref Type: Personal Communication
28. Sommer A, Katz J, Quigley HA, et al. Clinically detectable nerve fiber atrophy precedes the onset of glaucomatous field loss. *Arch Ophthalmol* 1991;109:77-83.
29. Zeyen TG, Caprioli J. Progression of disc and field damage in early glaucoma. *Arch Ophthalmol* 1993;111:62-5.
30. Leon Ortega JE, Sakata LM, Kakati B, et al. Effect of glaucomatous damage on repeatability of confocal scanning laser ophthalmoscope, scanning laser polarimetry, and optical coherence tomography. *Invest Ophthalmol Vis Sci* 2007;48:1156-63.
31. Leung CK, Cheung CY, Lin D, et al. Longitudinal variability of optic disc and retinal nerve fiber layer measurements. *Invest Ophthalmol Vis Sci* 2008;49:4886-92.
32. Lin D, Leung CK, Weinreb RN, et al. Longitudinal evaluation of optic disc measurement variability with optical coherence tomography and confocal scanning laser ophthalmoscopy. *J Glaucoma* 2009;18:101-6.
33. Schuman JS, Pedut-Kloizman T, Hertzmark E, et al. Reproducibility of nerve fiber layer thickness measurements using optical coherence tomography. *Ophthalmology* 1996;103:1889-98.
34. Bayraktar S, Cebeci Z, Kabaalioglu M, et al. Peripapillary Retinoschisis in Glaucoma Patients. *J Ophthalmol* 2016;2016:1612720.
35. Farjad H, Besada E, Frauens BJ. Peripapillary schisis with serous detachment in advanced glaucoma. *Optom Vis Sci* 2010;87:E205-E217.
36. Hwang YH, Kim YY, Kim HK, Sohn YH. Effect of peripapillary retinoschisis on retinal nerve fibre layer thickness measurement in glaucomatous eyes. *Br J Ophthalmol* 2014;98:669-74.
37. Kahook MY, Noecker RJ, Ishikawa H, et al. Peripapillary schisis in glaucoma patients with narrow angles and increased intraocular pressure. *Am J Ophthalmol* 2007;143:697-9.
38. Lee EJ, Kim TW, Kim M, Choi YJ. Peripapillary retinoschisis in glaucomatous eyes. *PLoS One* 2014;9:e90129.

39. Lee JH, Park HL, Baek J, Lee WK. Alterations of the Lamina Cribrosa Are Associated with Peripapillary Retinoschisis in Glaucoma and Pachychoroid Spectrum Disease. *Ophthalmology* 2016.
40. Bowd C, Zangwill LM, Medeiros FA, et al. Structure-function relationships using confocal scanning laser ophthalmoscopy, optical coherence tomography, and scanning laser polarimetry. *Invest Ophthalmol Vis Sci* 2006;47:2889-95.
41. Mai TA, Reus NJ, Lemij HG. Structure-function relationship is stronger with enhanced corneal compensation than with variable corneal compensation in scanning laser polarimetry. *Invest Ophthalmol Vis Sci* 2007;48:1651-8.
42. Rao HL, Zangwill LM, Weinreb RN, et al. Structure-function relationship in glaucoma using spectral-domain optical coherence tomography. *Arch Ophthalmol* 2011;129:864-71.
43. Reus NJ, Lemij HG. Relationships between standard automated perimetry, HRT confocal scanning laser ophthalmoscopy, and GDx VCC scanning laser polarimetry. *Invest Ophthalmol Vis Sci* 2005;46:4182-8.
44. Curcio CA, Allen KA. Topography of ganglion cells in human retina. *J Comp Neurol* 1990;300:5-25.
45. Oddone F, Lucenteforte E, Michelessi M, et al. Macular versus Retinal Nerve Fiber Layer Parameters for Diagnosing Manifest Glaucoma: A Systematic Review of Diagnostic Accuracy Studies. *Ophthalmology* 2016.
46. Zeimer R, Asrani S, Zou S, et al. Quantitative detection of glaucomatous damage at the posterior pole by retinal thickness mapping. A pilot study. *Ophthalmology* 1998;105:224-31.
47. Povazay B, Hofer B, Hermann B, et al. Minimum distance mapping using three-dimensional optical coherence tomography for glaucoma diagnosis. *J Biomed Opt* 2007;12:041204.
48. Chen TC. Spectral domain optical coherence tomography in glaucoma: qualitative and quantitative analysis of the optic nerve head and retinal nerve fiber layer (an AOS thesis). *Trans Am Ophthalmol Soc* 2009;107:254-81.
49. Yang Z, Tatham AJ, Zangwill LM, et al. Diagnostic ability of retinal nerve fiber layer imaging by swept-source optical coherence tomography in glaucoma. *Am J Ophthalmol* 2015;159:193-201.
50. Yang Z, Tatham AJ, Weinreb RN, et al. Diagnostic ability of macular ganglion cell inner plexiform layer measurements in glaucoma using swept source and spectral domain optical coherence tomography. *PLoS One* 2015;10:e0125957.
51. Takayama K, Hangai M, Kimura Y, et al. Three-dimensional imaging of lamina cribrosa defects in glaucoma using swept-source optical coherence tomography. *Invest Ophthalmol Vis Sci* 2013;54:4798-807.
52. Wang B, Nevins JE, Nadler Z, et al. Reproducibility of in-vivo OCT measured three-dimensional human lamina cribrosa microarchitecture. *PLoS One* 2014;9:e95526.
53. Omodaka K, Horii T, Takahashi S, et al. 3D evaluation of the lamina cribrosa with swept-source optical coherence tomography in normal tension glaucoma. *PLoS One* 2015;10:e0122347.
54. Leung CK, Weinreb RN. Anterior chamber angle imaging with optical coherence tomography. *Eye (Lond)* 2011;25:261-7.
55. McKee H, Ye C, Yu M, et al. Anterior chamber angle imaging with swept-source optical coherence tomography: detecting the scleral spur, Schwalbe's Line, and Schlemm's Canal. *J Glaucoma* 2013;22:468-72.

56. Cense B, Chen TC, Park BH, et al. In vivo birefringence and thickness measurements of the human retinal nerve fiber layer using polarization-sensitive optical coherence tomography. *J Biomed Opt* 2004;9:121-5.
57. Gotzinger E, Pircher M, Hitzenberger CK. High speed spectral domain polarization sensitive optical coherence tomography of the human retina. *Opt Express* 2005;13:10217-29.
58. Elmaanaoui B, Wang B, Dwelle JC, et al. Birefringence measurement of the retinal nerve fiber layer by swept source polarization sensitive optical coherence tomography. *Opt Express* 2011;19:10252-68.
59. Kocaoglu OP, Cense B, Jonnal RS, et al. Imaging retinal nerve fiber bundles using optical coherence tomography with adaptive optics. *Vision Res* 2011;51:1835-44.

10

Summary & Samenvatting

SUMMARY

Glaucoma is a heterogeneous group of progressive optic neuropathies characterised by an accelerated degeneration of retinal ganglion cells (RGCs) and their axons, resulting in a typical appearance of the optic nerve head and a matching pattern of irreversible visual field loss. Worldwide, approximately 12% of all blindness is due to glaucoma, which makes it the second leading cause of blindness. The most important risk factor is an increased intraocular pressure (IOP). In eyes with ocular hypertension, the IOP is increased without an optic neuropathy and visual field loss. The higher the IOP, the higher the risk of developing glaucoma. The IOP is currently the only factor that can be altered therapeutically. Lowering the IOP has been shown to slow down the progression of glaucoma.

To date, there is still no technique that measures the exact nature of the disease (the death of the RGCs and their axons). All techniques developed in the past decades indirectly measure the functional and structural loss. In measuring glaucoma, the function of the eye is determined by measuring the visual field by perimetry. Several types of perimetry have been developed to measure the functional glaucomatous loss. The structural loss due to glaucoma is determined by measuring the optic nerve head (ONH), which changes due to loss of RGCs and its axons, leading to a typical cupping of the ONH and the subsequent loss or thinning of the retinal nerve fiber layer. These structural changes are currently measured by several imaging techniques, such as optical coherence tomography (OCT), confocal scanning laser ophthalmoscopy (CSLO) and scanning laser polarimetry (SLP).

The objective of the research presented in this thesis was to evaluate various techniques used in daily glaucoma practice to diagnose and monitor glaucoma.

In chapter 2, we compared 2 types of perimetry, standard automated perimetry (SAP), which is mainly used in daily care, and short wavelength automated perimetry (SWAP). SWAP had been claimed to predict conversion to glaucoma 3-4 years before SAP defects occur. Our purpose was to compare the moment of glaucomatous conversion between SWAP and SAP in a large group of eyes with ocular hypertension. Our results did not support the notion that SWAP generally predicts conversion to glaucoma in SAP. Instead, SAP appeared to be at least as sensitive to conversion as SWAP in a large majority of eyes.

In chapters 3 & 4, we presented the results of a large randomised controlled trial into ocular hypertension and the effect of betablockers to prevent eyes from converting to glaucoma. Chapter 3 presented the rate of conversion from ocular hypertension to glaucoma defined by progression analyses on visual fields and SLP. SLP flagged conversion to glaucoma earlier than SAP in the large majority

of cases, potentially leading to earlier treatment preventing further progression to moderate or severe glaucoma. In [Chapter 4](#), we presented the effect of topical beta-blockers on the rate of conversion of ocular hypertension to glaucoma, using the definition of conversion as presented in Chapter 3. This study showed a higher rate of conversion to glaucoma in ocular hypertensive eyes treated with beta-blockers, as well as with placebo eye drops, than other trials have described before. We showed that, in general, beta-blockers do not prevent eyes with ocular hypertension from converting to glaucoma.

In [Chapter 5 & 6](#), we presented data on judging optic discs by professional glaucoma caregivers by assessing stereoscopic ONH photographs in diagnosing (Chapter 5) and monitoring (chapter 6) glaucoma. Firstly in [Chapter 5](#), we assessed the ability of ophthalmologists across Europe to match stereoscopic photographs of various optic discs to their corresponding visual fields, from a selection of visual fields of varying severity. European ophthalmologists correctly matched stereoscopic optic disc photographs to their corresponding visual field in only approximately 59% of cases. In most mismatches, the clinicians overestimated the visual field damage. Apparently, because of their poor agreement, both clinical ONH judgment and evaluation of visual field test results remain important mainstays in daily clinical care. In [Chapter 6](#), we determined the association between glaucoma progression in SAP and clinical assessment of stereoscopic ONH photographs. It also investigated any differences between various eye-care professionals in their ability to detect progression on sequential stereoscopic ONH photographs. We found a poor agreement between clinical assessment of serial stereoscopic ONH photographs and progression analysis on visual fields in glaucoma. In general, glaucoma specialists judged ONH photographs slightly more consistently than did less experienced eye care professionals.

In [Chapter 7 & 8](#) we presented the newest commercially available technique to assist clinicians to diagnose and monitor glaucoma, the OCT. New techniques lead to new insights. [Chapter 7](#) presented a newly described phenomenon in glaucomatous eyes. We showed 7 cases with a transient focal microcystic schisis of the retinal nerve fiber layer (RNFL) in glaucomatous eyes in images obtained with spectral domain OCT (SD-OCT). Our data suggest that this phenomenon is associated with glaucomatous wedge defects in the RNFL. We compared the OCT-images with other techniques measuring glaucoma and this phenomenon was best observed with SD-OCT and it was absent in healthy eyes. Further research will be required to explore its course and its pathogenesis.

In [chapter 8](#), we presented the first results of a newly developed parameter in OCT, the optical attenuation coefficient. In this chapter, we demonstrated the effect of glaucoma on the optical attenuation coefficient of the RNFL in SD-OCT

images. The measurements clearly demonstrated that the attenuation coefficient of the RNFL decreased with increasing disease severity. Future studies are needed to clarify the role of the attenuation coefficient of the RNFL in diagnosing and following glaucoma with SD-OCT, potentially leading to a new method to quantify glaucoma in SD-OCT images.

In summary, we evaluated various techniques used in daily glaucoma practice to diagnose and monitor glaucoma. SAP remains an important mainstay in daily glaucoma care, whereas SWAP turned out to be less sensitive than SAP. Accurately measuring structural change due to glaucoma remains a challenging goal. While SLP and CSLO have proven their additional value to the clinical assessment of the ONH, which, however, still remains challenging in ophthalmic care, the general focus of structural measurements for glaucoma has shifted towards SD-OCT. It has been shown to provide comparable diagnostic accuracy to the other structural measurements. In addition, SD-OCT allows the development of other types of measures in glaucoma than only the thickness of the RNFL, such as measures of the morphology of the ONH or the attenuation coefficient of the RNFL. SD-OCT is a promising technique with its ongoing technical development and the creation of new parameters, leading to a broader view on glaucoma and therefore to new insights. With the complexity of defining glaucoma and the ongoing current technical development, diagnosing and monitoring glaucoma is an everyday complex challenge!



SAMENVATTING

Glaucoom is een heterogene groep van progressieve aandoeningen van de oogzenuw gekenmerkt door een versneld verlies van retinale ganglioncellen (RGCs) en hun axonen, waardoor er een typisch uiterlijk van de oogzenuw en een bijpassend patroon van onomkeerbare gezichtsvelduitval ontstaat. Wereldwijd wordt ongeveer 12% van alle blindheid veroorzaakt door glaucoom, wat het de tweede belangrijkste oorzaak van blindheid maakt. De belangrijkste risicofactor is een verhoogde intra-oculaire druk (IOD). In ogen met oculaire hypertensie is de IOD verhoogd zonder aantasting van de oogzenuw en gezichtsvelduitval. Hoe hoger de IOD, hoe hoger het risico op het ontwikkelen van glaucoom. De IOD is momenteel de enige factor die kan worden beïnvloed met behandeling. Het is aangetoond dat het verlagen van de IOD de achteruitgang (progressie) van glaucoom doet vertragen.

Tot op heden is er nog geen techniek die de exacte aard van de ziekte (de dood van de RGCs en hun axonen) meet. Alle technieken die in de afgelopen decennia zijn ontwikkeld, meten indirect de functionele en structurele schade. Bij het meten van glaucoom wordt de functie van het oog bepaald door het gezichtsveld, dat wordt gemeten met behulp van perimetrie. Er zijn verschillende soorten perimetrie ontwikkeld om functionele schade ten gevolge van glaucoom te meten. De structurele schade als gevolg van glaucoom wordt bepaald door het meten van de oogzenuw (papil), die door verlies van RGCs en axonen verandert, wat leidt tot een typische 'excavatie' van de papil en het daaropvolgende verlies of verdunning van de retinale zenuwvezellaag. Deze structurele veranderingen kunnen worden gemeten door verscheidene beeldvormende technieken, zoals optische coherentie tomografie (OCT), confocale scanning laser ophthalmoscopie (CSLO) en scanning laser polarimetrie (SLP).

Het doel van het in dit proefschrift gepresenteerde onderzoek was om de verschillende technieken te evalueren die in de dagelijkse praktijk worden gebruikt om glaucoom te diagnosticeren en monitoren.

In hoofdstuk 2 hebben we twee soorten perimetrie met elkaar vergeleken, i.e. standaard automatische perimetrie (*Standard Automated Perimetry*, SAP), die vooral wordt gebruikt in de dagelijkse glaucoomzorg en *Short-Wavelength Automated Perimetry* (SWAP; in Nederland ook wel blauw-geel perimetrie genoemd). Van SWAP is bewezen dat het de conversie naar glaucoom 3-4 jaar eerder voorspelt dan dat SAP afwijkingen laat zien. Ons doel was om het moment van conversie naar glaucoom tussen SWAP en SAP te vergelijken in een grote groep van ogen met oculaire hypertensie. Onze resultaten ondersteunden niet de overtuiging dat SWAP conversie naar glaucoom in SAP voorspelt. In plaats daarvan bleek SAP minstens even gevoelig voor conversie als SWAP in verreweg de meeste ogen.

In hoofdstuk 3 & 4 hebben we de resultaten van een grote gerandomiseerde studie gepresenteerd naar oculaire hypertensie en het effect van topicale bètablokkers in het voorkomen van het converteren naar glaucoom. Hoofdstuk 3 presenteerde het percentage conversie van oculaire hypertensie naar glaucoom, gedefinieerd door de progressie-analyses van gezichtsvelden en SLP. SLP detecteerde conversie naar glaucoom eerder dan SAP in de grote meerderheid van de gevallen, wat in potentie kan leiden tot het eerder behandelen om verdere progressie tot matig of ernstig glaucoom te voorkomen. In hoofdstuk 4, presenteerden we het effect van topicale bètablokkers op het percentage conversie van oculaire hypertensie naar glaucoom, met behulp van de definitie van conversie zoals gepresenteerd in hoofdstuk 3. Deze studie toonde een hoger percentage conversie naar glaucoom in ogen met oculaire hypertensie behandeld met bètablokkers, evenals met placebo oogdruppels, dan andere studies eerder beschreven. We toonden aan dat in het algemeen, bètablokkers ogen met oculaire hypertensie niet beschermen tegen conversie naar glaucoom.

In hoofdstuk 5 & 6 presenteerden we de uitkomsten van 2 studies naar het beoordelen van de oogzenuw door professionele glaucoom-zorgverleners, gebruik makend van stereoscopische foto's van de oogzenuw bij het diagnosticeren (hoofdstuk 5) en monitoren (hoofdstuk 6) van glaucoom. In hoofdstuk 5 onderzochten we het vermogen van oogartsen in heel Europa om stereoscopische foto's van verschillende oogzenuwen te koppelen aan de bijbehorende gezichtsvelden, door te kiezen uit een selectie van gezichtsvelden van verschillende ernst van glaucoom. Europese oogartsen hebben in slechts ongeveer 59% van de gevallen de stereoscopische foto van de oogzenuw correct gekoppeld aan het corresponderende gezichtsveld. In de meeste mismatches overschatte de arts het gezichtsvelduitval. Blijkbaar, vanwege hun slechte overeenkomst zullen zowel het klinische beoordelen van de oogzenuw als de evaluatie van gezichtsvelduitval belangrijke pijlers blijven van het beoordelen van de ernst van glaucoom in de dagelijkse klinische zorg. In hoofdstuk 6 hebben we de associatie tussen progressie op het gezichtsveld en de klinische beoordeling van achteruitgang van de oogzenuw met behulp van stereoscopische foto's onderzocht. Ook zijn eventuele verschillen bekeken tussen de diverse oogheelkundige professionals in hun vermogen om progressie te detecteren op sequentiële stereoscopische foto's van de oogzenuw. We vonden een slechte overeenkomst tussen de klinische beoordeling van de oogzenuw middels de seriële stereoscopische foto's en progressie analyse van de gezichtsvelden in glaucoom. In het algemeen, glaucoom specialisten beoordeelden de oogzenuw iets consequenter dan wat minder ervaren oogzorg professionals.

In hoofdstuk 7 & 8 presenteerden we de nieuwste commercieel beschikbare techniek om klinici te helpen bij het diagnosticeren en monitoren van glaucoom, de OCT. Nieuwe technieken leiden tot nieuwe inzichten. Hoofdstuk 7 presen-

teerde een nieuw beschreven verschijnsel op OCT in ogen met glaucoom. We toonden 7 gevallen met een tijdelijke focale microcysteuze schisis van de retinale zenuwvezellaag (retinal nerve fiber layer, RNFL) in ogen met glaucoom in spectraaldomein OCT (SD-OCT). Onze data suggereren dat dit fenomeen geassocieerd is met glaucomateuze wig-defecten in de RNFL. We vergeleken de OCT-beelden met andere technieken waarmee men glaucoom kan meten en het bleek dat dit fenomeen het beste werd waargenomen met SD-OCT; deze microcysteuze schisis zagen we niet in gezonde ogen. Verder onderzoek zal nodig zijn om het beloop en de pathogenese verder te onderzoeken.

In hoofdstuk 8, presenteerden we de eerste resultaten van een nieuw ontwikkelde parameter in OCT, de attenuatie-coëfficiënt. In dit hoofdstuk hebben we het effect aangetoond van glaucoom op de attenuatie-coëfficiënt van de RNFL in SD-OCT metingen. De metingen laten duidelijk zien dat de attenuatie-coëfficiënt van de RNFL afneemt met het toenemen van de ernst van de ziekte. Toekomstige studies zijn nodig om meer inzicht te krijgen in de rol van de attenuatie-coëfficiënt van de RNFL in het diagnosticeren en monitoren van glaucoom, mogelijk leidend tot een nieuwe methode om glaucoom te kwantificeren in SD-OCT beelden.

Samengevat evalueerden we verschillende technieken in de dagelijkse glaucoomzorg om glaucoom te diagnosticeren en te monitoren. SAP blijft een belangrijke steunpilaar in de dagelijkse glaucoomzorg, terwijl SWAP minder gevoelig bleek te zijn dan SAP. Nauwkeurig meten van structurele veranderingen als gevolg van glaucoom blijft een uitdagend doel. Hoewel SLP en CSLO hun waarde hebben bewezen in de klinische beoordeling van de oogzenuw en de RNFL, is de algemene aandacht voor het structureel meten van glaucoom verschoven naar SD-OCT. Er blijkt vooralsnog een vergelijkbare diagnostische nauwkeurigheid ten opzichte van de andere structurele metingen. Daarnaast faciliteert de SD-OCT de ontwikkeling van nieuwe parameters voor het meten van glaucoom dan alleen de dikte van de RNFL, zoals het meten van de morfologie van de ONH of de attenuatie-coëfficiënt van de RNFL. SD-OCT is een veelbelovende techniek met een voortdurende technische ontwikkeling en met de ontwikkeling van nieuwe parameters, wat leidt tot een bredere kijk op glaucoom en dus tot nieuwe inzichten. Met de complexiteit van het definiëren van glaucoom en de voortdurende huidige technische ontwikkeling, is het diagnosticeren en monitoren van glaucoom een alledaagse complexe uitdaging!



Dankwoord
List of Publications
Portfolio
Curriculum Vitae

DANKWOORD

Promoveren is als het bewandelen van een labyrint: wie dat ene pad van promoveren betreedt, is op weg naar de uiteindelijke bestemming: de promotie. Dit pad heeft vele windingen, steeds weer onzichtbaar waar de weg heen gaat. Af en toe gaat het vlak langs het einddoel, om er weer weg van te geraken; een proeve van vastberadenheid en doorzettingsvermogen. De weg zelf leidt tot inzichten, minstens net zo belangrijk als het einddoel.

Mijn pad is lang geweest en heeft ook vele windingen gekend. Nu is het zover dat het einddoel bereikt is. Zonder de weg geen einddoel. En deze weg heb ik bewandeld met velen naast mijn zijde, mij inspirerend, motiverend, vergezellend, leidend (en soms afleidend) en volgend. Jullie hebben mijn promotieweg mede kleur gegeven, verlicht en het waard gemaakt te bewandelen, waarvoor allen dank! Een aantal mensen wil ik in het bijzonder danken:

Allereerst mijn co-promotor Hans Lemij. Het is inmiddels ruim 10 jaar geleden dat ik als co-assistent een ochtend met jouw spreekuur meekeek. Die ochtend raakten we in gesprek over oogheelkunde en onderzoek en heb je mij geïnspireerd een ander pad te bewandelen dan ik tot dan toe voor ogen had. Vanaf toen heb jij mij zijdelings gevolgd op mijn weg naar waar ik nu sta. Je hebt me met je geduld, vertrouwen en gidsend vermogen af en toe de weg gewezen, en me vooral mijn eigen pad laten volgen. Ik vind je een inspirerend arts, een creatief mens en een kritisch en kundig wetenschapper. Dank voor jouw zijn op mijn pad.

Mijn promotor Prof. Jan van Meurs. Ook jou heb ik als co-assistent voor het eerst ontmoet tijdens je spreekuren en operaties waarbij je pigmentblad-transplantaties uitvoerde. Ik dacht dat dit de normaalste zaak van de wereld was binnen de oogheelkunde, echter dit was toch wat onderschat. Je bescheidenheid en ontspannen houding leidde ertoe dat ik er later pas achter kwam dat dit jouw eigen pionierswerk was. Dank voor het zijn van een inspiratie hierin. Ik ben vereerd jou als promotor te mogen hebben.

De leden van de leescommissie, Prof. J.R. Vingerling, Prof. N.M. Jansonius en Prof. C.A.B. Cremers dank ik hartelijk voor het kritisch beoordelen van mijn proefschrift en het plaatsnemen in mijn commissie.

Deze studie was niet mogelijk geweest zonder de jarenlange toewijding van alle aan de studie vrijwillig deelnemende mensen. Met veel plezier en gezelligheid heb ik menig uurtjes met jullie gevuld voor de metingen.

Koen Vermeer, dank je wel voor je geduld en je duidelijke uitleg van die ingewikkelde fysische principes aan mij als leek. Je kritische niet-medische blik was verhelderend in onze artikelen. Dank voor het zijn van zo'n prettige persoonlijkheid en een fijne collega. Nic Reus en Thomas Colen, jullie hebben de basis gelegd voor deze jarenlange studie en een fantastische database gecreëerd. Jullie conscentieuze werk en daarnaast jullie kritisch en heldere oog voor detail bij de artikelen waardeer ik enorm. I would like to thank all European co-authors of the ESAFAT-group and all ophthalmologists participating in this trial for their share in our publication.

Alle mensen van het ROI wil ik bedanken voor de prettige tijd die ik heb ervaren tijdens mijn onderzoek. In het bijzonder Netty Dorresteyn. Ik wil je bedanken voor je kritische blik en begeleiding in het wel en wee van onderzoeksland om zo onze studie binnen de gegeven kaders te laten verlopen. Johannes de Boer & Rene Wubbels, dank jullie wel voor het vooral op de achtergrond meewerken aan het vorderen van het onderzoek. Annemiek, Carolien, Jetty & Marja: dames, dank jullie wel voor jullie ondersteuning, zowel professioneel als persoonlijk! Alle mede-onderzoekers: dank voor het zijn van een klankbord, inspiratie en voor alle gezelligheid! Leonieke, Esther, Maartje, Myrthe & Toine, weten jullie nog wat een ommezwaaai het was om bij de oprichting van het ROI van de donkere kamertjes in het OZR naar de met zon overgoten kamers te gaan met de Rotterdam skyline als uitzicht? Dank jullie wel dat ik dat met jullie vanuit hetzelfde perspectief heb mogen ervaren!

In het bijzonder wil ik Mieke Triesscheijn bedanken. Mieke, zo warm, conscentieus en doorzettend als je altijd bent geweest. Je werkte zo hard, cijferde jezelf vaak weg voor anderen; eigenschappen waardoor je in je werk enorm gewaardeerd werd. Ik heb je gelukkig ook persoonlijk mogen leren kennen als een fijne, lieve vrouw en het is een enorm gemis dat je niet meer bij ons bent.

Alle collega's van het Oogziekenhuis Rotterdam wil ik bedanken voor hun interesse in mijn onderzoek. Daarnaast wil ik de afdeling Perimetrie en Fotografie (de huidige Beeld- & Functie-afdeling) bedanken voor hun vele jaren trouwe hulp. In het bijzonder Marjo van der Horst, Gerard de Graaf, Melania Simileer, Cees van

Ostende, dank voor jullie inzet. Dank aan de MID/ICT voor het telkens maar weer draaiende krijgen van computers, software en apparaten.

Alle oogartsen en arts-assistenten wil ik bedanken voor hun jarenlange interesse in mijn promotie-onderzoek. In het bijzonder wil ik de glaucoomspecialisten Peter de Waard, Jelle de Vries, Antoinette Niessen, Jan-Geert Bollemeijer en Theo Nieuwendijk bedanken voor het aanleveren van patiënten, het delen van jullie onuitputtelijke kennis en het zijn van zo'n heterogene en daarmee elkaar aanvullende groep!

Lieve Karin Littink & Jocelyn van Brakel, mijn paranimfen. Wat ben ik bevoorrecht dat ik jullie aan mijn zijde heb staan! Beiden met dezelfde bagage in onderzoeksland. Karin, ik bewonder je harde werken, je altijd oprechte interesse in anderen en je warme openheid. Het is fijn dat ik je altijd als collega zal hebben, al is de afstand straks wat groter. Jos, het is ons beiden dan toch gelukt! Ik ben blij dat ik je al die jaren al ken en ben trots op je dat je je doelen niet alleen nastreeft, maar ook bereikt, getuige je nieuwe baan!

Alle lieve vrienden en familie, het zal niet altijd en voor iedereen even duidelijk zijn geweest waar ik al die jaren toch mee bezig ben geweest. Desondanks heb ik altijd jullie steun mogen ervaren. Dank jullie wel daarvoor!

Lieve Alie, wat vind ik het fijn dat we 16 jaar geleden samen uit het hoge noorden naar Rotterdam zijn gegaan en nog steeds vriendinnen zijn. Ik wens dat we de tijd minstens nog zullen verdubbelen! Claire, ik heb bewondering voor hoe je staat en gaat voor je idealen, ondanks de mening van anderen. Lieve Mark & Sibrecht, wat vind ik het fijn dat jullie in mijn leven zijn gekomen. De vele avonden en wandelingen met goede gesprekken zijn me dierbaar en ik wens ze nog vaak met jullie te mogen delen!

Lieve Anne, Mirjam & Giuseppe, Sjoeke & Koos, Cor & Nel, Han, Maaïke & Robert. Mijn lieve (schoon)familie, dank voor jullie blijvend vertrouwen in het slagen van mijn missie! Dank voor jullie soms kritische blik en onvoorwaardelijke steun.

Lieve Gert en Tia. Papa en mama, dank jullie wel voor het zijn van een vast baken, al jullie vertrouwen en liefde. Jullie hebben me altijd de vrijheid en ruimte gegeven mijn eigen keuzes te maken, wat me heeft geleid tot hier.

Lieve Ference, dit boekje was er nooit geweest zonder jou aan mijn zijde! Wat ben ik bevoorrecht jouw vrouw te zijn. Dank je wel voor jouw altijd blijvende vertrouwen in dit pad dat ik nu bewandeld heb, en voor je aansporing het steeds weer op te pakken. Dank je wel voor je onvoorwaardelijke liefde. Ik heb de eindbestemming bereikt! Vanaf nu ga ik dolgraag met jou en de jongens een nieuw pad in: wortelen op onze nieuwe plek. Ik kijk er erg naar uit om onze eigen plek van leven, rust en plezier te creëren! Ik hou van je.

Lieve Lucas en Mels, m'n lieve schatten! Wat hebben jullie mijn leven verrijkt! Dank dat jullie in mijn leven zijn gekomen, om een heel stuk samen mijn levenspad te bewandelen. Lucas, je hebt de zin "ik ga aan het werk" je eigen gemaakt, omdat je het te vaak hebt gehoord. Ik zal het niet meer zeggen. Lieve jongens, dank voor het zijn van mijn spiegel. Ik hou van jullie, zielsveel!

De vraag 'Hoe is het nou met je studie?' van mensen die wellicht denken dat ik een eeuwige student ben, kan ik nu na vele jaren positief beantwoorden: 'Het is klaar!'.

Josine van der Schoot



LIST OF PUBLICATIONS

van der Schoot J, Vermeer KA, Lemij HG.

Transient Peripapillary Retinoschisis in Glaucomatous Eyes.

J Ophthalmol. 2017;2017:1536030.

Hernández R, Burr JM, Vale L, Azuara-Blanco A, Cook JA, Banister K, Tuulonen A, Ryan M, Botello-Pinzon A, Takwoingi Y, Vazquez-Montes M, Elders A, Asaoka R, **van der Schoot J**, Fraser C, King A, Lemij H, Sanders R, Vernon S, Kotecha A, Glasziou P, Garway-Heath D, Crabb D, Perera R, Deeks J.

Monitoring ocular hypertension, how much and how often? A cost-effectiveness perspective.

Br J Ophthalmol. 2016 Sep;100(9):1263-8.

Takwoingi Y, Botello AP, Burr JM, Azuara-Blanco A, Garway-Heath DF, Lemij HG, Sanders R, King AJ, Deeks JJ, Hernández R, Vazquez-Montes M, Elders A, Asaoka R, Banister K, **van der Schoot J**, Fraser C, Vernon S, Tuulonen A, Kotecha A, Glasziou P, Crabb D, Vale L, Perera R, Ryan M, Cook J.; Surveillance for Ocular Hypertension Study Group..

External validation of the OHTS-EGPS model for predicting the 5-year risk of open-angle glaucoma in ocular hypertensives.

Br J Ophthalmol. 2014 Mar;98(3):309-14.

van der Schoot J, Reus NJ, Garway-Heath DF, Saarela V, Anton A, Bron AM, Faschinger C, Holló G, Iester M, Jonas JB, Topouzis F, Zeyen TG, Lemij HG.

Accuracy of matching optic discs with visual fields: the European Structure and Function Assessment Trial (ESAFAT).

Ophthalmology. 2013 Dec;120(12):2470-5.

Vermeer KA, **van der Schoot J**, Lemij HG, de Boer JF.

RPE-normalized RNFL attenuation coefficient maps derived from volumetric OCT imaging for glaucoma assessment.

Invest Ophthalmol Vis Sci. 2012 Sep 12;53(10):6102-8.

Burr JM, Botello-Pinzon P, Takwoingi Y, Hernández R, Vazquez-Montes M, Elders A, Asaoka R, Banister K, **van der Schoot J**, Fraser C, King A, Lemij HG, Sanders R, Vernon S, Tuulonen A, Kotecha A, Glasziou P, Garway-Heath D, Crabb D, Vale L, Azuara-Blanco A, Perera R, Ryan M, Deeks J, Cook J.

Surveillance for ocular hypertension: an evidence synthesis and economic evaluation.

Health Technol Assess. 2012 Jun;16(29):1-271, iii-iv.

van der Schoot J, Vermeer KA, de Boer JF, Lemij HG.

The effect of glaucoma on the optical attenuation coefficient of the retinal nerve fiber layer in spectral domain optical coherence tomography images.

Invest Ophthalmol Vis Sci. 2012 Apr 30;53(4):2424-30.

van Zeeburg EJ, Cereda MG, **van der Schoot J**, Pertile G, van Meurs JC.

Early perfusion of a free RPE-choroid graft in patients with exudative macular degeneration can be imaged with spectral domain-OCT.

Invest Ophthalmol Vis Sci. 2011 Jul 29;52(8):5881-6.

Vermeer KA, **van der Schoot J**, Lemij HG, de Boer JF.

Automated segmentation by pixel classification of retinal layers in ophthalmic OCT images.

Biomed Opt Express. 2011 Jun 1;2(6):1743-56.

van der Schoot J, Reus NJ, Colen TP, Lemij HG.

The ability of short-wavelength automated perimetry to predict conversion to glaucoma.

Ophthalmology. 2010 Jan;117(1):30-4.

PORTFOLIO

Name PhD student: Josine van der Schoot	PhD period: 2007 - 2017
Erasmus MC Department: The Rotterdam Eye Hospital / the Rotterdam Ophthalmic Institute	Promotor: Prof. Dr. J.C. van Meurs
	Supervisor: Dr. H.G. Lemij

1. PhD training

	Year	Workload
General courses		
- Good Clinical Practice, ICH-training en advies	2008	8 hours
- Statistische begrippen in de medische literatuur, deel 1& 2, Pfizer	2008	8 hours
- 2nd Research Course in Ophthalmology and Visual Science	2010	6 hours
Seminars and workshops		
- Stichting Anatomy and Function of the Eye (SAFE)	2007, 2008	12 hours
- ARVO-NED annual meeting	2008	6 hours
- Rotterdam Glaucoma Symposium	2008, 2009	12 hours
- Science Day - Rotterdam Ophthalmic Institute / Rotterdam Eye Hospital	2008-2011	24 hours
- Weekly ophthalmologic seminars - Rotterdam Eye Hospital	2008-2016	180 hours
- Monthly scientific seminars - Rotterdam Eye Hospital (including 2 oral presentations)	2008-2016	100 hours
- Monthly scientific seminars - Rotterdam Ophthalmic Institute	2008-2011	36 hours
Presentations		
- Several seminars at the Rotterdam Eye Hospital and several conferences (ARVO, IMAGE, NOG)	2008-2016	100 hours
(Inter)national conferences		
- The Association for Research in Vision and Ophthalmology (ARVO) – poster presentation	2008 - 2011	200 hours
- Imaging Morphometry Association for Glaucoma in Europe (IMAGE) – oral presentation	2008 - 2011	144 hours
- het Nederlands Oogheelkundig Genootschap (NOG) – oral presentation	2008 - 2016	180 hours
- European Glaucoma Course for Residents – European Glaucoma Society	2016	16 hours
- 12 th European Glaucoma Society Congress	2016	30 hours
Other		
- Guest in online Podcast 'As Seen From Here' by Joshua A. Young – Title: 'No Need to SWAP'	2010	8 hours

2. Teaching

	Year	Workload
Lecturing		
- Stichting Anatomy and Function of the Eye (SAFE)	2010	40 hours
- Glaucoma Symposium Rotterdam	2012	40 hours
- Glaucoomdag van Glaucoomvereniging (patientenvereniging)	2012	28 hours
Supervising Bachelor's theses		
- Bachelor Biomedische wetenschappen	2010	40 hours

CURRICULUM VITAE

Josine van der Schoot was born in Groningen on October 30th, 1981. After graduation from the Willem Lodewijk Gymnasium in Groningen, she studied psychology studies at the University of Groningen in 2000. In 2001 she was admitted to medical studies at the Erasmus University Rotterdam. During her studies she worked as a medical student and nurse at the Department of Internal Medicine (geriatrics and oncology) of the former Dijkzigt Hospital (Erasmus Medical Centre) in Rotterdam. Her graduation research project she performed on the department of Internal Medicine and was led by Dr. J.G. Langendonk. They investigated the effect of red wine on blood vessels.



On 16th November 2007, she received her medical degree and she subsequently started her research on diagnosing and monitoring glaucoma, supervised by Dr. H.G. Lemij at the Rotterdam Ophthalmic Institute and the Rotterdam Eye Hospital. The results of the PhD study are described in this thesis and were presented at several national and international meetings. In November 2011 she started her residency in Ophthalmology at the Rotterdam Eye Hospital (Prof. Dr. J.C. van Meurs), which she completed in November 2016. Subsequently, she attended a fellowship on glaucoma and glaucoma surgery at the same institute to become a glaucoma specialist. In 2017 she will start working as an ophthalmologist at the Rijnstate Hospital in Arnhem/Velp, combining allround ophthalmology with her special interest in glaucoma.



